`

Analytical Approach for Estimating the Wave Transmission Coefficient for Floating Structures in Deep Water

Abubaker Ali Alamailes

Submitted to the
Institute of Graduate Studies and Research
in partial fulfillment of the requirements for the degree of

Doctor of Philosophy
in
Civil Engineering

Eastern Mediterranean University
May 2019
Gazimağusa, North Cyprus

Approval of the Institute of Graduate Studies and Research

Prof. Dr. Ali Hakan Ulusoy
Acting Director

I certify that this thesis satisfies the requirements as a thesis for the degree of Doctor of Philosophy in Civil Engineering.

Assoc. Prof. Dr. Serhan Şensoy
Chair, Department of Civil Engineering

We certify that we have read this thesis and that in our opinion it is fully adequate in scope and quality as a thesis for the degree of Doctor of Philosophy in Civil Engineering.

Prof. Dr. Umut Türker
Supervisor

Examining Committee

1. Prof. Dr. Can Elmar Balas
2. Prof. Dr. Esin Çevik
3. Prof. Dr. Umut Türker
4. Assoc. Prof. Dr. Mustafa Ergil
5. Assoc. Prof. Dr. Mehmet Cemal Geneş

`

ABSTRACT

This thesis presents a simplified analytical approach, based on power transmission theory, to estimate the transmission coefficient of box and π-shaped floating structures with finite width. In evaluating the transmitted wave power, this approach considers both the incident wave power and the heave oscillation of the floating structure. Additional power due to the acceleration of the floating body and the hydrodynamic mass increases the transmitted wave power behind the floating structure and consequently increases the transmission coefficient. The proposed theoretical approach is validated using laboratory-scale experimental data obtained from the literature for floating breakwaters and wave energy converters. The results of the proposed approach are in good to excellent agreement with those of experimental studies. In addition, the reliability of the present model is assessed by comparing its results with those of other theoretical approximations. The effects of sea depth, relative draft, and incident wave height on the magnitude of the transmission coefficient distinguish the proposed model from others in the existing literature.

Keywords: Floating Structure, Hydrodynamic mass, Incident power, Transmission coefficient, Transmitted power, Wave transmission

`

ÖZ

Bu tez, sonlu genişlikte yüzen kutu ve π-şekilli yapıların öncesinde ve sonrasında yarattıkları dalga yüksekliklerindeki değişimleri, dalga enerji teorisini kullanarak basit analitik yaklaşımlarla çözerek iletim katsayısını hesaplamayı hedeflemektedir. İletim katsayısının belirlenmesinde kullanılan analitik yaklaşım yüzen yapıya yaklaşan dalga enerjisinin yarattığı etkinin yanında yapının ağır salınımını da göz önünde bulundurmuştur. Yüzen gövdenin hızlanması ve hidrodinamik kütlenin neden olduğu ek güç yüzer yapının kıyı tarafına iletilen dalga gücünü artırmakta ve sonuç olarak iletim katsayısının da artmasını sağlamaktadır. Önerilen teorik yaklaşım, yüzen dalgakıranlar ve dalga enerjisi dönüştürücüler için literatürde önceden elde edilen laboratuvar ölçeğinde deneysel verileri kullanarak doğrulanmıştır. Önerilen yaklaşımın sonuçları, deneysel çalışmaların sonuçları ile uyum içindedir. Ayrıca, mevcut modelin güvenilirliği, diğer teorik yaklaşımlarla karşılaştırılarak da değerlendirilmiştir. Deniz derinliğinin, yüzen yapı draftının ve yapıya yaklaşan dalga yüksekliğinin iletim katsayısının büyüklüğü üzerindeki etkileri, önerilen modeli mevcut literatürdeki diğer çalışmalardan ayırmaktadır.

Anahtar Kelimeler: Yüzen yapı, Hidrodinamik kütle, Yaklaşan dalga gücü, Iletim katsayısı, Iletilen güç, Dalga iletimi

`

Dedicated to:

My father. May his soul rest in Paradise

My soft-hearted mother

My wife and children

`

ACKNOWLEDGMENT

At the end of this challenging and interesting journey, I would like to thank my country, Libya for supporting this study through the High Education Scholarship program.

I would like to express my gratitude and appreciation to my advisor, Prof. Dr. Umut Türker. This study was made possible by his dedication, guidance, support, and encouragement. His office has been always a welcoming place where I learned and gained many skills in the academic aspects.

My biggest thanks go to my family. To my deceased father who was and still my inspiration in this life. I will never ever forget his wise words and his support and encouragement. To my beloved mother who has endured all of these years of separation. To my lovely wife who has withstood with me under all different circumstances. To my four children who have filled my life with joy and happiness. To my brothers and sisters.

`

TABLE OF CONTENTS

`

`

`

LIST OF TABLES

`

LIST OF FIGURES

`

`

`

`

LIST OF SYMBOLS

B	(m)	floating Structure Width
c	(m/s)	Wave Phase Velocity
D	(m)	Floating Structure Draft
d	(m)	Water Depth
E	(J/m^2)	Wave-Induced Energy Per Unit Wave Length
E_k	(J/m^2)	Wave Kinetic Energy Per Unit Wave Length
E_{po}	(J/m^2)	Wave Potential Energy Per Unit Wave Length
g	(m/s^2)	Gravitational Acceleration
H	(m)	Wave Height
H_i	(m)	Incident Wave Height
H_s	(m)	Significant Wave Height
H_t	(m)	Transmitted Wave Height
k	(rad/m)	Wave Number
K_t		Transmission Coefficient
$K_{t.D.e}$		Wave Dragon Experimental Transmission Coefficient
L	(m)	Wave Length
L_p	(m)	Peak Wave Length
M_b	(kg)	Floating Body Mass
M_h	(kg)	Hydrodynamic Mass
$P_{I.1}$	(kW/m)	Kinetic Part of the Incident Wave Power
$P_{I.2}$	(kW/m)	Induced Pressure Part of Wave Power
$P_{I.tot}$	(kW/m)	Total Incident Wave Power
$P_{L.S}$	(kW/m)	Leeside Wave Power

`

$P_{T.1}$	(kW/m)	Kinetic Energy Contribution to The Transmitted Wave Power
$P_{T.2}$	(kW/m)	Induced Pressure Energy Contribution to The Transmitted Wave Power
$P_{T.3}$	(kW/m)	Floating Mass and Added Mass Contribution to The Transmitted Wave Power
$P_{T.tot}$	(kW/m)	Total Transmitted Power
p_{wave}	(N/m^2)	Wave-Induced Pressure
T	(s)	Mean Wave Period
T_n	(s)	Natural Period for Heave Oscillation
T_p	(s)	Peak Wave Period
u_x	(m/s)	Orbital Velocity in The *X* Direction
u_z	(m/s)	Orbital Velocity in The *Z* Direction
α		Added Mass Correction Factor
δ	(m)	Equivalent Added Mass Depth
η	(m)	Displacement of Water Surface
ρ	(kg/m^3)	Density of Water
ω	(1/s)	Wave Circular or Radian Frequency

`

Chapter 1

INTRODUCTION

1.1 Background and Statement of the Problem

Offshore structures include floating breakwaters (FBs), which attenuate the impact of waves on the shoreline, and floating wave energy converters (WECs), which capture energy from waves and convert it into electric power. FBs reduce the impact of waves by reflecting and dissipating the incident wave power, whereas the main purpose of WECs is to harvest wave energy. Moreover, as WECs interact with incident waves, they absorb, transmit, and reflect the incident wave power. Consequently, the wave height behind these devices is reduced. Thus, WECs can also be used as coastal protection devices.

Several studies have investigated FBs as energy harvesting devices (Goggins and Finnegan, 2014; Ning et al., 2016), whereas, other studies have mainly focused on elucidating the hydrodynamic performance of floating structures by optimizing wave attenuation behind WECs and estimating the impact of the transmitted waves on the coastline (Venugopal and Smith, 2007; Palha et al., 2010; Beels et al., 2010; Ruol et al., 2011; Diaconu and Rusu, 2013). In experimental investigations, Burcharth et al. (2015) described the ability of four types of floating WECs—the Wave Dragon (WD), Seabreath, DEXA, and Blow-Jet—to reduce incident wave heights.

`

The commonly accepted standard for evaluating the performance of a floating structure as a wave attenuator is the transmission coefficient K_t. The transmission coefficient K_t is defined as the ratio of transmitted wave height H_t to incident wave height H_i. In linear wave theory, the transmission coefficient can also be defined as the square root of the transmitted wave power P_t over the incident wave power P_i (Hales, 1980; McCartney, 1985; Türker and Kabdasli, 2004).

Some simplified theoretical approaches have been derived from linear wave theory to estimate the performance of FBs. In general, these approaches provide a fair preliminary estimation of the transmission coefficient. In all these theoretical approaches, the effect of wave kinetic energy transport has been ignored when evaluating the hydrodynamic performance and estimating the transmission coefficient of floating structures. Moreover, most of these theories ignore the effect of the floating structure's movement. The present study proposes a simple theoretical approach for estimating the transmission coefficient of relatively wide floating structures using power transmission theory and considering the transport of the wave kinetic energy as a variable that affects the magnitude of the transmission coefficient. In addition, the hydrodynamic (added) mass effect resulting from the heaving motion of the floating structure is considered. The additional kinetic energy flux due to the structure mass and the hydrodynamic mass effect is expected to increase the effect of the kinetic part of the power of incident waves.

In general, floating structures have six degrees of freedom in response to the periodic wave water loads (see Figure 1.1). In three-dimensional domain, the periodic loads make the floating structure accelerates and displaces. Three movements: surge, sway, and heave are described as translational motions of floating structures. Heave is the

`

linear up and down (vertical) motion and the surge is the backward and forward motion of the floating structures. Sway, on the other hand, is represented as the side-to-side motion (left to right or vice versa) of the floating structures. Rotational motions of floating structures are the movements around the vertical, longitudinal and transverse axes. They are known as roll, pitch, and yaw. Pitch is the rotation around transverse axes, roll is the tilting rotation around longitudinal axes and yaw is the rotation around longitudinal axes.

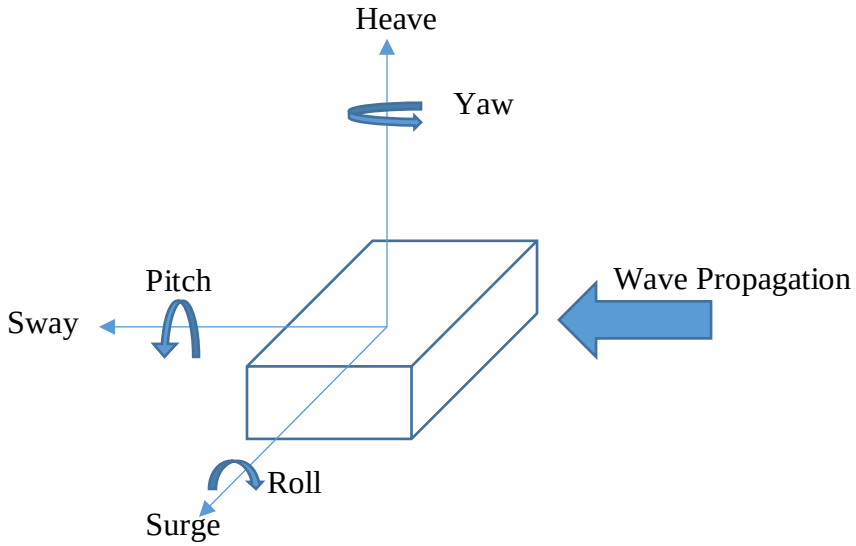

Figure 1.1: Degrees of freedom for a floating body in a three-dimensional space.

This study considers only heave oscillation, as it always occurs and is not significantly affected by mooring systems (Ruol et al., 2013). The transmission coefficient calculated using the present approach is validated by laboratory-scale experimental data obtained from the literature for several types of floating structures, including box FBs, π-shaped FBs and WECs. In addition, to assess the reliability of the proposed model, the transmission coefficient calculated using the proposed approach is compared with those calculated by other researchers, including Macagno (1954), Kriebel and Bollmann (1996), and Ruol et al. (2013).

`

As with other theoretical models, the proposed model is derived using a 2D assumption and validated using 2D experimental data. Thus, diffraction effects due to the floating structure's finite length are not considered. Nevertheless, in practice, floating structures are usually connected to each other or arranged such that they can be considered as a single long body. The effects of the wave propagating angle and the layouts of floating structures on the transmission coefficient have been investigated by Martinelli et al. (2008) and Diamantoulaki and Angelides (2011).

1.2 Aims and Objectives of the Research

The main aim of this study is to propose a simplified analytical approach, based on power transmission theory, to estimate the transmission coefficient of a floating structure with finite width. In evaluating the transmitted wave power, this approach considers both the wave power and the heave oscillation of the floating structure. Additional power resulting from the kinetic energy transport owning to the acceleration of the floating body and the hydrodynamic mass increases the transmitted wave power behind the floating structure and consequently increases the transmission coefficient.

As a simplified approach, this study introduces two additional variables that are in correlation with the performance of the floating structure. These two variables include the effect of the wave kinetic energy transport (flux of wave kinetic energy) according to linear wave theory, and the effect of the heaving motion of the floating structure.

1.3 Research Questions

- Why is the transport of the wave kinetic energy usually ignored when deriving formulas based on linear wave theory?
- How does the transport of the wave kinetic energy effect the transmission coefficient of the floating structures?

`

- Why is the hydrodynamic mass that is attached to the floating structure considered in the new approach?
- Why does the transmission coefficient change as the incident wave height changes?
- Is the closeness of the floating structure to sea bottom affecting the transmission behavior of the floating structure?
- How do the change in the wave conditions and the structure properties affect the transmission coefficient?

1.4 The Proposed Methodology

Wave decay on floating structures can be related to the ratio between incoming wave height H_i and transmitted wave height H_t. As a wave passes a floating structure, it decays and attains new height, H_t. Such wave attenuation can be expressed by the wave transmission coefficient K_t. The transmission coefficient can range from 0 to 1, where 0 indicates no transmission and 1 indicates complete transmission (i.e., no energy loss). The dimensionless transmission coefficient can be defined as a function of flow, fluid, and structure properties, and can also be defined in terms of incident and transmitted wave energies using power transmission theory (Türker, 2014).

The approach of this study is developed based on a fundamental balance in the energy flux. As it summarized in the flowchart (Figure. 1.2), the wave energy is a function in the wave height and the incident wave power can be calculated based on the wave climate. Also, based on the FB properties, the transmitted power can be estimated and the transmission coefficient can be calculated when the transmitted wave height is obtained. The study is assuming tall and wide floating structures, so overtopping is unlikely to occur. In this case, the wave transmission depends on the amount of wave

`

power transmitted to the lee side from underneath the floating structure.

The incident wave energy includes potential, kinetic, and wave-induced pressure energy. In general, under the assumptions of linear wave theory, the energy transport in the wave propagation direction is estimated by considering only the power resulting from the work done by the wave-induced pressure and by ignoring the transport of wave kinetic energy (kinetic part of the wave power), owing to approximation to a certain order of accuracy (Holthuijsen, 2010). In the presence of floating structures, kinetic part of the wave power should be considered because their heaving behavior significantly affects the total transmitted power. Therefore, the kinetic part of the wave power together with the kinetic energy flux generated from the heaving oscillation of the floating structures increase the total transmitted power and hence, the transmission coefficient. Therefore, the total incident wave power comprises the kinetic part of the wave power in addition to the wave-induced pressure part.

Part of the total incident wave power is transmitted from beneath the floating structure draft to the lee side. The transmitted power includes the transmitted kinetic part of the wave power and wave-induced pressure part. In addition to these two transmitted contributions, kinetic energy flux per unit floating structure width resulting from the heaving motion of the floating structure is also transmitted horizontally to the lee side. This contribution consists of two parts: the kinetic energy flux from the heaving body of the floating structure and the kinetic energy flux from the hydrodynamic mass that accelerates simultaneously with the floating body.

The transmitted wave (at the lee side of the floating structure) carries a total power that equals the total transmitted power. The transmitted wave becomes the incident wave

`

toward the coastline with a height of H_t, which is attained after attenuation of the sea-side incident wave. The leeside incident wave carries a total power that comprises the wave-induced pressure and kinetic parts of wave power. This power is a function of H_t, and once the value of H_t is obtained and the transmission coefficient K_t can be calculated.

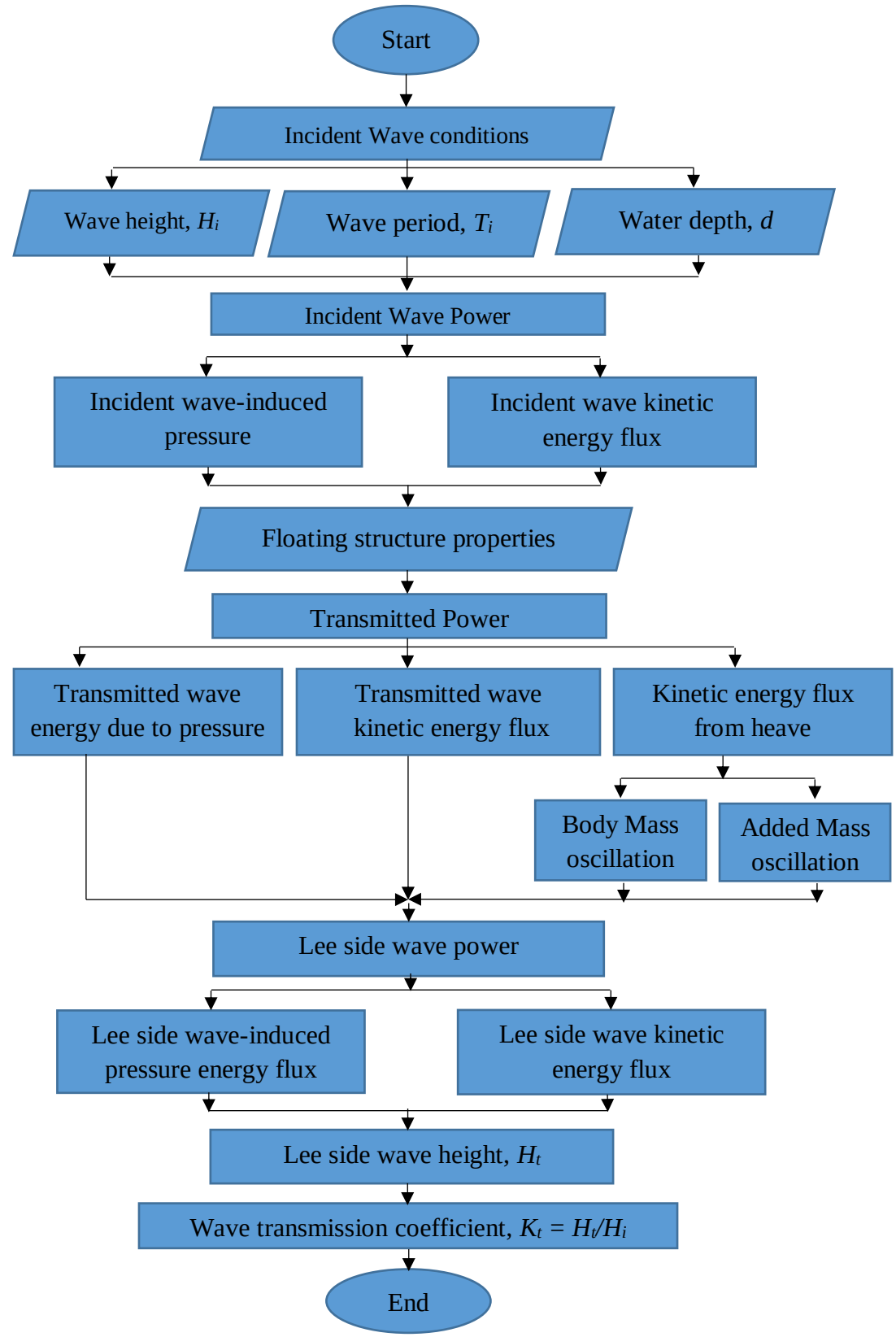

Figure 1.2: Summary of the proposed methodology.

`

1.5 Outline of the Study

This study includes six chapters. The first one is the introductory chapter in which background about the research problem, the aims and importance of the study, and proposed methodology are presented. The second chapter presents information about the previous theoretical approaches that dealt with the wave transmission phenomena. In the third chapter, the proposed methodology on the balance of the wave energy transport and wave transmission coefficient are discussed in details. Chapter four includes the assessment of the proposed approach using experimental data obtained from literature. Chapter five shows the results and discussions. Finally, chapter six contains the conclusions and recommendation for future studies.

1.6 Importance of the Study

The reliance on floating structure has increased in these days in various aspects. For instance, due to the high prices of oil and its negative effects on the environment, there is a global trend to increase the use of alternative energy sources including waves. The high construction cost of different kinds of the floating structures has led to cost-sharing strategy in which an application can be used for a secondary purpose beside its main use. For example, using the wave energy converters for coastline protection purpose is one of the ways of reducing the capital cost of the application (Ning et al., 2016). Therefore, evaluating the wave reduction behind any floating structure is an important key to assess the visibility of using this structure as a protecting device. The wave reduction can be evaluated by obtaining the wave transmission coefficient. This study is providing a simplified analytical approach to estimate the wave transmission coefficient for different types of floating structures. The approach is derived by using a simple wave energy transport balance based on the linear wave theory. However, it is aiming to provide more reliable and reasonable methodology by considering more

`

variables including the heaving oscillation of the floating structure and the wave kinetic energy transport which had been ignored in the previous theoretical models.

1.7 Limitations of the Study

The model of this study is based on the well-known linear wave theory which is used to define the wave dynamics and kinematics. Therefore, the approximation of the model is accurate under wave conditions that are compatible with linear wave theory assumptions. Also, the model is developed to estimate the transmission coefficient for non-fixed floating structures with finite width since the effects of the hydrodynamic mass is basically depending on the oscillation of the structure. Therefore it will not be reasonable to use it with fixed structures that have very limited widths. The model is also limited to reflective floating structures which typically reduce the impact of the incident wave by reflecting the wave energy and allowing small amount of this energy to pass beyond them. Therefore, this model should not be used in case of dissipative floating structures whose main effect is to dissipate the wave energy by friction, turbulence and etc. Finally, the model is not valid when the structure's freeboard is not sufficiently high to block overtopping. The excessive amount of wave power transmitted with the overtopped water will increase the total transmitted power and that will lead to reaching inaccurate estimation for the transmission coefficient.

`

Chapter 2

LITERATURE REVIEW

WAVE TRANSMISSION THEORIES

This chapter presents the different theoretical models, available in literature, to estimate the wave transmission of floating structures. Later in chapter 4, some of these theories will be compared with the proposed theory of this research and experimental data obtained from different studies to assess the reliability of the present approach.

2.1 Performance of Floating Structures as Wave Attenuators

The performance of floating structures as wave attenuators is determined by the amount of wave reduction, which basically depends on the amount of wave power that is reflected, dissipated, or transmitted to the leeside of the structure (see Figure. 2.1). Typically, most of the wave transmission theories are associated with the wave energy transport and their derivations are based on linear wave theory.

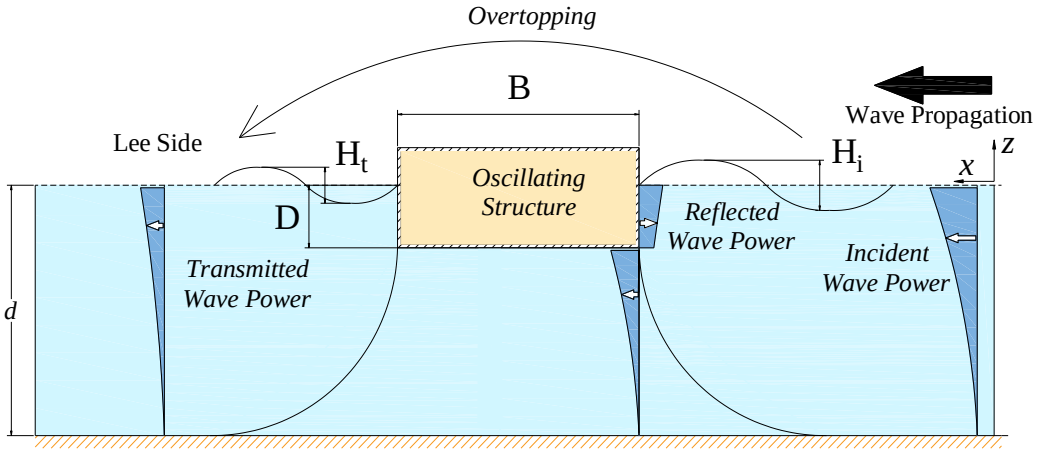

Figure 2.1: Basic interactions between waves and floating breakwaters.

`

For effective performance; in term of wave attenuation; the floating structure should be able to prevent the wave energy from transferring to the lee side. This requires the obstruction of the upper part of the water column where the major part of the wave energy is typically concentrated in case of short waves. However, in the presence of longer and higher waves, deeper structure draft will be required to block the transport of the larger amount of the wave energy which is extended deeper in the water column toward the sea bed (Hales, 1980 and McCartney, 1985).

The performance of the floating structures can be defined by the wave transmission coefficient K_t which is generally defined by the ratio between the transmitted wave height H_t and the incident wave height H_i. The transmission coefficient can range from 0 to 1, where 0 indicates no transmission and 1 indicates complete transmission (i.e., no energy loss). The dimensionless transmission coefficient can be defined as a function of flow, fluid, and structure properties, and can also be defined in terms of incident and transmitted wave energies using power transmission theory (Türker, 2014).

2.2 Floating Structures Classifications and Transmission Theories

Floating structures can be classified based on the wave attenuation process as reflective or dissipative structures (Oliver et al., 1994). Reflective floating structures is usually attenuate the impact of the incident wave by reflecting the wave energy and allowing small amount of this energy to pass beyond them. On the other hand, dissipative floating structures dissipate the wave energy by friction, turbulence and etc.

Floating structures can be also classified based on the formation properties as rigid or flexible structures. For a rigid structure, each member of the structure remains in the same position relative to the other members. Therefore, the relative displacement of

`

each member to the other members is null. Contrarily, in case of flexible structure, the relative displacement is considerable. Rigid floating structures attenuate waves mostly by reflection; meanwhile, flexible structure achieve wave attenuation basically by dissipation (Bouwmeester and Van der Breggen, 1984).

In addition to the two previous classifications, floating structures may be classified based on their relative movement to the sea bed as fixed or non-fixed structures. When the movements of the floating structures are restrained and relatively negligible, the structures are considered fixed unlike the case of non-fixed structures whose movements are considerable.

These classifications have been presented since the theoretical approaches for estimating the wave transmission that have been developed are basically different based on the type and the properties of each structure. In this study, an analytical approach is developed to estimate the wave transmission for reflective rigid structures. Therefore, a review for relative theories is presented in the following sections.

2.3 Wave Transmission Theories for Fixed Structures

Some simplified approaches have been derived from linear wave theory to estimate the performance of FBs. In general, these approaches provide a fair preliminary estimation of the transmission coefficient. One of the first such studies was performed in 1947 by Ursell, who established a theory for the partial transmission and reflection of waves in deep water for rigid and fixed submerged structures with extremely small widths. Another well-known formula was developed by Macagno (1954), who assumed a rigid, fixed, and finite-width structure installed in deep water. Several years later, Wiegel (1960) developed the power transmission theory, which assumes that all

`

of the incident wave power between the structure draft and the seabed is fully transmitted. Processes such as, turbulence, radiation due to the motions of the floating structure and overtopping are neglected by these approaches.

2.3.1 Ursell 1947

Uresell developed his theory for a vertical floating barrier in deep water using the linear wave theory. The assumptions of this theory are that the barrier is rigid and fixed with extremely small width, no overtopping occurs, and the wave energy encountered by the barrier is completely reflected. Uresell achieved the following expression (Eq. (2.1)) to estimate the transmission coefficient by using the modified Bessel functions to solve the second order ordinary differential equation of Bessel (Bouwmeester and Van der Breggen, 1984).

$$K_{t,Ursell} = \frac{k_1 \frac{2\pi D}{L_i}}{\pi^2 I_1^2 \frac{2\pi D}{L_i} + k_1^2 \frac{2\pi D}{L_i}} \tag{2.1}$$

Where $k_1 \frac{2\pi D}{L_i}$ and $I_1 \frac{2\pi D}{L_i}$ are the modified Bessel functions, L_i is the incident wave length, and the D is the draft of the floating structure.

The study of Uresell concluded that the relative draft (D/L_i) had a significant effect on the wave transmission. It showed (see Figure. 2.2) that as the draft is extended deeper, more wave energy blockage happened resulting in a smaller transmission coefficient.

`

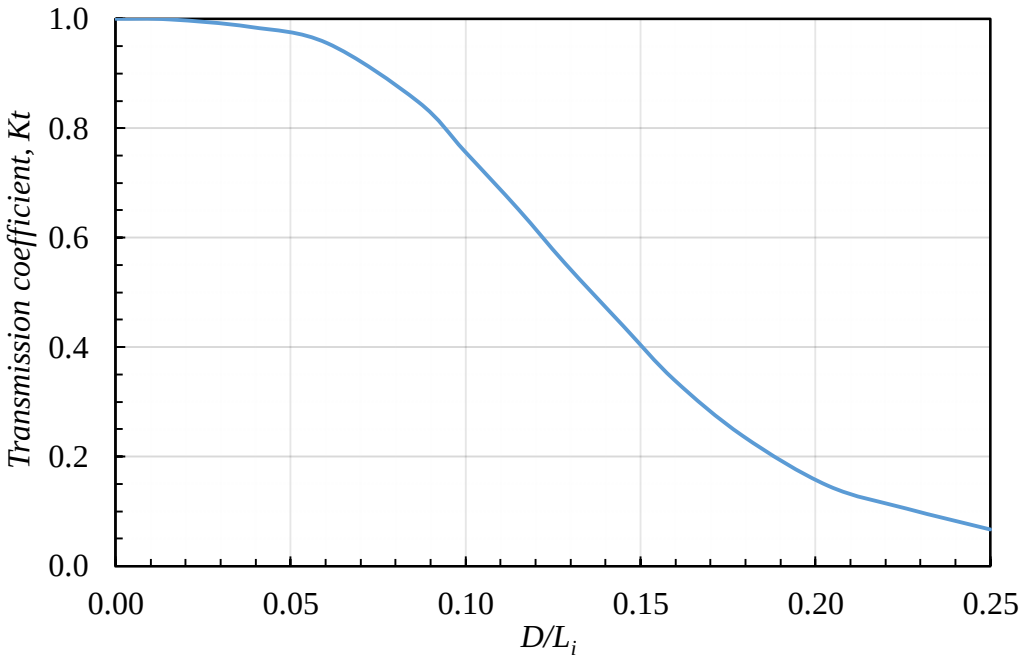

Figure 2.2: Change in Ursell's transmission coefficient with respect to the change of relative structure's draft D/Li (modified from Uresell, 1947).

2.3.2 Macagno (1954)

Macagno developed a formula to estimate the wave transmission coefficient for a rigid fixed box-type floating breakwater. This 2-dimential approach was developed based on linear wave theory without any consideration for the structure oscillations and the wave overtopping (see Figure. 2.3).

Based on the previous assumptions Macagno achieved the following expression (Eq. (2.2)) to calculate the transmission coefficient (Ruol et al., 2103).

$$K_{t,Macagno} = \frac{1}{\sqrt{1 + \left[kB\ \frac{\sinh(kd)}{2\cosh(kd - kD)}\right]^2}} \qquad (2.2)$$

Where k is the wave number (= $2\pi/L$), L is the wave length, B is the structure's width, and d is the water depth.

`

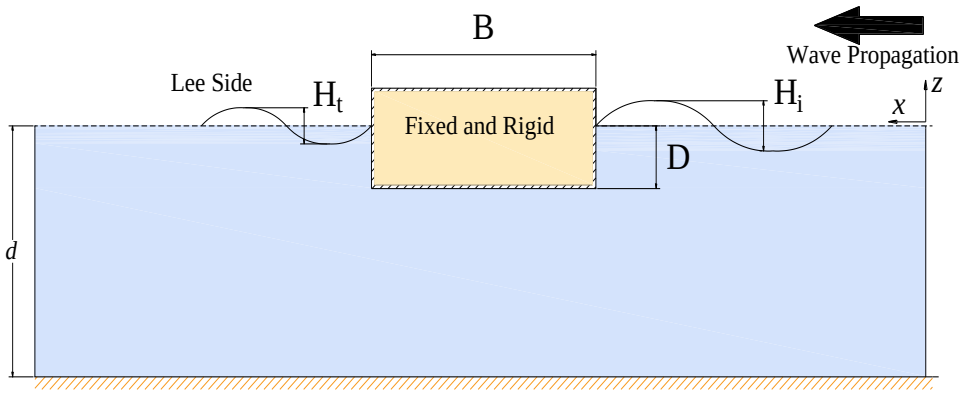

Figure 2.3: Definitions of Macagno's theory (modified from Bouwmeester and Van der Breggen, 1984).

The results of Macagno's formula is given in Figure. 2.4. The figure presents the change in the transmission coefficient with respect to the change in the wave period (wave length) and the change of the structure's width. It can be clearly seen that under constant wave depth and structure's draft as the wave period increases the transmission coefficient also increases minimizing the effect of floating structure. This approves the fact that longer waves require deeper draft to effectively attenuate the incoming wave energy impact.

`

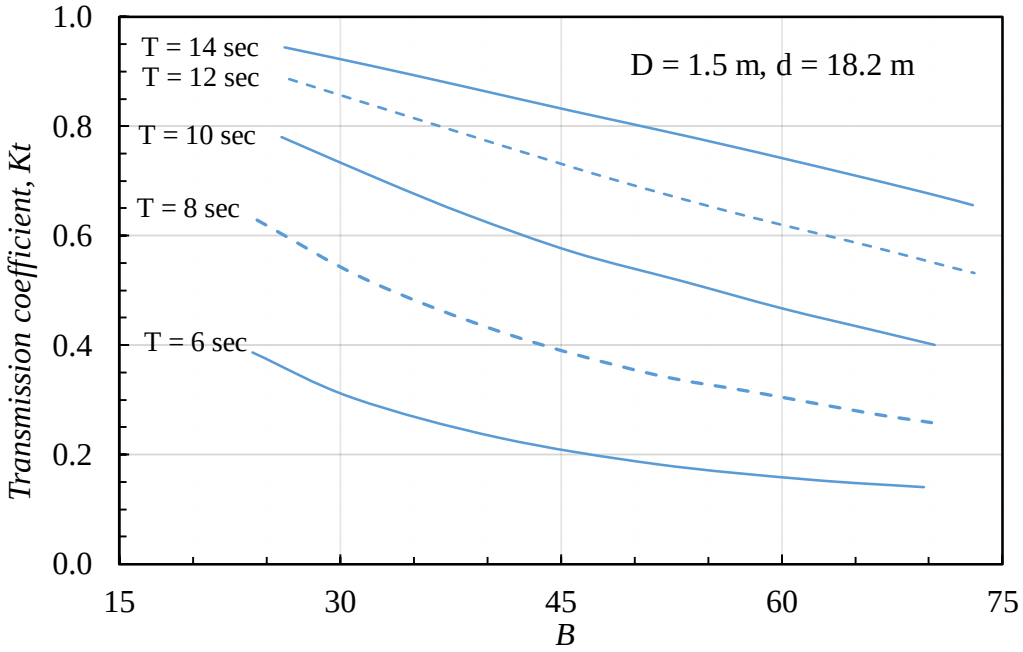

Figure 2.4: Change in Macagno's transmission coefficient with respect to the change of structure's width *B* and the wave period *T* (modified from Bouwmeester and Van der Breggen, 1984).

2.3.3 Wiegel (1960)

Wiegel in 1960 presented a theoretical approach called "Power Transmission Theory" to predict the wave transmission coefficient for the vertical submerged barrier which was assumed to be fixed and rigid. This theory was developed based in linear wave theory without accounting the reflection from the structure nor the wave overtopping.

In this theory, Wiegel supposed that the transmitted wave power is only the wave energy transported between the bottom of the structure (the draft) and the sea bed (see Figure. 2.5).

`

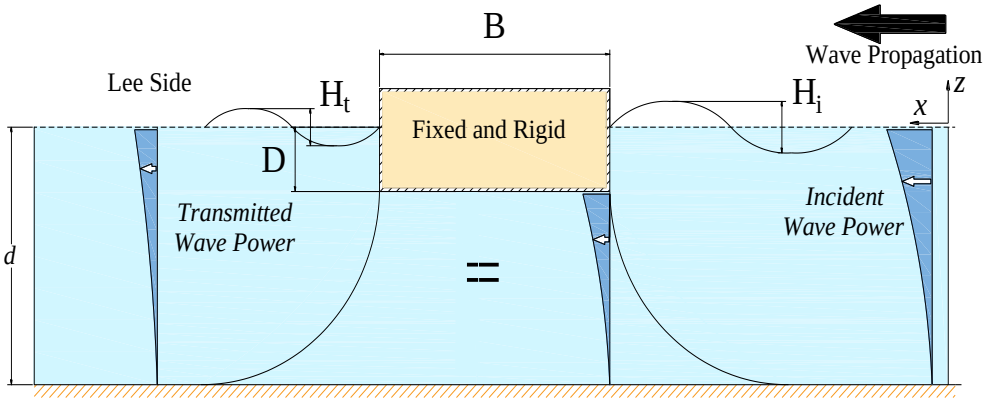

Figure 2.5: Definitions of Wiegel's theory.

Wiegel, however, considered only the transport of the wave energy that is resulted from the wave-induced pressure (p_{wave}) while he neglected the transport of the wave kinetic energy. The incident wave power ($P_{I.Wiegel}$) in this theory (Eq. (2.3)) is resulted for the time-averaging over one wave period integration of the wave-induced pressure by the wave horizontal orbital velocity from the average water surface (z = 0) to the sea bed (z = d). Meanwhile, the transmitted wave power ($P_{T.Wiegel}$) (Eq. (2.4)) is resulted for the time-averaging over one wave period integration of the wave-induced pressure by the wave horizontal orbital velocity from bottom of the structure (z = D) to the sea bed (z = d) as

$$P_{I.Wiegel} = \overline{\int_{-d}^{0} (p_{wave})\, u_x \, dz} \tag{2.3}$$

$$P_{T.Wiegel} = \overline{\int_{-d}^{D} (p_{wave})\, u_x \, dz} \tag{2.4}$$

Using the linear wave theory expressions for wave-induced pressure and the wave or-

`

bital velocity, Wiegel reached the following expressions for the incident and the transmitted wave power (Hals, 1981)

$$P_{I.Wiegel} = 1 + \frac{\frac{4\pi d}{L_i}}{\sinh(\frac{4\pi d}{L_i})} \tag{2.5}$$

$$P_{T.Wiegel} = \frac{\frac{4\pi\ (d+D)}{L_i}}{\sinh(\frac{4\pi d}{L_i})} + \frac{\sinh(\frac{4\pi\ (d+D)}{L_i})}{\sinh(\frac{4\pi d}{L_i})} \tag{2.6}$$

Wiegel then obtained the formula that estimates the transmission coefficient which is equal to the square root of the ratio of the transmitted wave power to the incident wave power as (Kriebel and Bollmann 1996)

$$K_{t,Wiegel} = \sqrt{\frac{P_{I.Wiegel}}{P_{T.Wiegel}}} = \sqrt{\frac{2k\ (d-D) + \sinh(2k(d-D))}{\sinh(2kd) + 2kd}} \tag{2.7}$$

According the theory of Wiegel, Figure. 2.6 shows the effect of the change of the structure draft (d) relative to the wave length (L) on the performance of the structure in different water depths. It can be seen that as the draft increases the transmission coefficient decreases indicating a better wave attenuation. Moreover, the figure shows that the performance of the floating structure is better in deep water than in shallower water for the same relative draft.

`

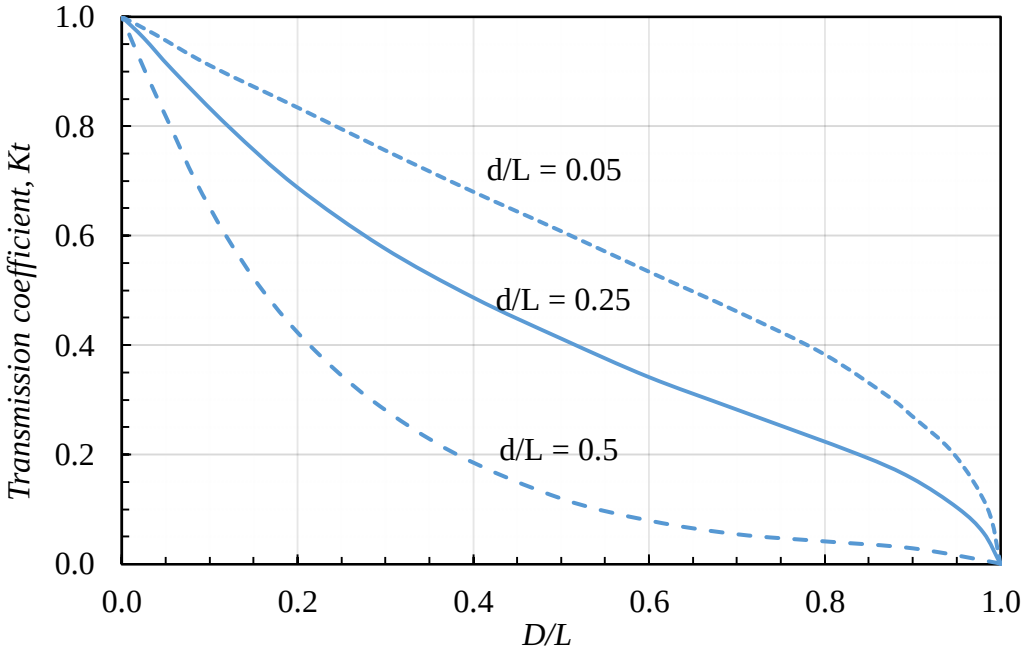

Figure 2.6: Change in Wiegel's transmission coefficient with respect to the change of structure's draft D relative to the wave length L in shallow (d/L =0.05), intermediate (d/L =0.25), and deep (d/L =0.5) waters (modified from Hales, 1981).

2.3.4 Kriebel and Bollmann (1996)

Kriebel and Bollmann (1996) modified Wiegel's theory by including partial wave reflection in the definition of the transmission coefficient. The researchers assumed that the wave-induced pressure under the floating structure equals the sum of the incident wave-induced pressure ($p_{wave.i}$) and the reflected wave-induced pressure ($p_{wave.r}$). Findings using this approach exhibit a higher net pressure under the structure than was assumed by Wiegel. In contrast, the orbital horizontal velocity (u_x), which is modified by subtracting the reflective horizontal velocity ($u_{x.r}$) from the incident horizontal velocity ($u_{x.i}$), is slower than the orbital horizontal velocity assumed by Wiegel. Therefore, the incident and the transmitted wave power proposed by Kriebel and Bollmann (1996) are

`

$$P_{I.Kriebel\ and\ Bollmann} = \overline{\int_{-d}^{0} (p_{wave.i} + p_{wave.r})\,(u_{x.i} - u_{x.r})\,dz} \tag{2.8}$$

$$P_{T.Kriebel\ and\ Bollmann} = \overline{\int_{-d}^{D} (p_{wave.t})\,u_x\,dz} \tag{2.9}$$

Since the wave reflection is taken in consideration in this model, two unknown variables appear in Eq. (2.8) and Eq. (2.9). Therefore, the researchers used the continuity of fluid velocities under the structure which is defined as, $u_x = u_{x.i} - u_{x.r}$ to overcome this problem. Then, using the linear wave theory and neglecting the wave dissipation and phase changing, the following expressions (Eq. (2.10)) were reached.

$$K_t + K_r = 1 \quad and \quad K_r = \frac{H_r}{H_i} \tag{2.10}$$

Where K_r is the wave reflection coefficient, H_r is the reflective wave height and H_i is the incident wave height.

With the use of these relations, Kriebel and Bollmann (1996) obtained Eq. (2.11) to estimate the transmission coefficient.

$$K_{t,Kriebel\ and\ Bollmann} = \frac{2K_{t,Wiegel}}{1 + K_{t,Wiegel}} \tag{2.11}$$

Then Kriebel and Bollmann compared their theory and the theory of Wiegel to the laboratory data provided by Wiegel, 1960. Figure 2.7 shows the change in the transmission coefficient in respect to the change in the relative draft (D/d) in deep water ($d/L = 0.7$). It can be observed that Wiegel's model overestimates the wave transmission coefficient while the modified theory provides better estimates.

`

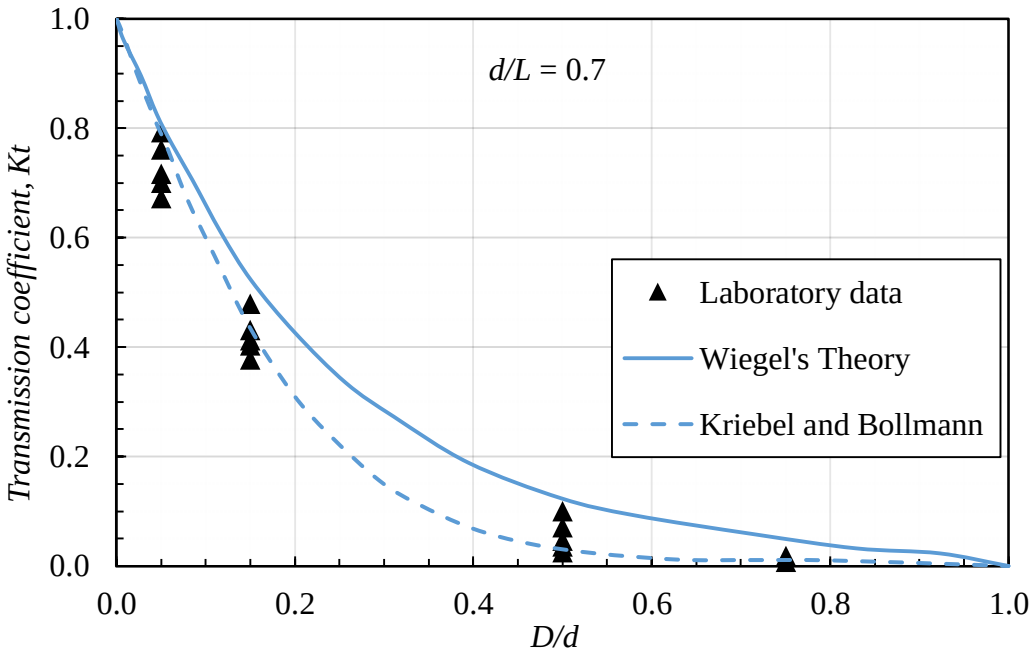

Figure 2.7: Comparison between experimental data from Wiegel (1960) with the outcomes of the theoretical approaches of Wiegel (1960) and Kriebel and Bollmann (1996) in deep water (modified from Kriebel and Bollmann, 1996).

2.4 Wave Transmission Theories for Non-Fixed Structures

The former theories are valid for floating structures that are fixed relative to the sea bed. Typically, floating breakwaters are non-fixed and have a certain degree of freedom; therefore, better estimations for wave transmission coefficient would be obtained when the oscillations of the floating structures are taken in consideration in the modeling. One of the earliest study that considered the structure's movement was performed by Carr (1951). The theory of Carr was developed for floating structures installed in shallow water and the structures were assumed to be freely move in the horizontal direction. Lately, Ruol et al. (2013) modified the theory of Macagno (1954) by introducing a correction factor on Macagno's formula in order to estimate the wave transmission coefficient for non-fixed floating breakwaters.

`

2.4.1 Carr (1951)

This theory was developed to predict the wave transmission coefficient for non-fixed floating structures. The theory assumed that the floating structures are anchored in a shallow water and made a use of linear wave theory considering only the wave hydro-static pressure. The motion of the structures was incorporated in the model by considering the horizontal natural period of the structure. Overtopping was not taken into account in the model. Based on these assumptions Carr (1951) obtained the following formula (Eq. (2.12)) to estimate the wave transmission coefficient.

$$K_{t,Carr} = \frac{1}{\sqrt{1 + \left(\frac{\pi M}{\gamma_w L d}\right)^2 \left(\left(\frac{T_n}{T}\right)^{-2} - 1\right)^2}} \qquad (2.12)$$

Where M is the mass per unit length of the floating structure (kg/m), γ_w is the unit weight of water (kg/m^3), L is the wave length (m), d is the water depth (m), T_n is the horizontal natural period of the structure (sec), and T is the wave period (sec).

The implementation of the formula (Figure. 2.8) of Carr shows that the transmission coefficient decreases as the mass per unit length of the floating structure increases relative to the wave mass. This indicates that for the same wave, extending the draft of the structure deeper results in better floating structure performance as a wave breaker.

`

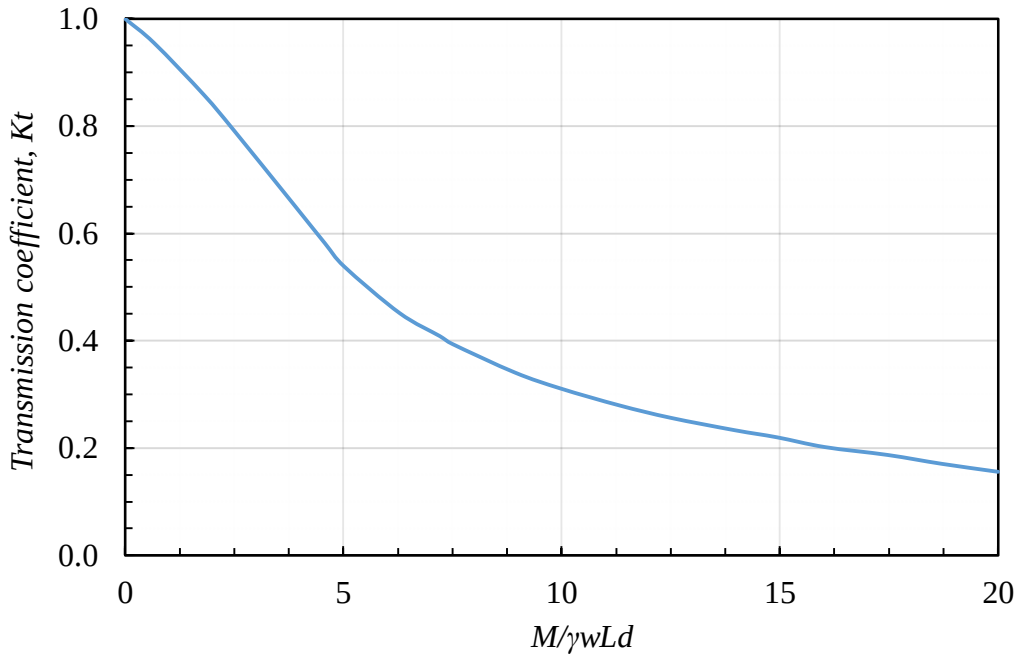

Figure 2.8: Change in Carr's transmission coefficient with respect to mass per unit length of floating structure relative to wave mass (modified from Carr, 1951).

2.4.2 Ruol et al. (2013)

The theory of Ruol et al. (2013) was initially developed to predict the wave transmission for π-shaped floating breakwater and then was found that it could also be applicable for box-type. It is basically a modification for Macagno's theory in which the floating structure was considered fixed. However, in the model of Ruol et al. (2013), the heaving motion of the floating structure was taken into account. The formula is a function of the relative period (χ), which is defined as the wave peak period (T_p) over the heave natural period (T_n). The formula was found to be valid for a relative draft ($0.20 \leq D/d \leq 0.60$) and for relative period ($0.50 \leq \chi \leq 1.5$). In these ranges, the modification on Macagno's formula was performed by introducing a factor donated as $\beta(\chi)$ which was achieved based on a dataset of experimental data to obtain the relative period. The natural period for the heave motion of the floating structure has to be found through experimental tests in which the hydrodynamic (added) mass has to be consid-

`

ered. The added mass is defined as the fluid mass that accelerates along with the floating structure. Thus, this mass has to be taken in consideration when the mass of the floating structure is involved in the modeling.

Based on the assumption that the buoyancy force is the only vertical force considered when calculating the moorings' stiffness for the chain moorings, Ruol et al. (2013) estimated the hydrodynamic mass M_h as the volume of water under the floating structure, where the volume boundary is described by a semicircle with a radius equal to half the width B of the structure (Figure. 2.9).

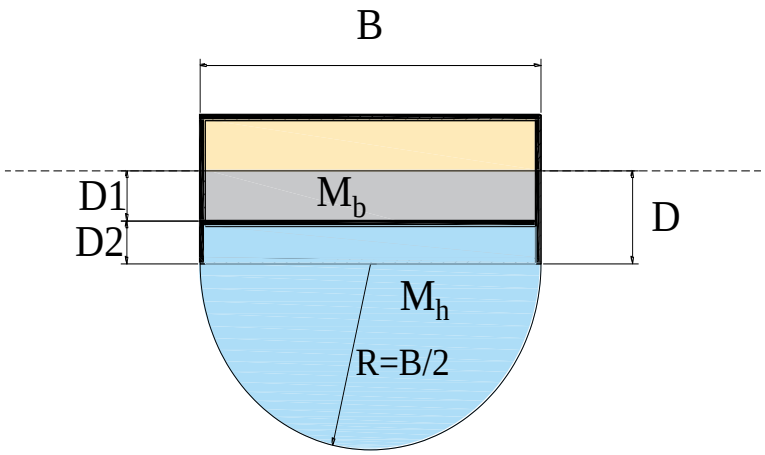

Figure 2.9: The estimated hydrodynamic mass for π-shaped floating structure (modified from Roul et al., 2013).

The natural frequency for the heaving motion of the floating structure (ω_n) considering the added mass was found to be (Ruol et al., 2013)

$$\omega_n = \sqrt{\frac{\rho g B}{M_b + M_h}} = \sqrt{\frac{g}{D + \frac{\pi}{8} B}} \qquad (2.13)$$

Where ρ is the water density, g is the gravitational acceleration, B is the width of the structure, $M_b = \rho\ B\ D$ representing the submerged mass of the floating body, and

`

$M_h = \rho \frac{\pi}{8} B^2$ representing the hydrodynamic mass.

Ruol et al. (2013) experimentally examined the natural heave period for π-shaped structure and compared the analytical calculations with experimental results. It was found out that the value π/8 = 0.39 should be 0.35. Therefore, the natural heave period was estimated as

$$T_n = \frac{2\pi}{\omega_n} = \frac{2\pi}{\sqrt{\frac{g}{D + .035B}}} \tag{2.14}$$

Therefore, the relative χ, which is defined as T_p/T_n is calculated as

$$\chi = \frac{T_p}{T_n} = \frac{T_p}{2\pi} \sqrt{\frac{g}{D + .035B}} \tag{2.15}$$

Equation (2.15) considers the peak wave period T_p, which implies irregular waves. In general, T_p is 10% larger than the mean wave period T (Ruol et al., 2013). Therefore, to apply this relation to regular waves with mean period T (as with Macagno's theory), T_p/T_n in Eq. (2.15) should be multiplied by a factor of 1.1, i.e., $T/T_n = 1.1\ T_p/T_n$.

Then, the modification factor $\beta(\chi)$ based on the best fit to the dataset of experimental data is

$$\beta(\chi) = \frac{1}{1 + \left(\frac{\chi - \chi_o}{\sigma}\right) e^{-\left(\frac{\chi - \chi_o}{\sigma}\right)^2}} \tag{2.16}$$

In which $\chi_o = 0.7919$ and $\sigma = 0.1922$ (with 95% confidence interval)

Therefore, the transmission coefficient formula by Ruol et al. (2013) becomes

$$K_{t,Ruol} = \beta(\chi)\, K_{t,Macagno} \tag{2.17}$$

`

Roul et al. (2013) validated the previous formula (Eq. (2.17)) by comparing the calculated transmission coefficient to a set of experimental data obtained from their own experiments and others taken from various studies on the performance of box and π-shaped floating breakwaters. These studies were conducted under different conditions of waves and mooring systems. Table (2.1) summarizes these studies and shows the legend symbol for each data set that are shown in figure (2.10).

Table 2.1: Summaries of the experimental studies used by Roul et al. (2013).

Study	**Legend**	**Type**	**Mooring**	**Wave**
Ruol et al., 2013	shaded circle	pi-type	cables	irregular
Martinelli et al., 2008	solid circle	pi-type	cables	irregular
Gesraha, 2006	square	pi-type	cables	regular
Pena et al., 2011 (Model A)	left triangle	pi-type	chains	regular
Pena et al., 2011 (Model B)	upward triangle	pi-type	cables	regular
Pena et al., 2011 (Model C)	right triangle	pi-type	cables	regular
Koutandos et al., 2005	diamond	Box-type	piles	regular
Cox et al., 2007	open asterisk	Box-type	piles	regular
Cox et al., 2007	solid asterisk	Box-type	piles	irregular

Figure (2.10) demonstrates the comparison between the measured results for floating breakwaters moored by piles and chains and the calculated results of the formula of Roul et al. (2013). The dash lines characterizes 20% confidence boundaries. Ruol et al. determined that an excellent agreements are reached for π-shaped FB moored by chains. However, models with FBs moored by cables are in good agreement with formula, while, FBs moored by piles are generally overestimated.

`

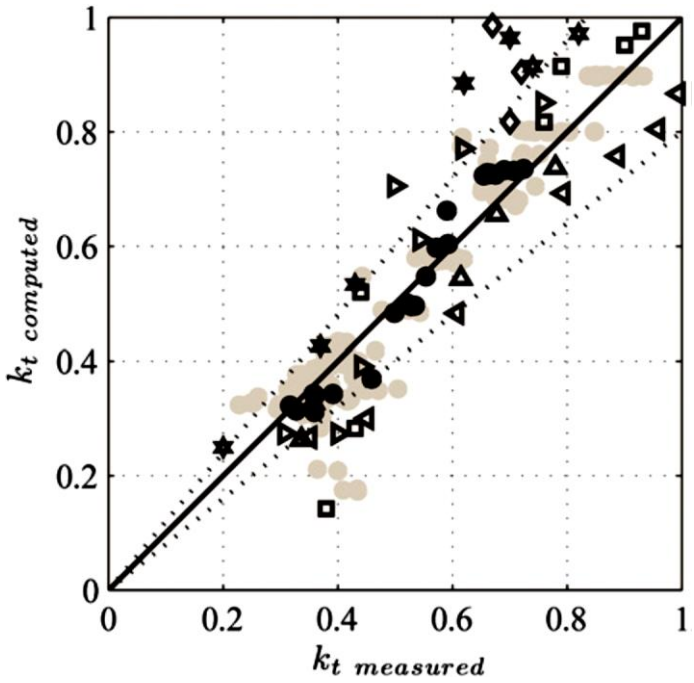

Figure 2.10: Measured results versus calculated transmission coefficients (Roul et al., 2013).

`

Chapter 3

METHODOLOGY

WAVE POWER TRANSMISSION

This chapter presents the methodology that is followed to estimate the wave transmission coefficient for two types of floating structures namely Box and π-shaped. The process is developed based on the balance between the incident wave power (wave energy transport before facing the floating structure) and the transmitted wave power (wave energy transport after passing the floating structure). The chapter initially explains the incident wave energy and the incident wave energy transport (wave power) for regular waves using the linear wave theory. In this part not only the transport of the wave energy resulted from the wave induced-pressure is considered but also the transport of the wave kinetic energy. Then, the transmitted wave power is described in details for both types of floating structure mentioned previously. The balance of the wave power transmission includes the incident wave power, the transmitted wave power and the kinetic energy transport resulted from the heave oscillation of the floating structure.

3.1 General Methodology

Wave decay on floating structures can be related to the ratio between incoming wave height H_i and transmitted wave height H_t. As a wave passes a floating structure, it decays and attains new height, H_t. Such wave attenuation can be expressed by the wave transmission coefficient K_t as

`

$$K_t = \frac{H_t}{H_i} \tag{3.1}$$

In case of tall and wide floating structures, overtopping is unlikely to occur; in this case, the wave transmission depends on the amount of wave power transmitted to the lee side from underneath the floating structure.

The incident wave energy includes potential, kinetic, and wave-induced pressure energy. Under the assumptions of linear wave theory, the energy transport (wave power) in the wave propagation direction is estimated by considering only the work done by the wave-induced pressure, yielding the well-known equation for wave power per unit wave length:

$$P_{Incident} = \frac{1}{8}\,\rho\, g H^2 \;\; \frac{1}{2}\left[1 + \frac{2kd}{\sinh(2kd)}\right]\frac{\omega}{k} \tag{3.2}$$

where H is the wave height, d is the water depth, ρ is the fluid density, g is the gravitational acceleration, ω is the wave circular or radian frequency (= $2\pi/T$), k is the wave number (= $2\pi/L$), T is the wave period, and L is the wave length.

Equation (3.2) is obtained by ignoring the transport of kinetic energy (kinetic part of the wave power), owing to approximation to a certain order of accuracy (Holthuijsen, 2010). However, in the presence of floating structures, the kinetic part of the wave power should be considered because their heaving behavior significantly affects the total transmitted power. Therefore, the kinetic part of the wave power together with the kinetic energy flux generated from the heaving oscillation of the floating structures increase the total transmitted power and hence, the transmission coefficient. Therefore, the total incident wave power $P_{I.tot}$ comprises the kinetic part of the wave power $P_{I.1}$ in

`

addition to the wave-induced pressure part $P_{I.2}$.

Part of these two wave powers is transmitted from beneath the floating structure draft D to the lee side (Figure 3.1(a)). The transmitted part includes the kinetic energy contribution to the wave power $P_{T.1}$ and the induced pressure energy contribution ($P_{T.2}$). In addition to $P_{T.1}$ and $P_{T.2}$, the kinetic energy flux per unit floating structure width resulting from the heaving motion of the floating structure ($P_{T.3}$) is transmitted in the x direction to the lee side. $P_{T.3}$ consists of two contributions: the kinetic energy flux of the heaving body of the floating structure and the kinetic energy flux of the hydrodynamic mass that accelerates simultaneously with the floating body.

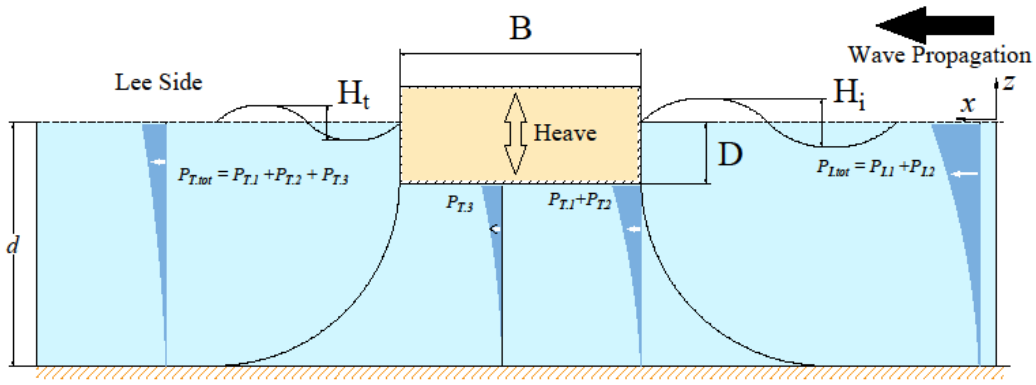

(a)

`

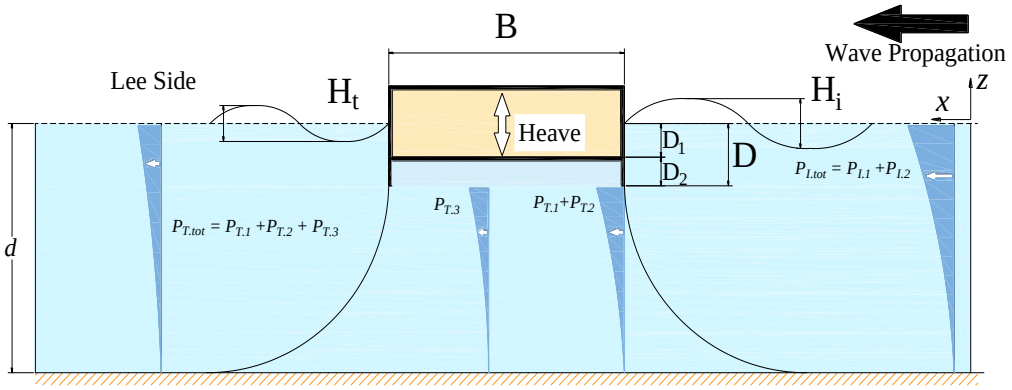

(b)

Figure 3.1: Wave transmission process for (a) box-type floating structures (b) π-shaped floating structures.

The transmitted wave (at the lee side of the floating structure) carries a total power that equals the total transmitted power ($P_{T.tot} = P_{T.1} + P_{T.2} + P_{T.3}$). The transmitted wave becomes the incident wave toward the coastline with a height of H_t, which is attained after attenuation of the seaside incident wave. The leeside incident wave carries a total power $P_{L.S}$ that comprises the wave-induced pressure and kinetic parts of wave power. $P_{L.S}$ is a function of H_t, and once the value of $P_{L.S}$ is found (i.e., $P_{L.S} = P_{T.tot}$), the value of H_t can be obtained and the transmission coefficient K_t can be calculated using Eq. (3.1).

3.2 Wave Energy

The presence of a wave at the water surface indicates that water particles have been motivated to move from their position at rest to some other position. To change the position of these particles, a work done against gravitation is required and this work represents potential energy (E_{po}). Moreover, the movement of water particles represents kinetic energy (E_k). To estimate the potential energy, a slice of water with thickness Δz in a column with horizontal surface area $\Delta x\, \Delta y$ is considered (see Figure 3.2).

`

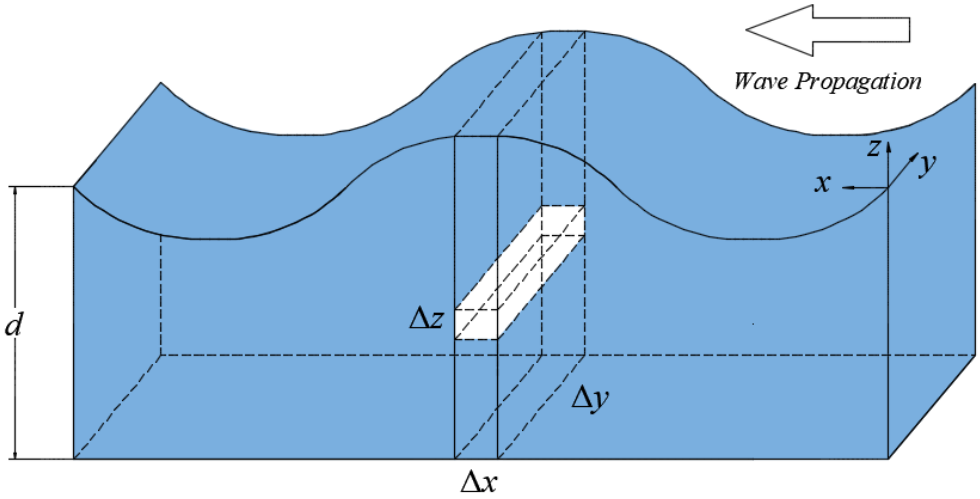

Figure 3.2: Column in a harmonic wave.

The instantaneous potential energy (i.e., mass × elevation, at a given moment in time) of this slice of water, relative to $z = 0$, is $\rho g z\, \Delta x\, \Delta y\, \Delta z$. The corresponding wave-induced potential energy in the entire column, from bottom to surface, is equal to the potential energy in the presence of the wave minus the potential energy in the absence of the wave. Per unit horizontal surface area (divide by the horizontal surface area of the column $\Delta x\, \Delta y$) and time-averaged over one period (represented by overbar), and for wave with amplitude $a = H/2$, the potential energy (E_{po}) is

$$E_{\mathrm{po}} = \overline{\int_{-d}^{\eta} \rho g z\, dz} - \overline{\int_{-d}^{0} \rho g z\, dz} = \overline{\int_{0}^{\eta} \rho g z\, dz} = \overline{\frac{1}{2}\rho g \eta^2} = \frac{1}{4}\rho g a^2 = \frac{1}{16}\rho g H^2 \tag{3.3}$$

where η is the displacement of water surface relative to still water level.

The instantaneous kinetic energy in the same slice of water as above (i.e., ½ ×mass ×velocity squared, at a given moment in time) is $\frac{1}{2}\, \rho\, \Delta x\, \Delta y\, \Delta z\, u^2$ (with $u^2 = u^2_x + u^2_z$).

`

Where u_x and u_z are the orbital particle velocity components in x and z directions respectively and can be obtained from cosine surface profile linear wave theory as

$$u_x = \omega \frac{H}{2} \frac{cosh(k(z+d))}{sinh(kd)} \cos(kx - \omega t) \tag{3.4}$$

$$u_z = \omega \frac{H}{2} \frac{sinh(k(z+d))}{sinh(kd)} \sin(kx - \omega t) \tag{3.5}$$

The corresponding time-averaged (over one period) kinetic energy (E_k) in the entire column, from bottom to surface, is then, per unit surface area, can be calculated as

$$E_k = \overline{\int_{-d}^{\eta} \frac{1}{2} \rho u^2 \, dz} \approx \int_{-d}^{0} \frac{1}{2} \rho u^2 \, dz \tag{3.6}$$

Substituting the orbital velocity terms from Eq. (3.4) and Eq. (3.5) in ($u^2 = u^2_x + u^2_z$) gives

$$E_k = \frac{1}{2} \rho \int_{-d}^{0} \left[\left(\omega \frac{H}{2} \frac{cosh(k(z+d))}{sinh(kd)} \cos(kx - \omega t) \right)^2 + \left(\omega \frac{H}{2} \frac{sinh(k(z+d))}{sinh(kd)} \sin(kx - \omega t) \right)^2 \right] dz \tag{3.7}$$

Recalling that $cosh\, x\, sinh\, x = \frac{1}{2} sinh\, 2x$ and simplifying the hyperbolic functions yields

$$E_k = \frac{1}{2} \rho \omega^2 \frac{H^2}{8} \frac{1}{sinh^2(kd)} \int_{-d}^{0} [(\, cosh(2k(z+d)))] \, dz \tag{3.8}$$

Solving the integration:

$$E_k = \frac{1}{2} \rho \omega^2 \frac{H^2}{8} \frac{1}{sinh^2(kd)} \left[\frac{\sinh\big(2k(z+d)\big)}{2k} \right]_{-d}^{0} \tag{3.9}$$

Inserting the integration limits gives:

`

$$E_k = \frac{1}{2}\,\rho\omega^2\,\frac{H^2}{8}\,\frac{1}{sinh^2(kd)}\left(\frac{\sinh(2kd)}{2k}\right) \tag{3.10}$$

Using the dispersion relationship $\omega^2 = gk\tanh(kd)$ gives

$$E_{\mathrm{k}} = \frac{1}{2}\,\rho\,g\,\frac{H^2}{8}\,\frac{\tanh(kd)}{2sinh^2(kd)}\,(\sinh(2kd)) \tag{3.11}$$

Now, simplifying the functions of $tanh\,x = \frac{sinh\,x}{cosh\,x}$ and $cosh\,x\,sinh\,x = \frac{1}{2}sinh\,2x$ results in the final form of the wave kinetic energy as

$$E_k = \frac{1}{4}\,\rho g a^2 = \frac{1}{16}\,\rho\,gH^2 \tag{3.12}$$

Therefore, the total wave energy (E), which is equal to the summation of the wave potential energy (E_{po}) and the wave kinetic energy (E_k), is given as

$$E = E_{po} + E_k = \frac{1}{16}\,\rho\,gH^2 + \frac{1}{16}\,\rho\,gH^2 = \frac{1}{8}\,\rho\,gH^2 \tag{3.13}$$

3.3 Incident Wave Power (Energy Transport) (Energy Flux)

As the waves propagate across the water's surface, they carry potential and kinetic energies. The rate at which energy is transported in the direction of wave propagation across a vertical plane perpendicular to the direction of wave advancement and extending downward to the maximum depth is called energy flux (or, frequently, wave power). To estimate the flux of these energies, consider the right-hand vertical side of the slice of water in the column (a window with cross-section $\Delta z\,\Delta y$; Figure. 3.3).

`

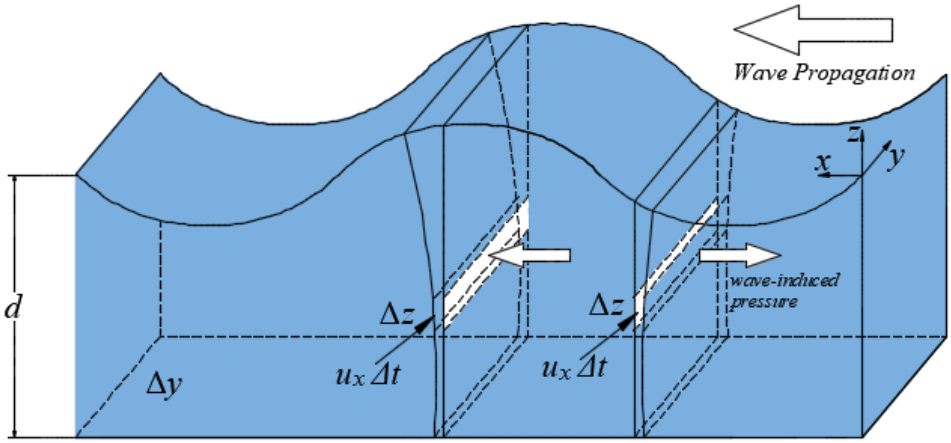

Figure 3.3: Horizontal flux of the wave energy.

The physical flux of potential energy ρgz through that slice in the x-direction (with the water particles, and therefore, with velocity u_x) in time interval Δt is given as $(\rho gz)u_x \Delta z \Delta y \Delta t$. Over the entire depth, from the bottom to the surface, this energy flux (power) is calculated as

$$P_{po} = \left(\int_{-d}^{\eta} (\rho gz) u_x \, dz \right) \Delta y \Delta t \tag{3.14}$$

Similarly, the physical flux of the kinetic energy, that is, $0.5\ \rho u^2$, integrated over the entire depth, is calculated as

$$P_k = \left(\int_{-d}^{\eta} \left(\frac{1}{2} \rho \, u^2 \right) u_x \, dz \right) \Delta y \Delta t \tag{3.15}$$

In addition to the physical flux of the potential and kinetic energies, energy is also transported horizontally by the work done through the pressure in the direction of wave propagation. This horizontal flux through a vertical plane in time interval Δt is equal to the pressure, p_{wave} multiplied by the distance moved in that interval (in the x-direction; $u_x \Delta t$). By integrating from the bottom to surface, the wave energy transported horizontally by the work done through pressure is written as

`

$$P_{pr} = \left(\int_{-d}^{\eta} (pu_x)\ dz \right) \Delta y \Delta t \tag{3.16}$$

where $p = -\rho g z + p_{wave}$ and p_{wave} is the wave-induced pressure which can be obtained from linear wave theory as

$$p_{wave} = \rho g\ \frac{H}{2} \frac{\cosh(k(d+z))}{\cosh(kd)} \sin(\omega t - kx) \tag{3.17}$$

The total energy flux or total incident wave power $P_{I.tot}$ per unit crest length and per unit time (i.e., divided by $\Delta y\ \Delta t$) and time-averaged can be written as the sum of the three contributions as

$$P_{I.tot} = \overline{P_{po}} + \overline{P_k} + \overline{P_{pr}} \tag{3.18}$$

The time-averaged energy fluxes given in Eq. (3.18) were evaluated by Dean and Dalrymple (1991) and Holthuijsen (2010), and can be estimated as

$$P_{I.tot} = \overline{\int_{-d}^{\eta} (\rho g z) u_x\ dz} + \overline{\int_{-d}^{\eta} \left(\frac{1}{2}\ \rho\ u^2\right) u_x\ dz} + \overline{\int_{-d}^{\eta} (-\rho g z + p_{wave})\, u_x\, dz} \tag{3.19}$$

The potential part of the wave power ($\rho g z.\ u_x$) given by the first term on the right-hand side of Eq. (3.19) cancels out the hydrostatic pressure ($-\rho g z.\ u_x$) given by the third term. The wave-induced pressure p_{wave} is in phase with the horizontal orbital motion and the surface elevation (Figure 3.3). If the water particles move in the wave direction, the surface elevation is higher than when the water particles move against the wave direction. Therefore, the net time-averaged effect is an energy flux in the wave direction (Holthuijsen, 2010).

For most applications of linear wave theory, the second term of the right-hand side of Eq. (3.19) is ignored as the integration is limited to a second-order approximation and

`

the kinetic part of the wave energy flux is of third order. Nevertheless, this study considered this part of the wave power because it is expected to substantially increase the magnitude of the total transmitted wave power when added under the structure to the kinetic energy flux owing to the heaving behavior of the floating body. This expectation is based on the fact that the floating structures investigated in this research (i.e., FBs and WECs) are usually installed in deep water and facing large amplitude waves. Under such conditions, the FBs are needed to attenuate the wave impact and the WECs are installed to capture more wave energy. The wave kinetic energy transport is associated with the wave amplitude which as it increases a higher magnitude of the wave energy transport obtained (Alamailes and Türker, 2019).

Therefore, the total incident wave power can be evaluated as

$$P_{I.tot} = \overline{\int_{-d}^{\eta} \left(\frac{1}{2}\,\rho\, u^2\right) u_x \; dz} + \overline{\int_{-d}^{\eta} (p_{wave})\, u_x \, dz} \tag{3.20}$$

Based on the assumptions of linear wave theory, integration from the seabed to the still water level results in the final form of the total incident wave power as

$$P_{I.tot} = \overline{\int_{-d}^{0} \left(\frac{1}{2}\,\rho\, u^2\right) u_x \; dz} + \overline{\int_{-d}^{0} (p_{wave})\, u_x \, dz} \;\; = P_{I.1} + \; P_{I.2} \tag{3.21}$$

The derivation of each part of Eq. (3.21) separately, according to linear wave theory, yields

$$P_{I.1} = \int_{-d}^{0} \left[\begin{array}{c} \dfrac{H\;\omega\;\;\rho \cos(kx-\omega t)\;\; cosh\big(k(z+d)\big)}{4\sinh(kd)} \\ \left(\dfrac{H^2\omega^2 sin^2(kx-\omega t)\; sinh^2\big(k(z+d)\big)}{4sinh^2(kd)} \right. \\ \left. + \dfrac{H^2\omega^2 cos^2(kx-\omega t)\; cosh^2\big(k(z+d)\big)}{4sinh^2(kd)} \right) \end{array} \right] dz \tag{3.22}$$

Applying linearity gives

`

$$P_{I.1} = \frac{\rho H^3 \omega^3 cos(kx-\omega t)}{16 sinh^3(kd)} \int_{-d}^{0} \Big[cosh\big(k(z+d)\big) \begin{pmatrix} sin^2(kx-\omega t)\, sinh^2\big(k(z+d)\big) \\ +cos^2(kx-\omega t)\, cosh^2\big(k(z+d)\big) \end{pmatrix} \Big] dz \quad (3.23)$$

Simplifying sums of squares of trigonometric/hyperbolic functions:

$$P_{I.1} = \frac{\rho H^3 \omega^3 cos(kx-\omega t)}{16 sinh^3(kd)} \int_{-d}^{0} \Big[cosh\big(k(z+d)\big) \Big(\big(sin^2(kx-\omega t) + cos^2(kx-\omega t) \big) sinh^2\big(k(z+d)\big) + cos^2(kx-\omega t) \Big) \Big] dz \quad (3.24)$$

By recalling that $\big(sin^2(kx-\omega t) + cos^2(kx-\omega t)\big) = 1$, a further simplified arrangement is obtained as

$$P_{I.1} = \frac{\rho H^3 \omega^3 cos(kx-\omega t)}{16 sinh^3(kd)} \int_{-d}^{0} cosh\big(k(z+d)\big) \Big(sinh^2\big(k(z+d)\big) + cos^2(kx-\omega t) \Big) dz \quad (3.25)$$

Now solving the integration

$$\int_{-d}^{0} cosh\big(k(z+d)\big) \Big(sinh^2\big(k(z+d)\big) + cos^2(kx-\omega t) \Big) dz \quad (3.26)$$

substituting $u = k(z+d) \rightarrow dz = \frac{1}{k}\, du$

$$\frac{1}{k} \int_{-d}^{0} cosh(u) \big(sinh^2(u) + cos^2(kx-\omega t) \big) du \quad (3.27)$$

Now solving

$$\int_{-d}^{0} cosh(u) \big(sinh^2(u) + cos^2(kx-\omega t) \big) du \quad (3.28)$$

`

substituting $v = \sinh(u) \rightarrow du = \frac{1}{\cosh(u)}\, dv$

$$\int_{-d}^{0} \left(v^2 + cos^2(kx - \omega t) \right)\ dv$$

$$= \int_{-d}^{0} v^2 dv + cos^2(kx - \omega t) \int_{-d}^{0} 1\, dv \qquad (3.29)$$

$$= \left[\frac{v^3}{3} + cos^2(kx - \omega t) v \right]_{-d}^{0}$$

Undo substituting $v = \sinh(u)$ gives

$$\int_{-d}^{0} \left(cosh(u) \left(sinh^2(u) + cos^2(kx - \omega t) \right) \right)\ du$$

$$= \left[\frac{sinh^3(u)}{3} + cos^2(kx - \omega t) \sinh(u) \right]_{-d}^{0} \qquad (3.30)$$

Inserting solved integrals and undo substituting *u = k (z +d)* yields

$$\frac{1}{k} \int_{-d}^{0} cosh(u) \left(sinh^2(u) + cos^2(kx - \omega t) \right) du \qquad (3.31)$$

$$= \left[\frac{sinh^3(k(z+d))}{3k} + \frac{cos^2(kx - \omega t) \sinh(k(z+d))}{k} \right]_{-d}^{0}$$

Similarly,

$$\frac{\rho H^3 \omega^3 cos(kx - \omega t)}{16 sinh^3(kd)} \int_{-d}^{0} cosh\big(k(z + d)\big) \left(sinh^2\big(k(z+d)\big) + cos^2(kx - \omega t) \right) dz \qquad (3.32)$$

$$= \left[\frac{\rho H^3 \omega^3 cos(kx - \omega t)\ sinh^3\big(k(z+d)\big)}{48\ k\ sinh^3(kd)} + \frac{\rho H^3 \omega^3 cos^3(kx - \omega t)\ sinh\big(k(z+d)\big)}{16\ k\ sinh^3(kd)} \right]_{-d}^{0}$$

The displacement of the water surface relative to still water level is $\eta =$

`

$\frac{H}{2}\cos(kx-\omega t)$. Therefore, rewriting Eq. (3.32) by replacing the displacement as time-varying function $|\eta| = \frac{H}{2}$ and by substituting ω^2 with $gk\tanh(kd)$, based on the dispersion relation, results in

$$P_{I.1} = \frac{\rho\, gH^3\omega}{48}\left[\frac{\tanh(kd)\sinh\big(k(d+z)\big)\big(sinh^2\big(k(d+z)\big)+3\big)}{sinh^3(kd)}\right]_{-d}^{0} \tag{3.33}$$

By plugging-in the integration limits and simplifying the hyperbolic functions, the last form of the kinetic part of the wave power is obtained as

$$P_{I.1} = \frac{\rho g H^3\,\omega}{24}\left(\frac{(sinh^2(kd)+3)}{\sinh(2kd)}\right) \tag{3.34}$$

For the second part of Eq. (3.21), the wave velocity in the *x*-direction u_x and the wave-induced pressure p_{wave} can be obtained from Eq. (3.4) and (3.17) respectively and substituted in second part of Eq. (3.21) as

$$P_{I.2} = \int_{-d}^{0}\left[\rho g\,\eta\,\frac{\cosh(k(z+d))}{\cosh(kd)}\right]\left[\omega\;\eta\;\frac{\cosh(k(z+d))}{\sinh(kd)}\right]dz \tag{3.35}$$

Applying linearity gives

$$P_{I.2} = \quad \frac{\rho g\omega\,\eta^2}{\cosh(kd)\sinh(kd)}\int_{-d}^{0} cosh^2\big(k(z+d)\big)dz \tag{3.36}$$

Now solving the integration

$$\int_{-d}^{0} cosh^2\big(k(z+d)\big)dz \tag{3.37}$$

substituting $u = k(z+d) \rightarrow dz = \frac{1}{k}\,du$ and solving

$$\frac{1}{k}\int_{-d}^{0} cosh^2(u)\;du = \left[\frac{1}{4}\sinh(2u)+\frac{u}{2}\right]_{-d}^{0} \tag{3.38}$$

Undo substituting $u = k\,(z+d)$ yields

`

$$P_{I.2} = \frac{\rho g \omega \, \eta^2}{\cosh(kd)\sinh(kd)} \left[\frac{1}{4}\sinh(2k(z+d) + \frac{k(z+d)}{2}\right]_{-d}^{0} \tag{3.39}$$

Replacing the time-varying function $|\eta| = \frac{H}{2}$ and plugging-in the integration limits with simplified hyperbolic functions, the last form of the induced pressure part of the wave power is obtained as

$$P_{I.2} = \frac{1}{16}\,\rho\, g H^2 \left[1 + \frac{2kd}{\sinh(2kd)}\right]\frac{\omega}{k} \tag{3.40}$$

It can be observed that the induced pressure part of the wave power in Eq. (3.40) is the same as the well-known formula that has been given in Eq. (3.2)

From the previous derivations, the total incident wave power is (Alamailes and Türker, 2019)

$$\begin{aligned} P_{I.tot} &= P_{I.1} + P_{I.2} \\ &= \frac{\rho g H^3\, \omega}{24}\left(\frac{(sinh^2(kd)+3)}{\sinh(2kd)}\right) \\ &+ \frac{\rho\, g H^2 \omega}{16k}\left[1 + \frac{2kd}{\sinh(2kd)}\right] \end{aligned} \tag{3.41}$$

The first part of Eq. (3.41) shows that $P_{I.1}$ is in third order of the wave amplitude. This makes this part negligible comparing to the second part ($P_{I.2}$) for waves with small amplitudes. However, this study suggests to take $P_{I.1}$ in consideration since in the typical wave conditions, under which the FBs and WECs usually installed, the wave amplitudes are relatively large and the water is deep. In these conditions, the linear wave theory is still applicable and $P_{I.1}$ magnitude fairly increases. For instance, in the North Sea the wave height reaches 5 m (Kramer and Frigaard, 2002; Goggins and Finnegan, 2014) and if considering H = 4 m in deep water (i.e., d = 50 m and T = 7 sec), $P_{I.1}$ will form about 10% of the total wave power (See Figure 3.4).

`

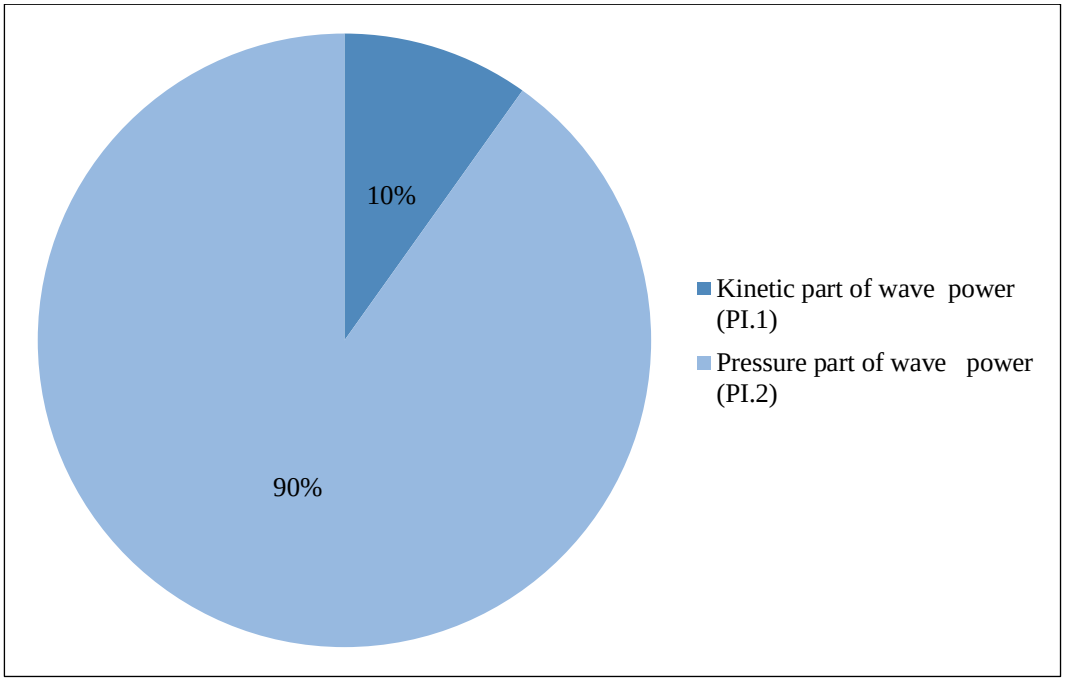

Figure 3.4: The percentages of the kinetic and induced pressure parts of the wave energy in the North Sea when the wave height is 4 m.

This amount should not be ignored when evaluating the transmitted wave power and hence K_t, and should be counted in when estimating the wave power for energy production especially when waves are propagating with significant heights (See Figure 3.5).

`

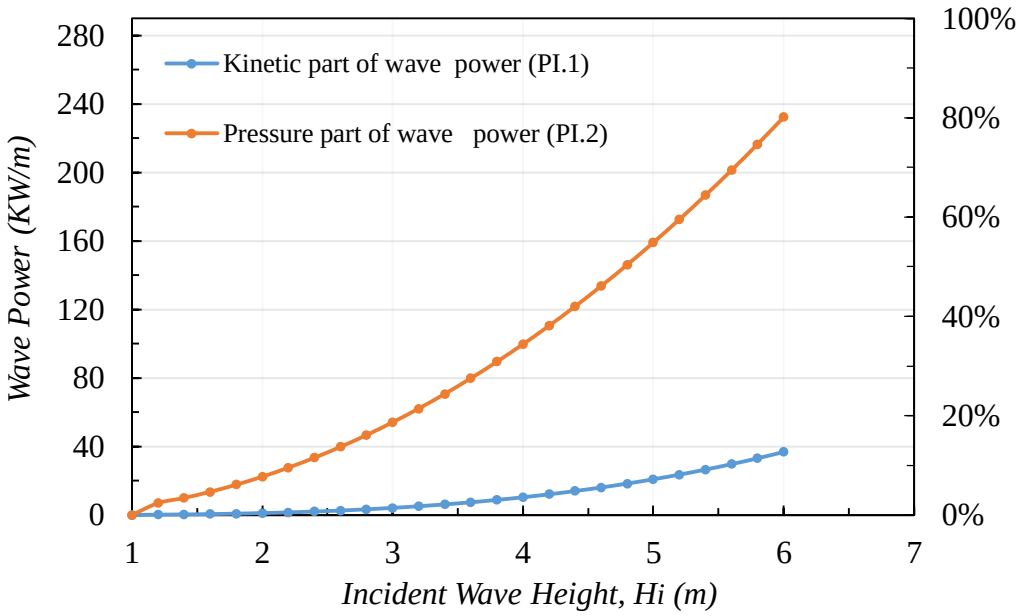

Figure 3.5: Change in the induced pressure and kinetic part of wave power with respect to the change in the incident wave height.

3.4 Transmitted Wave Power

The transmitted wave power depends basically on the portion of incident wave power that is transmitted to the leeside underneath the floating structure when the overtopping is ignored. In this study, the approach is generalized for different structures with various dimensions assuming that the freeboard is sufficiently high to prevent the occurrence of overtopping. For both investigated types of floating structures (Box and π-shaped), part of total incident wave power (with the incident pressure and kinetic energy contributions) is transmitted between the draft of the structure and the seabed. In addition, the transmitted wave power includes the horizontal transport of the kinetic energy that is generated by the heaving oscillation of the floating structure.

3.4.1 Transmitted Wave Kinetic Energy flux

The wave kinetic energy contribution to the transmitted wave power ($P_{T.1}$) can be obtained as by integrating the horizontal flux of the kinetic energy from the draft of the floating structure -*D* to the seabed -*d* as

`

$$P_{T.1} = \int_{-d}^{-D} \left(\frac{1}{2}\,\rho\, u^2\right) u_x \; dz \tag{3.42}$$

This integration has been evaluated using the linear wave theory terms and the result is shown in Eq. (3.33). With the changed integration limits; however, the final form the wave kinetic energy contribution to the total transmitted wave power is

$$P_{T.1} = \frac{\rho g H^3 \omega}{48} \left[\frac{tanh(kd)\, sinh\big(k(d-D)\big)\left(sinh^2\big(k(d-D)\big)+3\right)}{sinh^3(kd)}\right] \tag{3.43}$$

3.4.2 Transmitted Wave-Induced Pressure Energy flux

Similarly, the wave-induced pressure contribution to the transmitted wave power can be obtain by integrating the horizontal flux of the wave-induced pressure energy from the draft of the floating structure -*D* to the seabed –*d* as

$$P_{T.2} = \int_{-d}^{-D} (p_{wave})\, u_x \, dz \tag{3.44}$$

This integration has also been evaluated using the linear wave theory terms and the result is shown in Eq. (3.39). With the changed integration limits; however, the final form the wave-induced pressure contribution to the total transmitted wave power is

$$P_{T.2} = \frac{\rho\, g H^2 \omega}{16k} \left[\frac{(sinh(2k(d-D)) + 2k(d-D)}{sinh(2kd)}\right] \tag{3.45}$$

3.4.3 Floating Structure Mass and Hydrodynamic Mass Kinetic Energy Flux

Kinetic energy flux $P_{T.3}$ (per unit width of the floating structure) that is produced by the heaving oscillation of the floating structure increases the magnitude of the transmitted wave power. It consists of two parts: (i) the kinetic energy flux from the heaving body of the floating structure and (ii) the kinetic energy flux from the hydrodynamic mass that accelerates simultaneously with the floating body.

`

The added mass is defined as the fluid mass that accelerates along with the floating structure. Therefore, this additional mass must be accounted for when the structure mass is considered.

For the heaving motion, Ruol et al. (2013) estimated the hydrodynamic mass M_h as the volume of water under the floating structure, where the volume boundary is described by a semicircle with a radius equal to half the width B of the structure in case of Box-type floating structures. However, in case of the π-shaped floating structures, the water trapped between the structure's appearing side plates is considered as a part of the hydrodynamic mass. This estimation was made assuming that the buoyancy force is the only vertical force considered when calculating the moorings' stiffness. The body mass M_b is equal to the mass of the displaced water, so the total estimated mass may be evaluated as the sum of M_b and M_h, as shown in Figure 3.6.

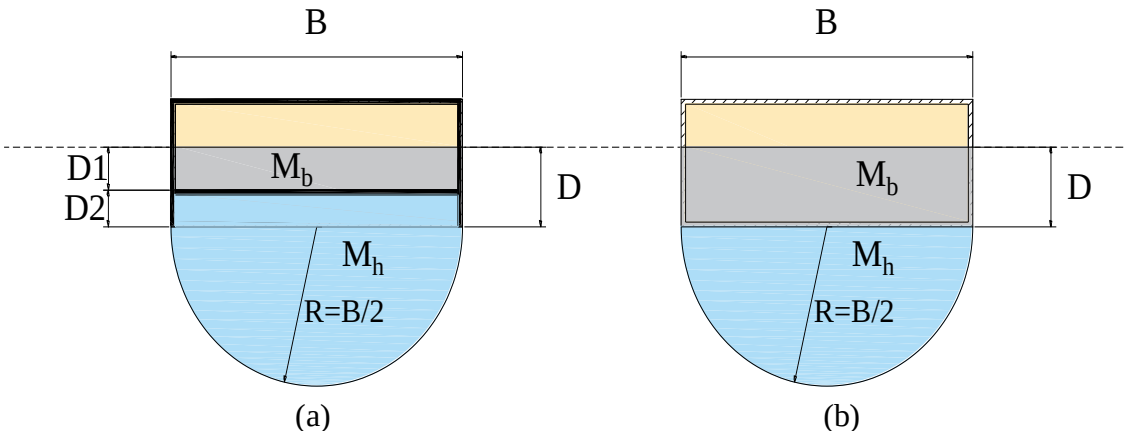

Figure 3.6: The estimated hydrodynamic mass for (a) π-shaped floating structure (b) box-type floating structure (modified from Roul et al., 2013).

According to Figure (3.6), per unit body length, the body mass M_b can be obtained using Archimedes' principle and the hydrodynamic mass M_b can be obtained by multiplying the area with the water density (ρ) as

`

For Box-type

$$M_b = \rho\, BD \tag{3.46}$$

$$M_h = \rho\, \frac{\pi}{8} B^2 \tag{3.47}$$

For the π-shaped

$$M_b = \rho\, BD_1 \tag{3.48}$$

$$M_h = \rho\, \frac{\pi}{8} B^2 + \rho\, BD_2 \tag{3.49}$$

When estimating the kinetic energy flux (per unit structure width) resulting from the total accelerating mass, the shape of the added mass should be reconsidered to simplify the calculation.

The added mass can be considered to be rectangular and can be fitted within the body width B and extended toward the seabed at depth δ (see Figure. 3.7).The cross-sectional area of the rectangular shape should be equal to the cross-sectional area of the semicircular shape. Such an arrangement provides equivalent added masses for both shapes.

`

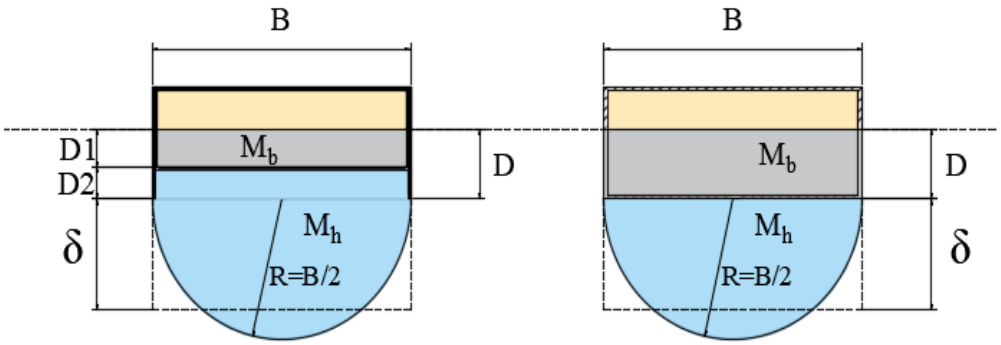

(a) (b)

Figure 3.7: Simplified shape of the added mass for (a) π-shaped floating structure (b) box-type floating structure.

The equivalence of the masses can be achieved when the depth $\delta = (\pi/8) \times B$. Then, the hydrodynamic mass becomes

For Box-type

$$M_h = \rho\, B\, \delta \tag{3.50}$$

For the π-shaped

$$M_h = \rho\, B(D_2 + \delta) \tag{3.51}$$

The kinetic energy flux generated by the structure's body (per unit body length) can be obtained by integrating $(0.5M_b \times u^2)\, u_x$ from the still water level to the structure draft $-D$. Meanwhile, the kinetic energy flux generated by the hydrodynamic mass can be obtained by integrating $(0.5M_h \times u^2)\, u_x$ from $-D$ to $-(D+\delta)$ for the box-type and from $-D_1$ to $-(D_1 + D_2 + \delta)$ for the π-shaped floating structure. The integrations are averaged over a wave period and per unit structure width as

`

For Box-type

$$P_{T.3} = \int_{-D}^{0} (\frac{1}{2}\rho\, u^2)\, u_x\, dz + \int_{-(D+\delta)}^{-D} (\frac{1}{2}\rho\, u^2)\, u_x\, dz \tag{3.52}$$

For the π-shaped

$$P_{T.3} = \int_{-D_1}^{0} (\frac{1}{2}\rho\, u^2)\, u_x\, dz + \int_{-D_2}^{-D_1} (\frac{1}{2}\rho\, u^2)\, u_x\, dz + \int_{-(D_1+D_2+\delta)}^{-D_2} (\frac{1}{2}\rho\, u^2)\, u_x\, dz \tag{3.53}$$

As the floating structure approaches the seabed, the hydrodynamic mass is apparently influenced by the close juxtaposition of the wall. Yamamoto et al. (1974) investigated the impact of the closeness of the seabed on the hydrodynamic mass of a cylinder, finding that, as the distance between the cylinder and seabed decreases, the hydrodynamic mass coefficient increases.

Therefore, Eq. (3.52) and Eq. (3.53) are only valid for cases with shallow drafts and deep water, when the effect of the seabed on the hydrodynamic mass is negligible. However, for deeper drafts or shallower water, a correction factor α should be introduced to reflect the change in the added mass owing to the effect of closeness to the seabed. Therefore, $P_{T.3}$ can be considered (per unit structure width) to be

For Box-type

$$P_{T.3} = \int_{-D}^{0} (\frac{1}{2}\rho\, u^2)\, u_x\, dz + \boldsymbol{\alpha} \int_{-(D+\delta)}^{-D} (\frac{1}{2}\rho\, u^2)\, u_x\, dz \tag{3.54}$$

`

For the π-shaped

$$P_{T.3} = \int_{-D_1}^{0} (\frac{1}{2}\rho\, u^2)\, u_x\, dz + \boldsymbol{\alpha}\left(\int_{-D_2}^{-D_1} (\frac{1}{2}\rho\, u^2)\, u_x\, dz + \int_{-(D_1+D_2+\delta)}^{-D_2} (\frac{1}{2}\rho\, u^2)\, u_x\, dz\right) \quad (3.55)$$

In a simplified form for π-shaped

$$P_{T.3} = \int_{-D_1}^{0} (\frac{1}{2}\rho\, u^2)\, u_x\, dz + \boldsymbol{\alpha} \int_{-(D_1+D_2+\delta)}^{-D_1} (\frac{1}{2}\rho\, u^2)\, u_x\, dz \quad (3.56)$$

This study ignores the effect of the closeness of the seabed on the added mass (i.e., α = 1), as the formula is generalized for the deep-water conditions in which FBs and floating WECs are usually installed. For shallow depths or deep drafts, the value of α increases.

When the floating body is large and is positioned at a depth less than or equal to its draft plus half of its width (i.e., $d \leq D + (B/2)$), the added mass can be assumed to be the mass trapped between the bottom of the structure and the seabed. However, under typical conditions (i.e., $d > D + (B/2)$), the added mass is extended to a depth of $\delta = (\pi/8)\, B$ (see Figure 3.7).

Thus, Eq. (3.54) and Eq. (3.56) are rewritten as

`

For Box-type

$$P_{T.3} = \int_{-(D+\delta)}^{-D} (\frac{1}{2}\rho\, u^2)\, u_x\, dz \tag{3.57}$$

For the π-shaped

$$P_{T.3} = \int_{-(D_1+D_2+\delta)}^{0} (\frac{1}{2}\rho\, u^2)\, u_x\, dz \tag{3.58}$$

The integration in Eq. (3.57) and Eq. (3.58) is similar to that in the first term on the right-hand side of Eq. (3.21). This integration has been evaluated using the linear wave theory terms and the result is shown in Eq. (3.33). With the changed integration limits; however, the contribution of the kinetic energy flux generated by the heaving oscillation to the total transmitted wave power is

For Box-type

$$P_{T.3} = \frac{\rho\, gH^3\omega}{48} \left[\frac{tanh(kd)\, sinh\big(k(d+z)\big)\left(sinh^2\big(k(d+z)\big)+3\right)}{sinh^3(kd)}\right]_{-(D+\delta)}^{0} \tag{3.59}$$

For the π-shaped

$$P_{T.3} = \frac{\rho\, gH^3\omega}{48} \left[\frac{tanh(kd)\, sinh\big(k(d+z)\big)\left(sinh^2\big(k(d+z)\big)+3\right)}{sinh^3(kd)}\right]_{-(D_1+D_2+\delta)}^{0} \tag{3.60}$$

From figure (3.7), it can be obtained that ($D_1 + D_2 = D$); therefore, Eq. (3.59) and Eq. (3.60) are presenting the same operation which delivers the transmitted kinetic energy flux generated by the heaving oscillation for both types of the floating structures (box-type and π-shaped).

Thus, plugging in the integration limits gives

`

$$P_{T.3} = \frac{\rho\, gH^3\omega}{48}\left[\left(\frac{(sinh^2(kd)+3)}{cosh(kd)\,sinh(kd)}\right) - \frac{tanh(kd)\,sinh(k(d-(D+\delta)))(sinh^2\left(k(d-(D+\delta))\right)+3)}{sinh^3(kd)}\right] \quad (3.61)$$

When $D + [(\pi/8)\, B]$ is less than the water depth d, then $\delta = [(\pi/8)\, B]$. In this case, $P_{T.3}$ is given by

$$P_{T.3} = \frac{\rho\, gH^3\omega}{48}\left[\left(\frac{(sinh^2(kd)+3)}{cosh(kd)\,sinh(kd)}\right) - \left(\frac{tanh(kd)\,sinh(k\left(d-D-\frac{\pi}{8}B\right)\,(sinh^2\left(k\left(d-D-\frac{\pi}{8}B\right)\right)+3)}{sinh^3(kd)}\right)\right] \quad (3.62)$$

In contrast, when $D + [(\pi/8)\, B]$ is greater than or equal to the water depth d, then $\delta = d\text{-}D$. In this case, $P_{T.3}$ is given by

$$P_{T.3} = \frac{EH\omega}{3}\left(\frac{(sinh^2(kd)+3)}{sinh(2kd)}\right) \quad (3.63)$$

3.4.4 Lee Side Wave Power

The total transmitted power obviously characterizes the wave power carried by a wave that passes the floating structure to the lee side. Naturally, the corresponding transmitted power $P_{T.tot}$ is equivalent to the incident wave power propagating toward the shore, $P_{L.S}$, which can be calculated by Eq. (3.41) as a function of transmitted wave height H_t. The magnitude of $P_{L.S}$ is obtained as (Alamailes and Türker, 2019)

$$P_{T.1} \times L + P_{T.2} \times L + P_{T.3} \times B = P_{T.tot} \times L = P_{L.S} \times L \quad (3.64)$$

Hence, $P_{L.S}$ is a cubic function of the transmitted wave height H_t. The cubic function

`

always has three roots and, in this study, the leeside wave power $P_{L.S}$ is always positive; therefore, there is always one real positive root for the equation, which is the resultant H_t. Once the value of H_t is obtained by solving Eq. (3.41), K_t can be calculated using Eq. (3.1).

`

Chapter 4

MODEL VALIDATION

This chapter presents an evaluation to the reliability and the validity of the proposed approach of this study. The analytical model is evaluated using laboratory data that were obtained from various experimental studies on different floating structures. First, two studies on the hydrodynamic performance of box-type FBs (Koutandos et al., 2005; Dong et al., 2008); second, two experimental studies on the hydrodynamic performance of two different WECs, wave dragon (Nørgaard and Andersen, 2012) and a pile-restrained WEC-style FB (Ning et al., 2016), both modeled as box shape; and finally, two experimental hydrodynamic performance on π-shaped FBs (Koutandos et al., 2005; Cox et al., 2007) are evaluated. In addition, earlier theoretical approaches from Macagno (1954), Kriebel and Bollmann (1996), and Ruol et al. (2013) were also considered using the same laboratory data and the results were compared with those of the approach proposed in this study.

4.1 Box-Type Floating Breakwater

Koutandos et al. (2005) and Dong et al. (2008) performed experimental studies to investigate the hydrodynamic performance of optimized FBs and compared them with box-type FBs. In these studies, the FBs were moored by slack moorings. Both studies were performed under regular wave conditions with varying wave properties (i.e., period and height).

`

4.1.1 Box-type Floating Breakwater with Heave Motion (Koutandos et al., 2005)

Koutandos et al. (2005) experimentally investigated four sets of floating breakwaters based on their configuration. One of these configuration was heave motion box-type FB which is compatible with the assumptions of the analytical proposed model of this study. The experiments took a place in the CIEM (Canal Investigació i Experimentació Marktima) flume at the Catalonia University of Technology, Spain. The flume is 100 m long, 3 m wide, and 4.5 m depth. The FB was positioned in the middle of the flume in 2 m water depth (Figure 4.1).

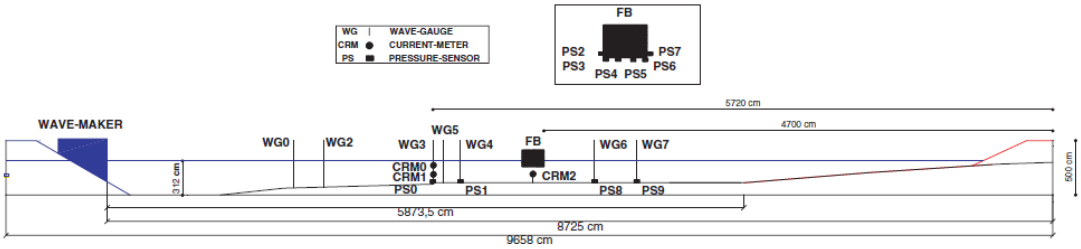

Figure 4.1: Dimensions of the CIEM Flume and the FB Position (Koutandos et al., 2005).

The FB physical model was restrained from all the oscillating motion but heave. Iron rails were installed on the flume walls to detain rotational and horizontal motions of the FB, while pneumatic wheels were attached on the structure to allow the free heaving motion (See Figure 4.2). The water depths and the details of the physical models employed in the study is summarized in Table 4.1.

Table 4.1: Box-type FB full-scale properties and regular wave conditions for experimental study of Koutandos et al. (2005).

Model Scale	Draft D (m)	Width B (m)	Incident Wave Height H_i (m)	Wave Period T (s)	Water depth d (m)
1:5	2	10	1	14.9, 12.4, 9.5, 7.5, 6.4, 5.4	10

`

Figure 4.2: Box-type FB with heave motion (Koutandos et al., 2005).

Figure. 4.3 compares the experimental and theoretical transmission coefficients. The curves show the relationship between the relative floating structure width B/L and the transmission coefficient K_t, as well as the relationship between the wave steepness H_i/L and K_t. In addition, the curves show the relationship between K_t and the relative wave period T/T_n, where T is the wave period and T_n is the natural period of the heave oscillation. This relation was proposed by Ruol et al. (2013) as in Eq (2.15).

As shown in Figure. 4.3, the proposed model is consistent with the experimental results of Koutandos et al. (2005), except when B/L = 0.19, at which point a sudden drop is observed in the experimental data, perhaps due to the natural period of the floating structure, which is ignored in theoretical approaches (Dong et al., 2008). Furthermore, better correlation can be observed at a small wave steepness H_i/L. The relationship

`

between K_t and the relative wave period T/T_n shows that the theoretical estimates deviate from the experimental measurement when the wave period becomes closer to the heave natural period. Generally, the theoretical results obtained from this study and those obtained by Kriebel and Bollmann (1996) give the best estimation for K_t compared with the experimental results, whereas the models from Macagno (1954) and Ruol et al. (2013) overestimate K_t.

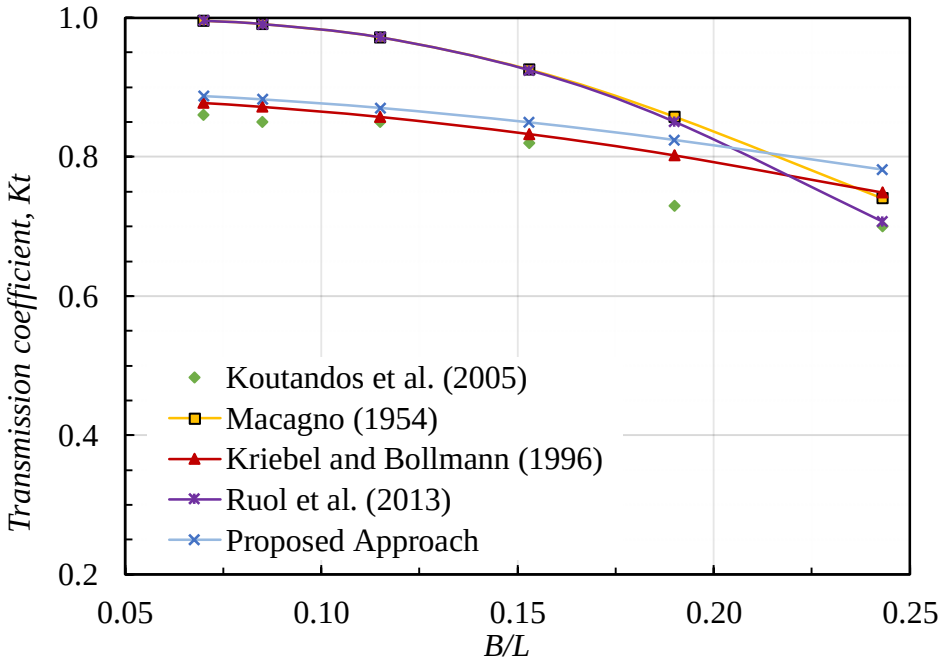

(a)

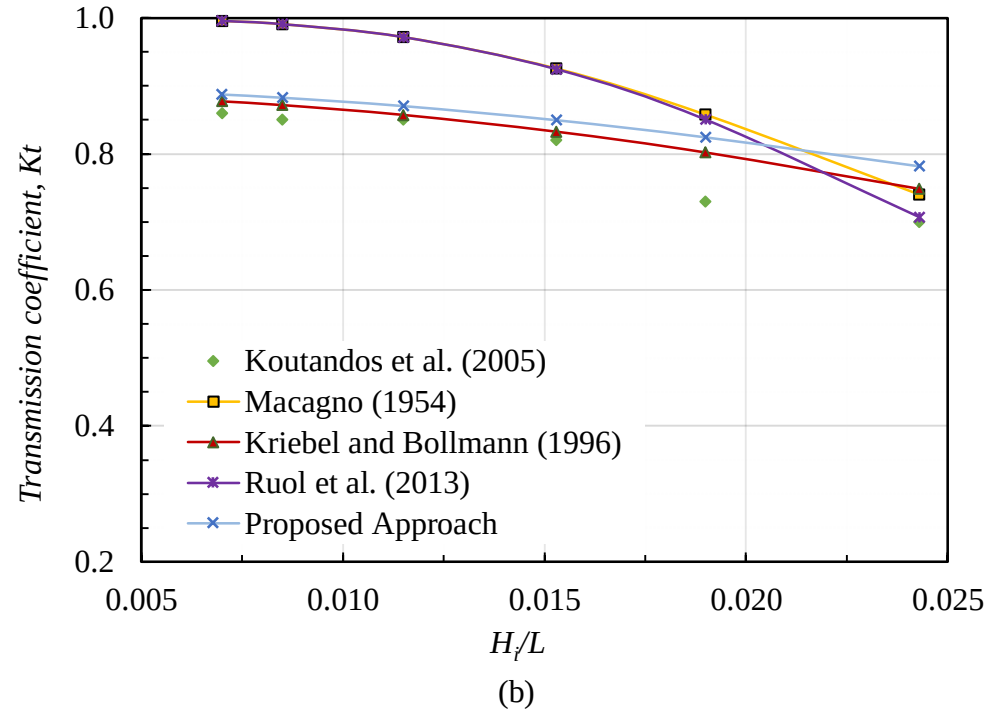

(b)

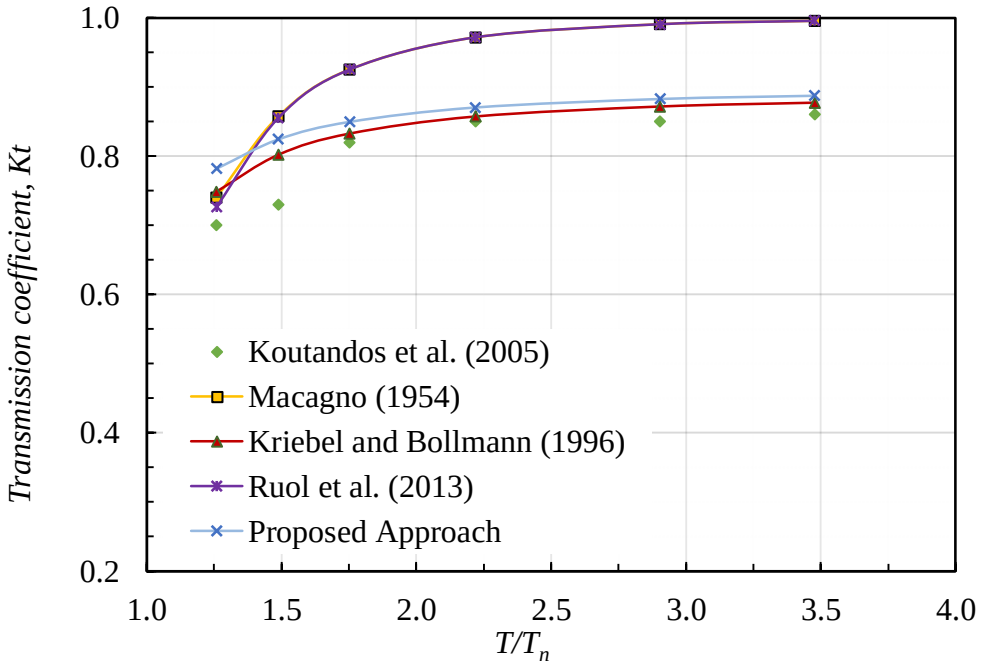

(c)

Figure 4.3: Change in the transmission coefficient of box-type FB with respect to (a) relative structure width B/L, (b) wave steepness H_i/L, and (c) relative wave period (T/T_n). The figure compares experimental results from Koutandos et al. (2005) with the outcomes of different theoretical approaches.

`

4.1.2 Box-type FB with Slack Mooring Chains (Dong et al., 2008)

Dong et al. (2008) experimentally investigated three types of floating breakwater and one of these types was the regular box-type. Two mooring systems were examined to evaluate the effect of the degree of tightness of the mooring chain. Since the analytical approach of the present study assuming free heaving motion, the slacker configuration of the physical model of Dong et al. (2008) for box-type FB is selected for model validation. The experiments of Dong et al. (2008) were conducted in the wave flume that is 50 m long, 3 m wide, and 1 m depth (see Figure 4.4).

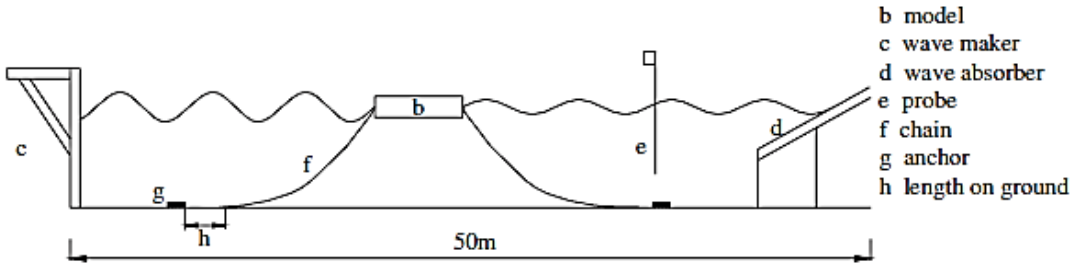

Figure 4.4: The experimental wave flume (Dong et al., 2008).

The experiments took a place at the State Key Laboratory of Coastal and Offshore Engineering, Dalian University of Technology, China. The water depth and the details of the physical models employed in the experiments is summarized in Table 4.2.

Table 4.2: Box-type FB full-scale properties and regular wave conditions for experimental study of Dong et al. (2008).

Model Scale	Draft D (m)	Width B (m)	Incident Wave Height H_i (m)	Wave Period T (s)	Water depth d (m)
1:40	4	20	2.5	6, 7, 8, 9, 10	20

The results plotted in Figure 4.5 include laboratory data from Dong et al. (2008) and theoretical data obtained from Macagno (1954), Kriebel and Bollmann (1996), Ruol

`

et al. (2013), and the present research.

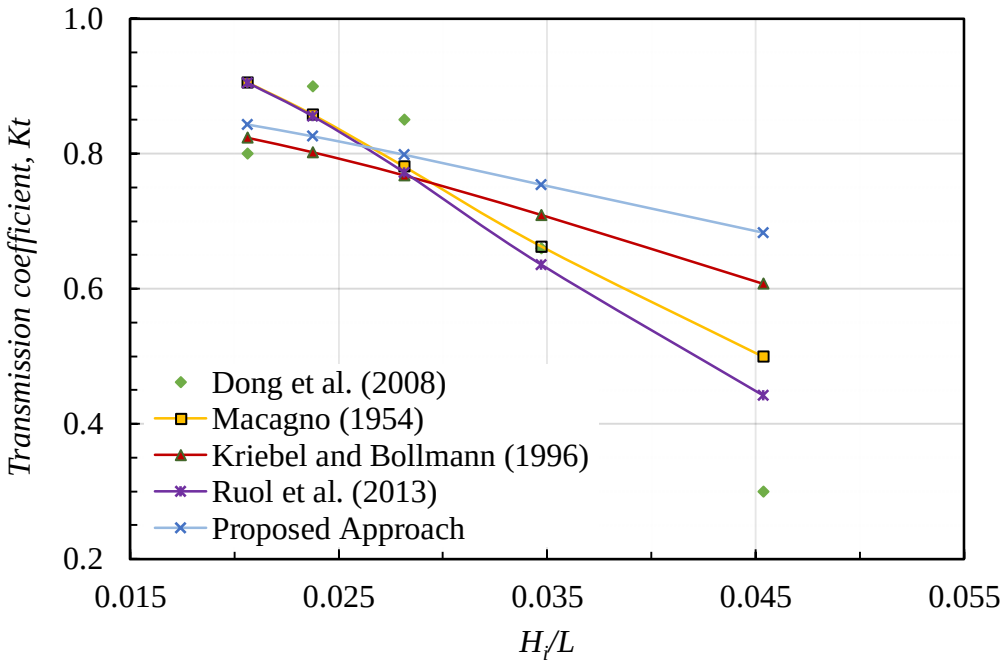

(a)

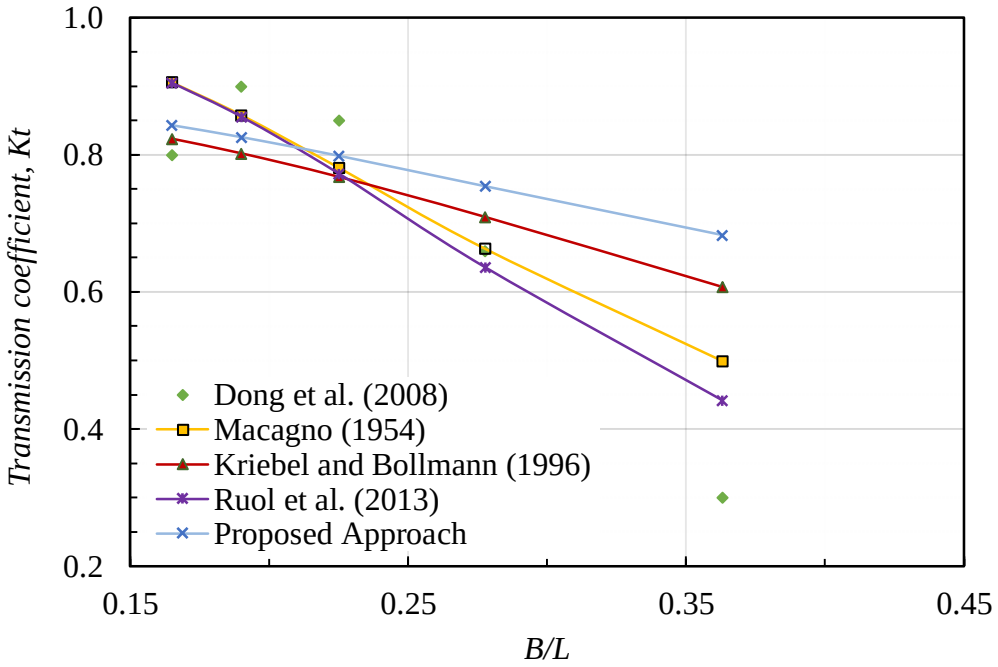

(b)

`

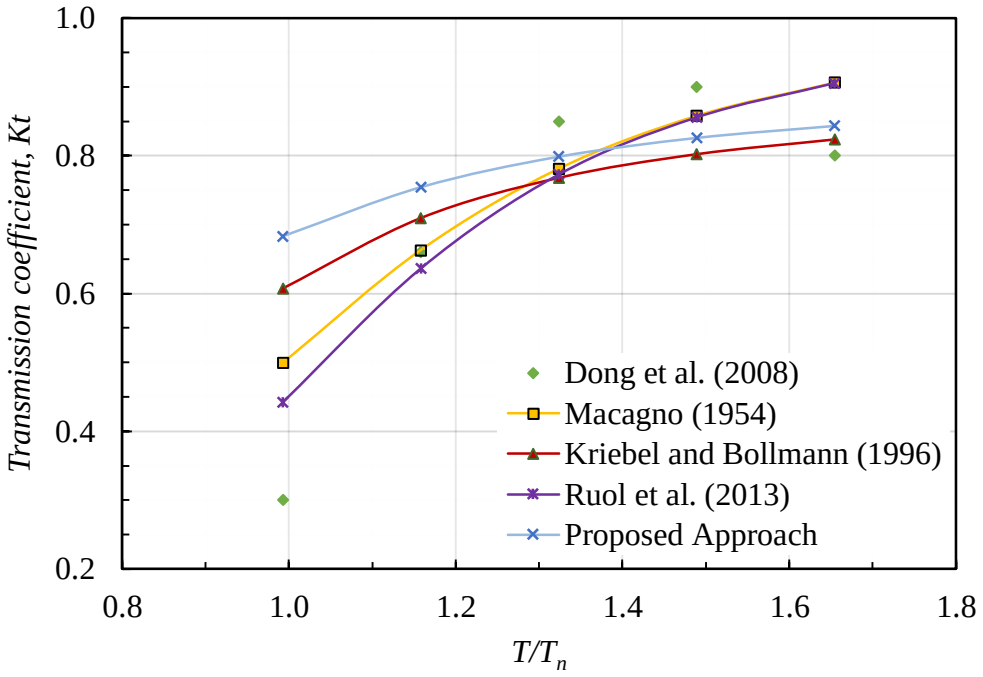

(c)

Figure 4.5: Change in the transmission coefficient with respect to (a) relative structure width B/L, (b) incident wave steepness H_i/L, and (c) relative wave period (T/T_n). The figure compares experimental results from Dong et al. (2008) with the outcomes of different theoretical approaches.

Overall, the proposed approach slightly underestimates K_t when B/L = 0.19. However, for 0.20 < B/L < 0.30, this approach estimates K_t well. Beyond the limit of B/L = 0.30, the proposed model overestimates K_t, and as B/L increases, the gap between the experimental and the theoretical data increases. In addition, the present method overestimates K_t as the wave steepness H_i/L increases, which can be explained by the research's reliance on linear wave theory, which is valid under a subset of wave steepness conditions. Finally, the relation between K_t and T/T_n shows that for larger T/T_n ratios (i.e., for waves with a long period), K_t increases as expected. Likewise, for smaller T/T_n (i.e., for short wave periods), K_t typically decreases.

4.2 Wave Energy Converters as Box-type FB

Utilizing the wave energy converters (WECs) as floating breakwater has been investigated by many researchers for the purpose of sharing cost as an effective economic

`

technique. Two types of WECs, that has been experimentally investigated to be FBs, are selected in this study to examine the validity of the analytical approach: (a) The Pile-Restrained WEC investigated by Ning et al. (2016) and (b) The Wave Dragon (WD) investigated by Nørgaard and Andersen (2012).

4.2.1 Pile-Restrained WEC-Style FB

Ning et al. (2016) experimentally investigated the hydrodynamic performance of an oscillating-buoy WEC that was vertically restrained by piles and used as a box-type FB. The WEC is restrained but undergoes heaving oscillation and is linked to a power take-off (PTO) that converts wave energy from the oscillating FB to electric power (Figure 4.6).

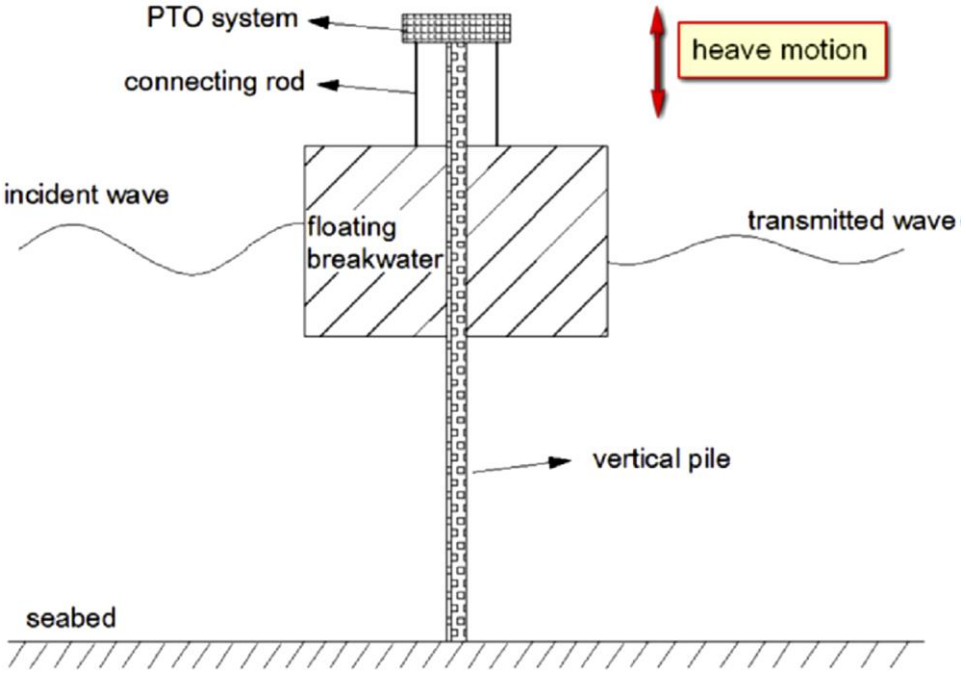

Figure 4.6: Sketch of the Pile-Restrained WEC-Style FB (Ning et al., 2016).

The tests were performed in a wave flume at the State Key Laboratory of Coastal and Offshore Engineering, Dalian University of Technology, China. The flume was 69 m long, 2 m wide and 1.8 m in depth. A wave-generator is installed at one end of the

`

flume, and a wave-absorbing layer was positioned at the other end to reduce the wave reflection (Figure 4.7).

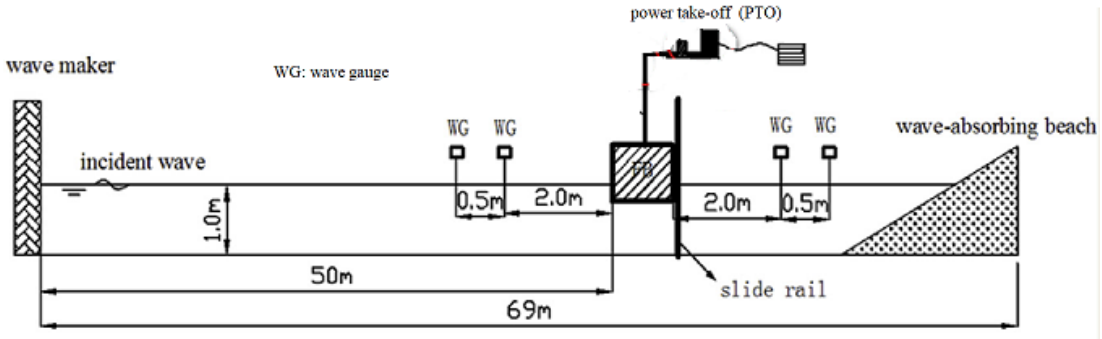

Figure 4.7: Pile-restrained WEC-Style FB tests (modified from Ning et al., 2016).

The water depths and the details of the physical models employed in the tests is summarized in Table 4.3.

Table 4.3: Box-type WEC-Style FB full-scale properties and regular wave conditions for experimental study of Ning et al. (2016).

Model Scale	Draft D (m)	Width B (m)	Incident Wave Height H_i (m)	Wave Period T (s)	Water depth d (m)
1:10	2	8	2	3.7, 4.3, 5.0, 5.7, 6.4, 7.6	10

The results of comparing the proposed approach to the experimental measurements of Ning et al. (2016) are shown in Figure 4.8. The proposed model to the experimental data approximates K_t well, especially when $B/L < 0.3$ and wave steepness, H_i/L is small. On the contrary, when $B/L > 0.30$ and $H_i/L > 0.065$, the theoretical approaches fail to predict K_t closely compared to the experimental results. Ruol et al. (2013) provided the closest prediction when $B/L = 0.38$ and $H_i/L = 0.095$, where their predicted $K_t = 0.37$ is 47% greater than the experimental $K_t = 0.25$. Meanwhile, this study predicted $K_t = 0.61$, which is 147% greater than the experimental K_t.

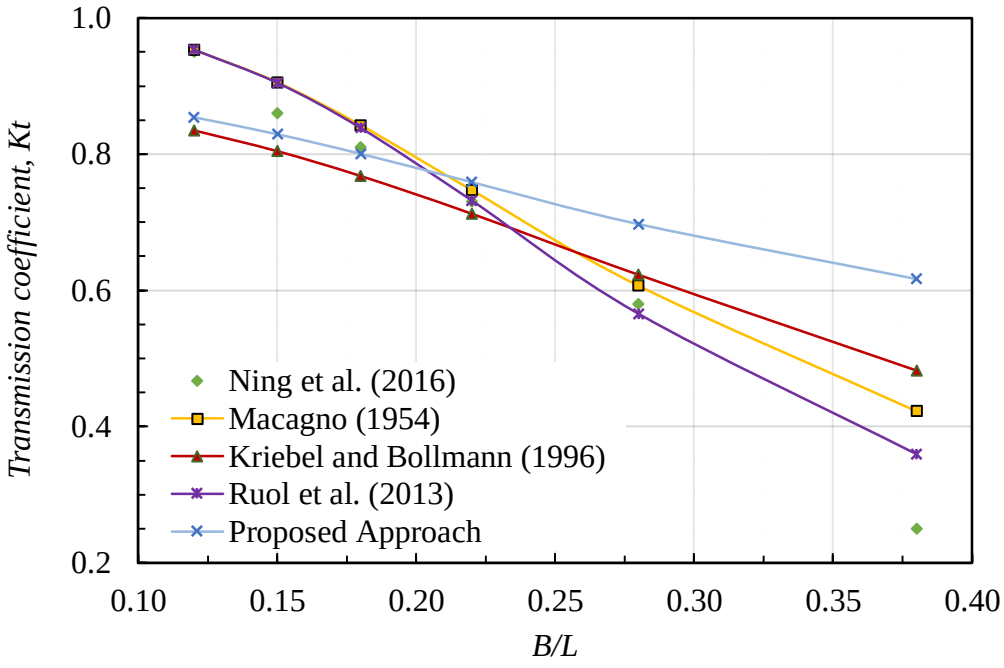
1.0
0.8
0.6
0.4
0.2
Transmission coefficient, Kt
0.10
0.15
0.20
0.25
0.30
0.35
0.40
B/L
Ning et al. (2016)
Macagno (1954)
Kriebel and Bollmann (1996)
Ruol et al. (2013)
Proposed Approach

(a)

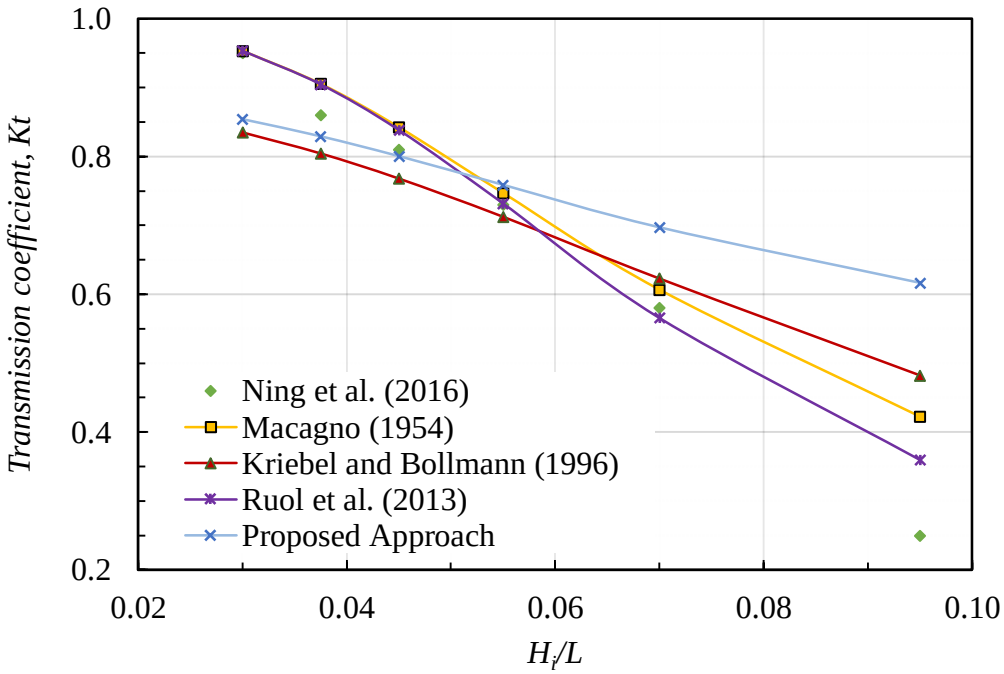
1.0
0.8
0.6
0.4
0.2
Transmission coefficient, Kt
0.02
0.04
0.06
0.08
0.10
Hi/L
Ning et al. (2016)
Macagno (1954)
Kriebel and Bollmann (1996)
Ruol et al. (2013)
Proposed Approach

(b)

`

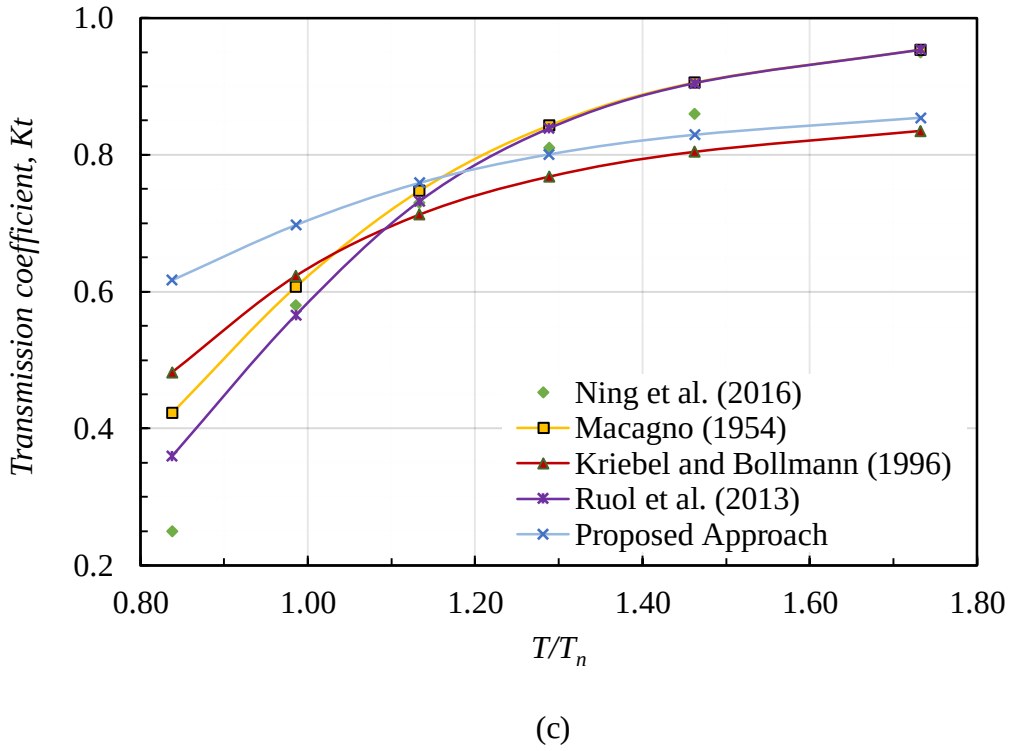

(c)

Figure 4.8: Change in the transmission coefficient with respect to (a) relative structure width B/L, (b) Incident Wave Steepness H_i/L, and (c) Relative Wave Period (T/T_n). The figure compares experimental results from Ning et al. (2016) with the outcomes of different theoretical approaches.

4.2.2 Overtopping Wave Energy Converter: Wave Dragon

The proposed methodology for defining the transmission coefficient has thus far been verified under various scales for box-type floating structures both experimentally and theoretically and it has been concluded that the approximation is reasonable. However, the main aim of the study is to provide good estimates under field conditions. Therefore, the proposed model was also tested using field data obtained by Nørgaard and Andersen (2012) for the Wave Dragon (WD) wave energy converter. The WD consists of a main body and two wave reflectors that guide the waves through a doubly curved ramp toward the main body (Figure 4.9).

`

Figure 4.9: Frontal view of the wave dragon in the North Sea (Bevilacqua, and Zanuttigh, 2011).

Under the typical wave conditions of the North Sea, the waves overtop the main body into the basin that is placed above the average sea water level. The power produced as the captured water in the basin is directed back to the sea via set of low-head hydro-turbines attached to generators (Figure 4.10).

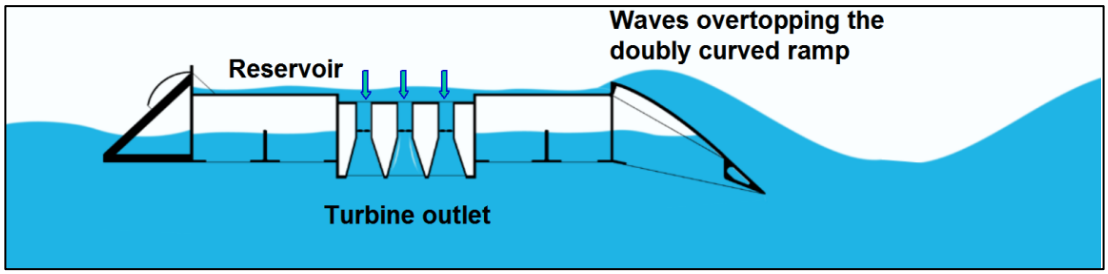

Figure 4.10: Basic principle of the Wave Dragon energy conversion (Parmeggiani et al., 2013).

The overall dimensions of the 24-kW/m WD are shown in Figure. 4.11. The draft of the reflectors increases from 6 m (at the seaside edge) in the first 37 m, to 8 m in the rest of the reflectors (the main body edge). The WD is moored by a single cable and has a certain degree of freedom to turn and face the incident waves.

`

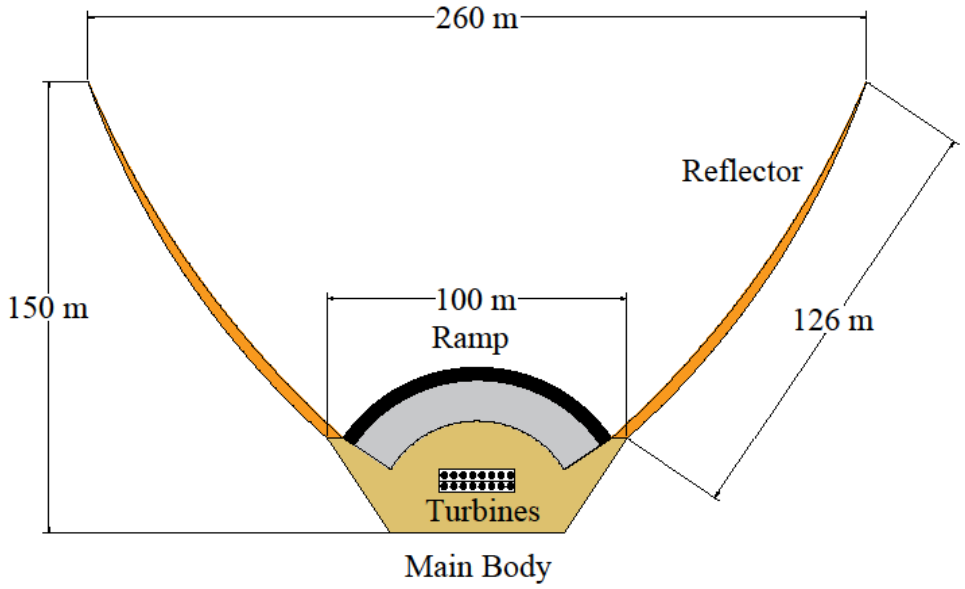

Figure 4.11: Wave Dragon dimensions. (Adapted from Nørgaard and Andersen 2012).

The reflectors increase the power density as the wave propagates toward the WD main body (Kramer and Frigaard, 2002). This increase in power was evaluated in the North Sea using a testing device developed by Kramer and Frigaard (2002), who established the efficiency factor η_{eff}, which is given by the ratio of the mean power in between the reflectors to the undisturbed incident wave power. The wave conditions in the North Sea (significant wave height H_s and peak wave period T_p) and incident wave power P_i are summarized in Table 4.4.

Table 4.4: Wave conditions in the North Sea (adapted from Nørgaard and Andersen 2012).

H_s (m)	T_p (s)	η_{eff}	P_i (KW/m)
1	5.6	1.86	2.50
2	7.0	1.45	12.30
3	8.4	1.24	33.30
4	9.8	1.20	69.00
5	11.20	1.15	123.20

`

Under the same conditions (i.e., wave climate and depth), this study examined the WD's wave attenuation performance by calculating the transmission coefficient using the present approach as well as the methods from Macagno (1954), Kriebel and Bollmann (1996), and Ruol et al. (2013).

Because the geometries of the WD components (reflectors and main body) are different, the transmission coefficient for each must be evaluated separately. The geometry of the main body is simplified to a rectangular box whose length L_b is equal to the distance between the wave reflectors in the cross section (i.e., L_b = 100 m) and width B_b is equal to the length of the reservoir (i.e., B_b = 45 m). The draft of the main body D_b is 16 m. The draft of the reflector increases from D_{r1} = 6 m, when the length perpendicular to the wave direction L_{r1} = 23.5 m, to D_{r2} = 8 m, when L_{r2} = 56.5 m (see Figure 4.12). The effect of simplifying the geometry of the WD to a rectangular box was experimentally investigated by Nørgaard and Andersen (2012) and by Beels (2009). Their results showed that this simplification did not lead to variance in the magnitude of the transmission coefficient.

`

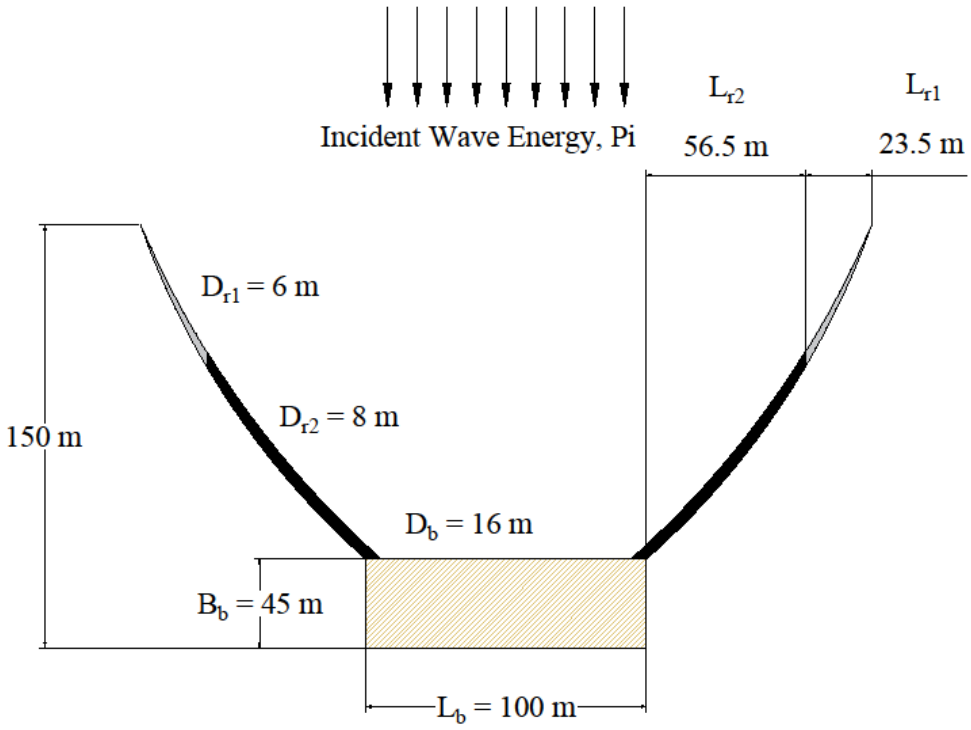

Figure 4.12: Schematic view of the simplified Wave Dragon model.

To determine the overall transmission coefficient value of the WD, the transmission coefficient for each component (i.e., main body and each part of the reflectors) must be calculated individually. Then, based on the length of each part, the weighted average transmission coefficient can be calculated using the following equation:

$$K_{t.D.t} = \frac{(K_{t.r1} \,.\, L_{r.1} \,.\, 2) + (K_{t.r2} \,.\, L_{r.2} \,.\, 2) + (K_{t.b} \,.\, L_b)}{(L_{wD})} \qquad (4.1)$$

where $K_{t.D.t}$ is the weighted average theoretical transmission coefficient for a single device, $K_{t.r.1}$ is the transmission coefficient for the part of the reflector for which D_{r1} = 6 m and L_{r1} = 23.5 m, $K_{t.r.2}$ is the transmission coefficient for the part of the reflector for which D_{r2} = 8 m and L_{r2} = 56.5 m, $K_{t.b}$ is the transmission coefficient of the main body, L_b is the length of the main body (i.e., 100 m), and L_{WD} is the total length of the WD (i.e., 260 m).

`

Figure 4.13 shows the relationship between the transmission coefficient and the non-dimensional relative structure width B/L_p, where B is the total width of the WD (B =150 m) and L_p is the peak length of the incident wave. The results of the proposed approach are in excellent agreement with the results obtained by Nørgaard and Andersen (2012). The models from Macagno (1954) and Roul et al. (2013) overestimate the transmission coefficient, whereas the model from Krieble and Bollmann (1996) underestimates the transmission coefficient under the same conditions.

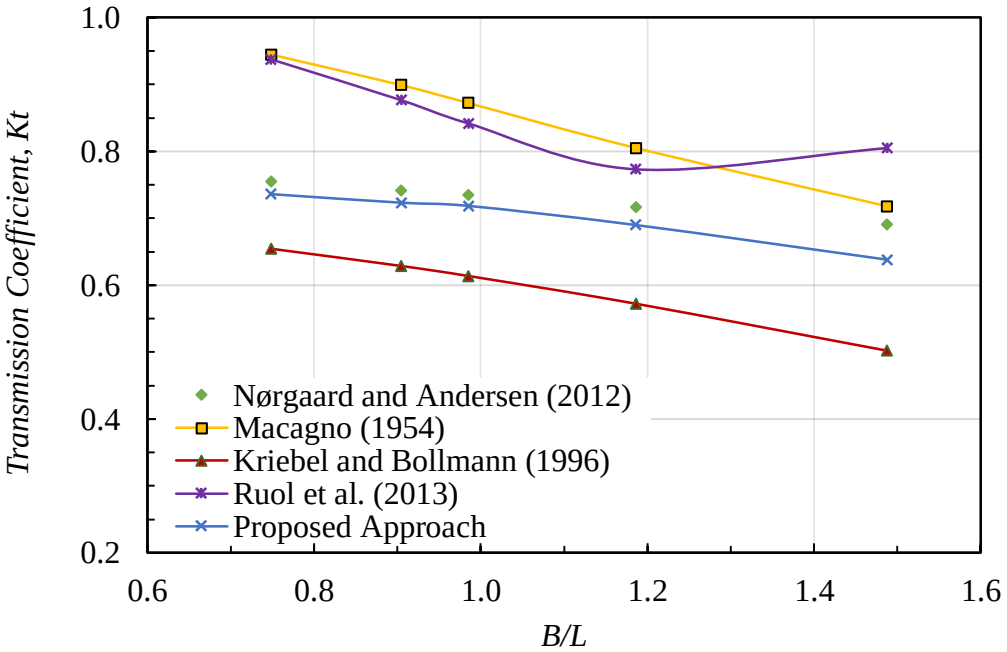

(a)

`

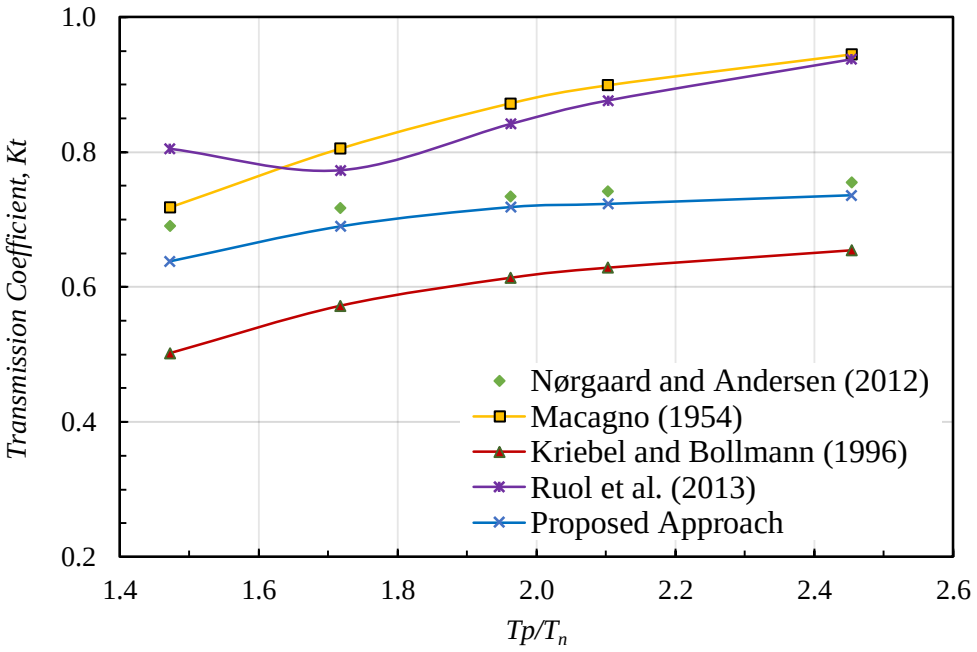

(b)

Figure 4.13: Change in the transmission coefficient with respect to (a) relative structure width B/L_p and (b) relative wave period (T/T_n). The figure compares experimental results from Nørgaard and Andersen (2012) with the outcomes of different theoretical approaches.

4.3 π-shaped Floating Breakwater

After examining the validity of the present analytical model against the experimental measurements for box-type floating structures, here in this section two experimental studies will be used to investigate if this model will be applicable for π-shaped floating structures. The first study was conducted by Koutandos et al. (2005) who investigated the performance of π-shaped FB in comparison to the box-type FB. The second experimental study was carried out by Cox et al. (2007) who investigated the wave transmission for FB under various wave climates.

4.3.1 Performance of π-shaped FB by Koutandos et al. (2005)

Koutandos et al. (2005) experimental investigated the efficiency of box-type FB with attached impermeable plate which turned the FB to be π-shaped. The purpose of the

`

study was to compare the hydrodynamic performance and the wave transmission behavior for the box and π-shaped structures. The tests were performed under the same settings that have been shown in Figure 4.1. The total draft of the attached plate was meant to be the same as the draft of the box-type FB. Therefore, the keel of the box-type was reduced to give the FB the π shape. The properties of the examined π-shaped FB and the wave conditions are shown in Table 4.5.

Table 4.5: π-shaped FB full-scale properties and regular wave conditions for experimental study of Koutandos et al. (2005).

Model Scale	Draft D (m)		Width B (m)	Incident Wave Height H_i (m)	Wave Period T (s)	Water depth d (m)
	FB	Plate				
1:5	1	1	10	1.5	14.9, 12.4, 9.5, 7.5, 6.4, 5.4	10
	Total = 2					

Figure. 4.14 shows a comparison between the experimental and theoretical transmission coefficients. The curves show the relationship between the relative floating structure width B/L and the transmission coefficient K_t, as well as the relationship between the wave steepness H_i/L and K_t. In addition, the curves depict the relationship between K_t and the relative wave period T/T_n.

As shown in Figure. 4.14, the calculated K_t using the present analytical model is in very good agreement with the experimental results of Koutandos et al. (2005) when $B/L < 0.19$, at which point an unexpected descent is observed in the measured data, possibly due to the natural period of the FB, which is ignored in theoretical approaches (Dong et al., 2008). Moreover, better correlation can be observed at a small wave steepness H_i/L which complies with the linear wave theory that is used in the derivations of the present approach. The relationship between K_t and the relative wave period

`

T/T_n shows that the theoretical estimates deviate from the experimental measurement when the wave period becomes closer to the heave natural period. Generally, the theoretical results obtained from this study give the best estimation for K_t compared with the experimental results, whereas the models from Kriebel and Bollmann (1996) Macagno (1954) and Ruol et al. (2013) overestimate K_t.

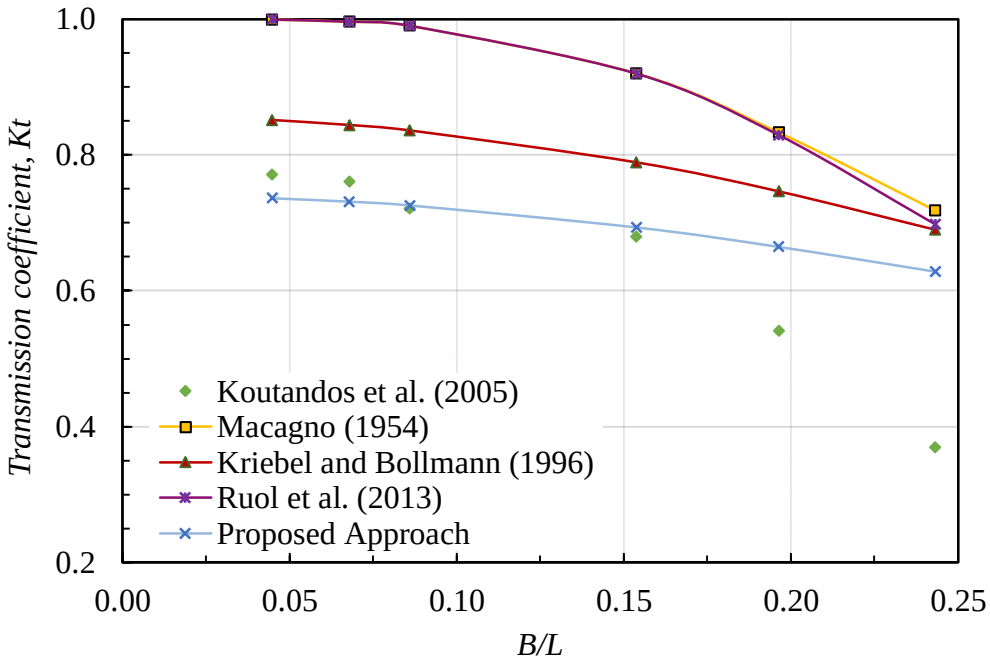

(a)

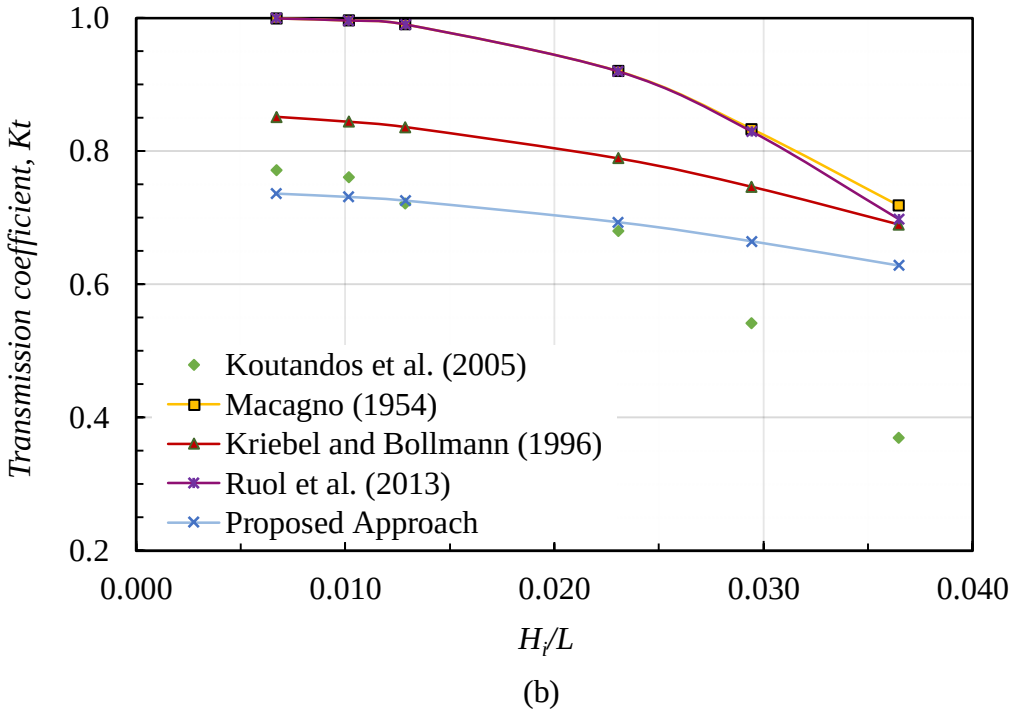

(b)

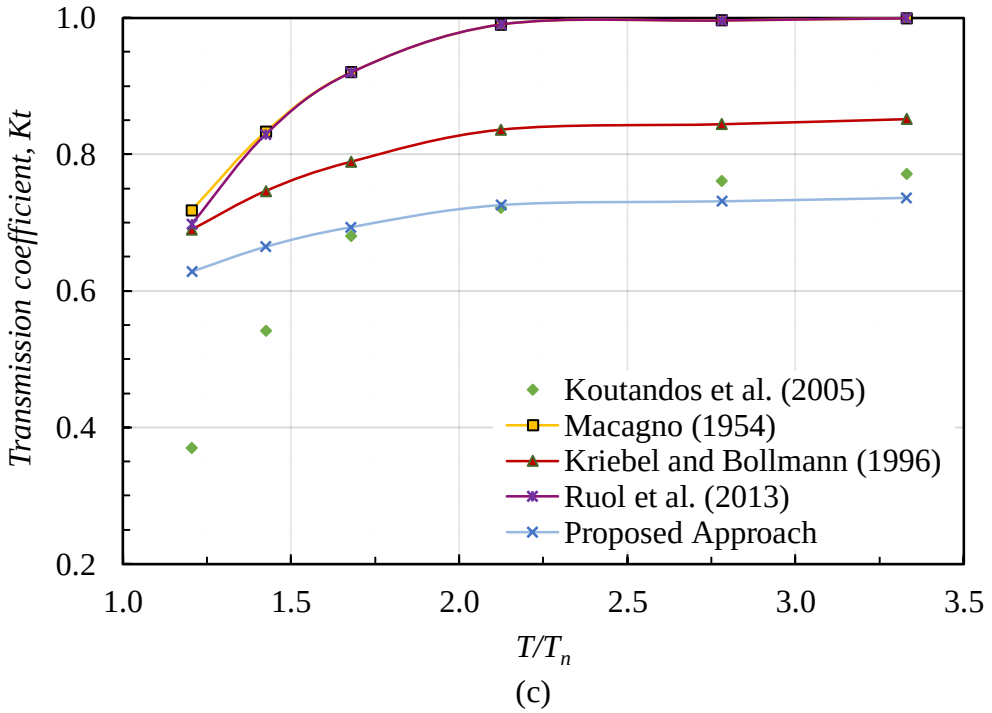

(c)

Figure 4.14: Change in the transmission coefficient of π-shaped FB with respect to (a) relative structure width B/L, (b) Wave Steepness H_i/L, and (c) relative wave period (T/T_n). The figure compares experimental results from Koutandos et al. (2005) with the outcomes of different theoretical approaches.

`

4.3.2 Performance of π-shaped FB by Cox et al. (2007)

Cox et al. (2007) experimentally investigated the performance of pile restrained π-shaped FB under various wave conditions. The FB was restrained from horizontal movements while it was allowed to move in the vertical direction. The experimental investigation took a place in a wave flume at the University of New South Wales, Many Vale Water Research Laboratory. The flume was 130 m in length, 0.7 m in depth, and 0.6 m in width. The FB was positioned in the middle of the flume as shown in Figure (4.15).

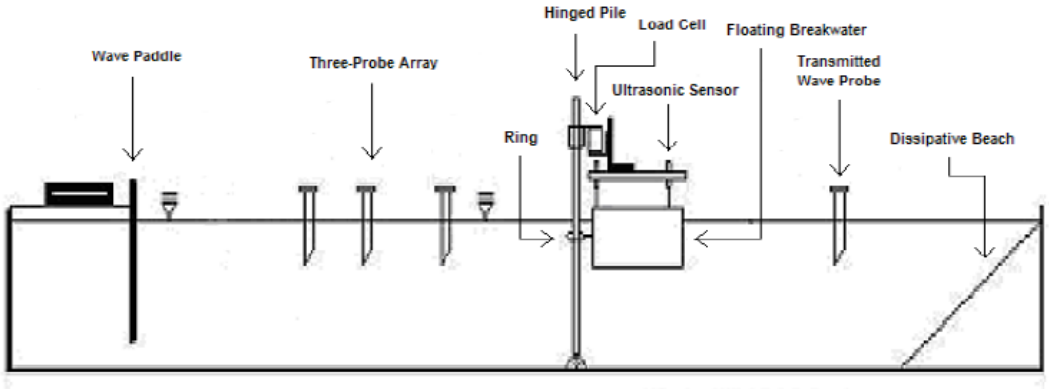

Figure 4.15: The set-up of the experiments for the FB (Cox et al., 2007).

The FB physical model is restrained by two piles which allow the structure to move vertically but limit its horizontal movement. The water depths and the details of the physical models employed in is summarized in Table 4.6.

Table 4.6: Full-scale properties of π-shaped FB and regular wave conditions for experimental study of Cox et al. (2007).

Model Scale	Draft D (m)	Width B (m)	Incident Wave Height H_i (m)	Wave Period T (s)	Water depth d (m)
1:5	2.1	2.4	0.4, 0.8	2, 3, 4, 5	7

`

Figure. 4.16 and Figure 4.17 compare the experimental and theoretical transmission coefficients under two different incident wave heights (i.e., H_i = 0.4 m and H_i = 0.8 m). The curves show the relationship between the relative floating structure width B/L and the transmission coefficient K_t, as well as the relationship between the wave steepness H_i/L and K_t. Furthermore, the curves present the relationship between K_t and the relative wave period T/T_n.

As it can be observed in Figure. 4.16, the proposed model follows the trend of the measured results of Koutandos et al. (2005). The analytical approach gives the best K_t estimation when B/L is around 0.17 and slightly underestimates K_t when B/L is larger or smaller. Furthermore, excellent correlation can be observed at a wave steepness H_i/L = 0.03. The relationship between K_t and the relative wave period T/T_n shows that the analytical estimates are closer to the experimental measurements when the wave T/T_n is around 1.

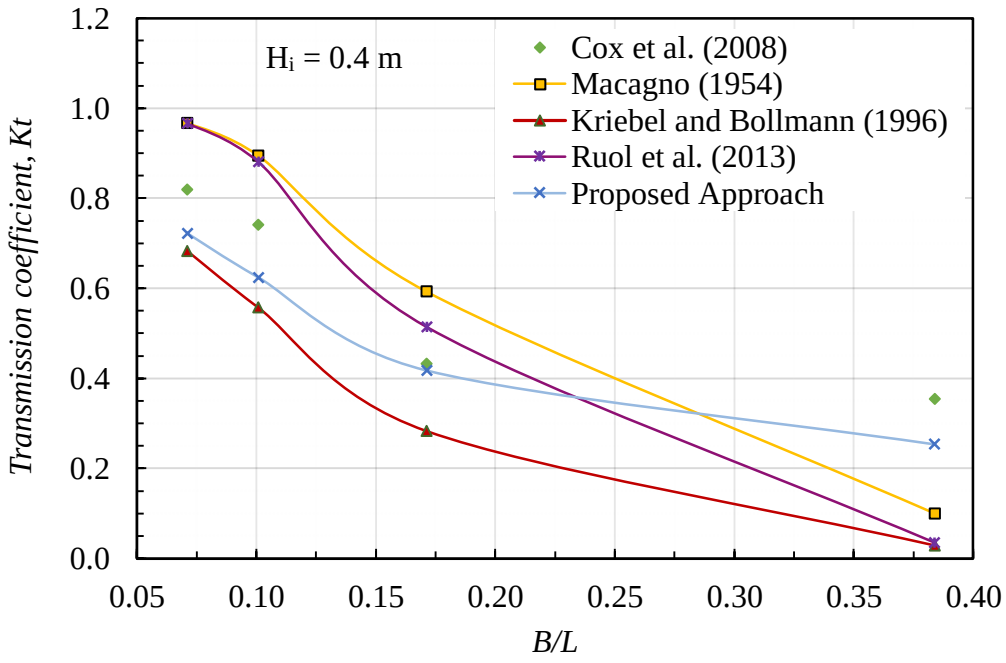

(a)

`

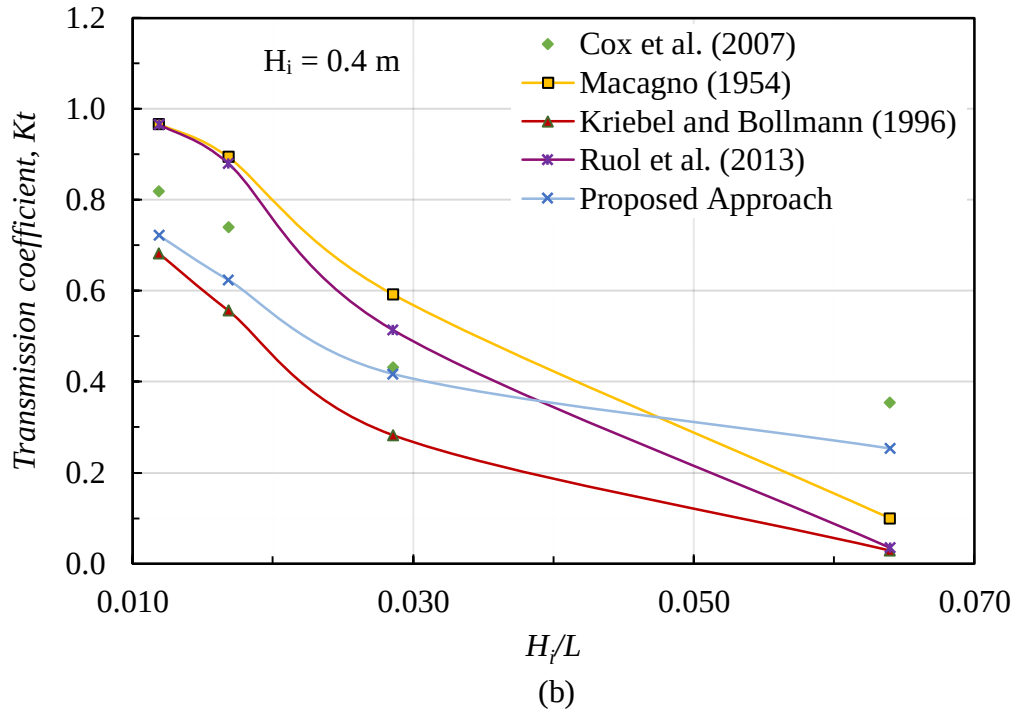

(b)

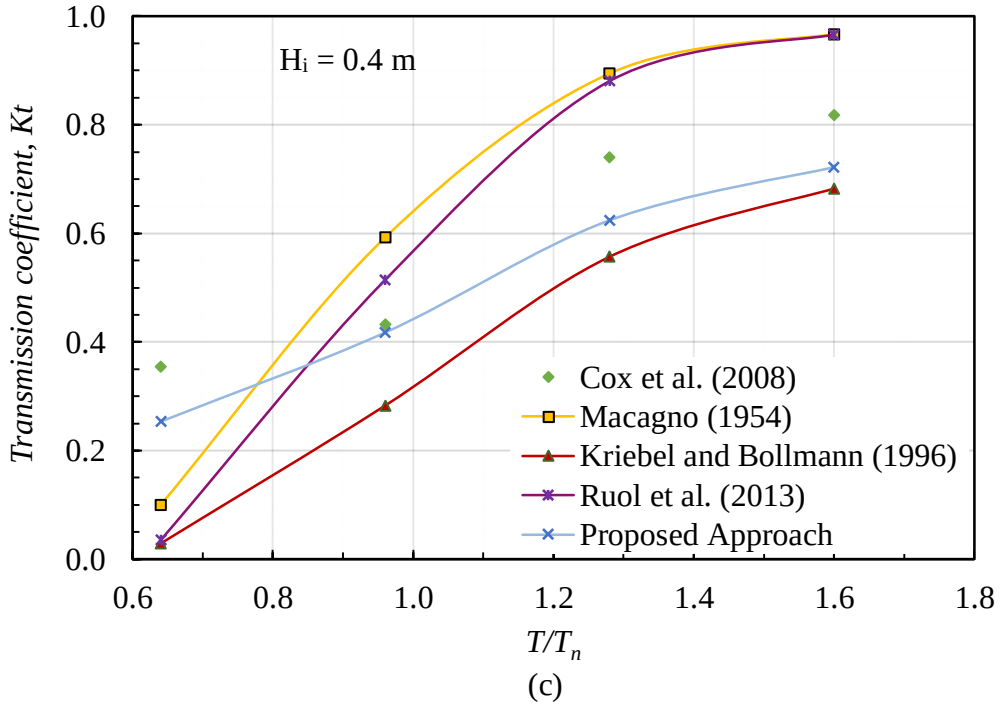

(c)

Figure 4.16: Change in the transmission coefficient of π-shaped FB with Respect to (a) Relative Structure Width *B/L*, (b) Wave Steepness H_i/L, and (c) relative wave period (T/T_n). The figure compares experimental results from Cox et al. (2007) with outcomes of different theoretical approaches when wave height H_i = 0.4 m.

Similar outcomes can be seen in Figure 4.17. The analytical approach of this study gives a trend following curve to the measured data of Cox et al, (2007). However, a

`

better correlation is obtained when the H_i = 0.8 m than when H_i = 0.4 m. Overall, the theoretical results obtained from this study gives the best estimations for K_t compared with the experimental results, whereas the models from Macagno (1954), Kriebel and Bollmann (1996), and Ruol et al. (2013) either overestimate or underestimate K_t.

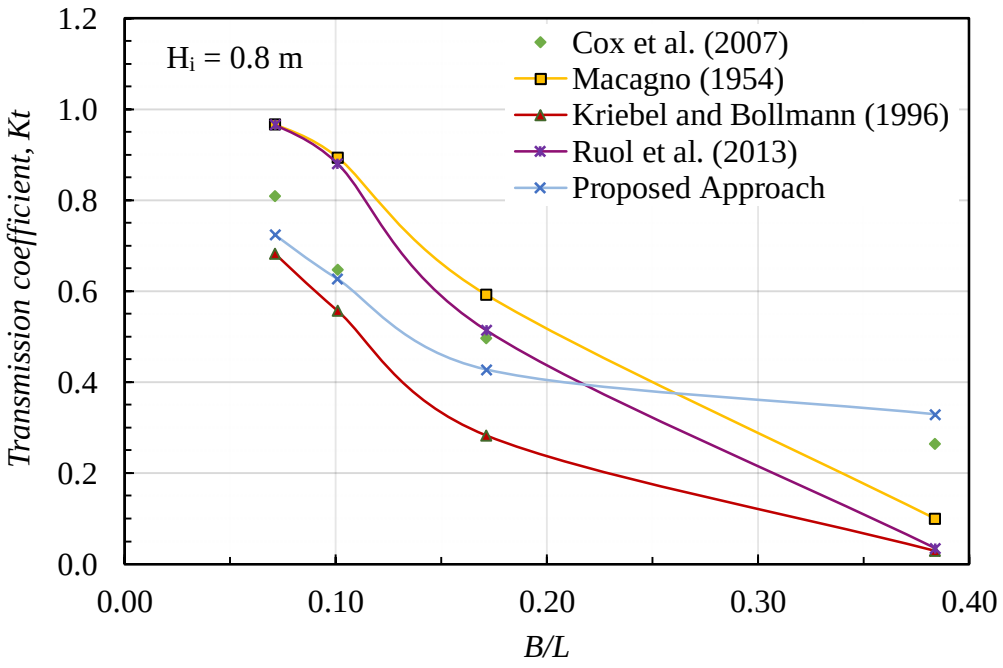

(a)

`

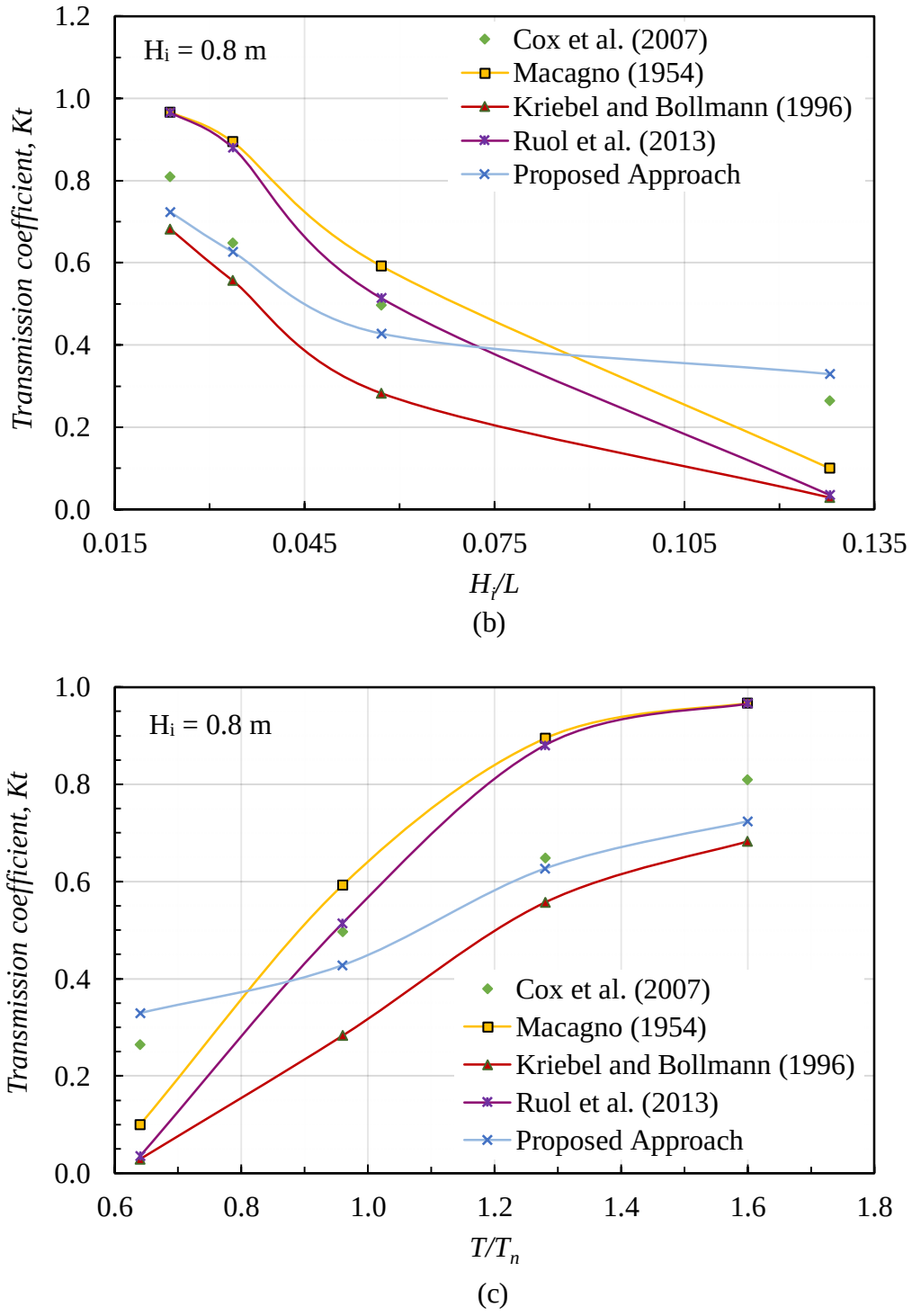

Figure 4.17: Change in the transmission coefficient of π-shaped FB with respect to (a) relative structure width B/L, (b) wave steepness H_i/L, and (c) relative wave period (T/T_n). The figure compares experimental results from Cox et al. (2007) with outcomes of different theoretical approaches when wave height H_i = 0.8 m.

An exceptional finding is obtained from the study of Cox et al. (2007) and it is shown in Table 4.7. The transmission coefficient calculated using all the theoretical models

`

except the proposed approach remains constant even though the incident wave height is changed. The experimental results shows a variation in the value of the transmission coefficient as the incident wave height increases from H_i = 0.4 m to H_i = 0.8 m and the same results are obtained from the theoretical results of the analytical model of this study. This finding is exclusively observed in the experimental study of Cox et al. (2007) since it is the only study in which all the variables are kept constant except the incident wave height. The dimensions of the FB remained unchanged and the wave periods and wave depth were the same in all experimental tests.

Table 4.7**:** The change in the measured and calculated transmission coefficient values for π-shaped floating structures with changing incident wave height.

Model	Transmission Coefficient, K_t							
	H_i = 0.4 m				H_i = 0.8 m			
	Wave Period (s)				Wave Period (s)			
	2	3	4	5	2	3	4	5
Cox et al. (2007)	0.35	0.43	0.74	0.82	0.26	0.50	0.65	0.81
Macagno (1954)	0.10	0.59	0.89	0.97	0.10	0.59	0.89	0.97
Kriebel and Boll-mann (1996)	0.03	0.28	0.56	0.68	0.03	0.28	0.56	0.68
Ruol et al. (2013)	0.04	0.51	0.88	0.97	0.04	0.51	0.88	0.97
Proposed Approach	0.25	0.42	0.62	0.72	0.33	0.43	0.63	0.72

`

Chapter 5

DISCUSSIONS AND CONCLUSIONS

This chapter contains an overview of the research and discusses the results that have been obtained according to the research designated plan. In addition, the chapter includes the conclusions that have been reached about the study. The discussion section explains the comparison between the proposed model of this study and the available models and shows the effects of the properties of the waves and the floating structures on the results. Finally, answers to the research questions will be presented within the conclusions.

5.1 Discussion

5.1.1 Comparison of Proposed and Available Models

Evaluations using the laboratory experimental data indicated that the proposed model estimates the transmission coefficient K_t well for smaller values of the relative structure width (i.e., $B/L \leq 0.3$). However, as the relative structure width exceeds this limit, both the present approach and existing theoretical approximations overestimate K_t, which may result from scale effects on the behavior of the floating structure. Figure 5.1 compares the measured and calculated transmission coefficients for the four aforementioned experimental studies; modeled as Box-type floating structures; and the four theoretical approaches (including the present model). For all applications, except for the WD, the theoretical approaches slightly underestimate K_t for relatively long waves (i.e., $B/L < 0.2$) and slightly overestimate it for relatively short waves (i.e., $0.2 < B/L < 0.3$). For the WD, the relative width B/L_p has different limits because the total width

`

of 150 m is considered for the overall WD transmission coefficient. Within these limits, the mean square error between the measured and calculated K_t for all theoretical approaches is summarized in Table 5.1.

Table 5.1**:** The mean square error between the measured and calculated transmission coefficient values for box-type floating structures.

Model	Koutandos et al. (2005)	Dong et al. (2008)	Ning et al. (2016)	Nørgaard and Andersen (2012)
Macagno (1954)	0.014	0.011	0.006	0.018
Kriebel and Bollmann (1996)	0.001	0.023	0.012	0.019
Ruol et al. (2013)	0.013	0.008	0.003	0.016
Proposed Approach	0.003	0.033	0.027	0.001

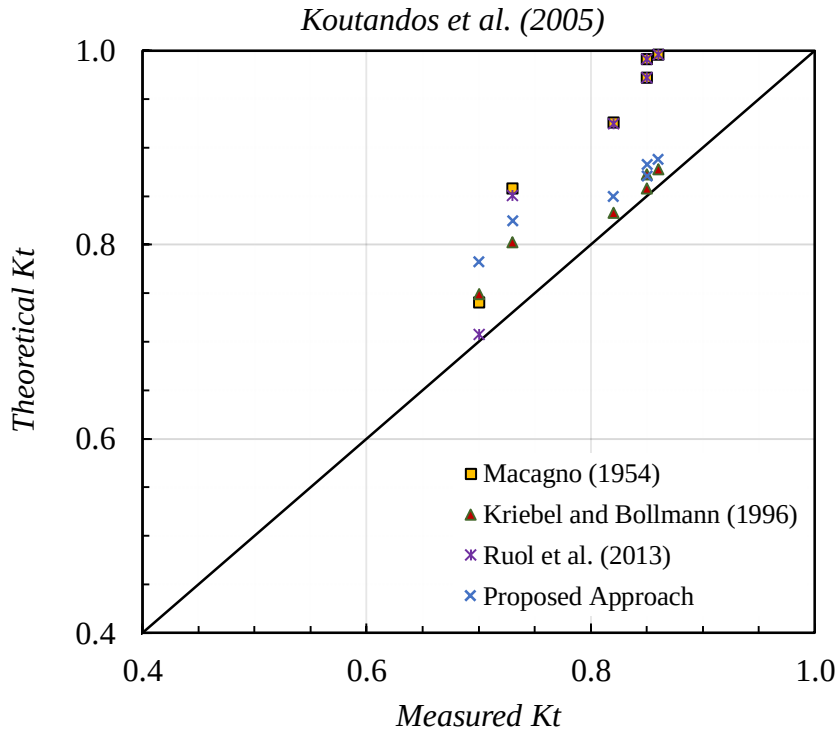

`

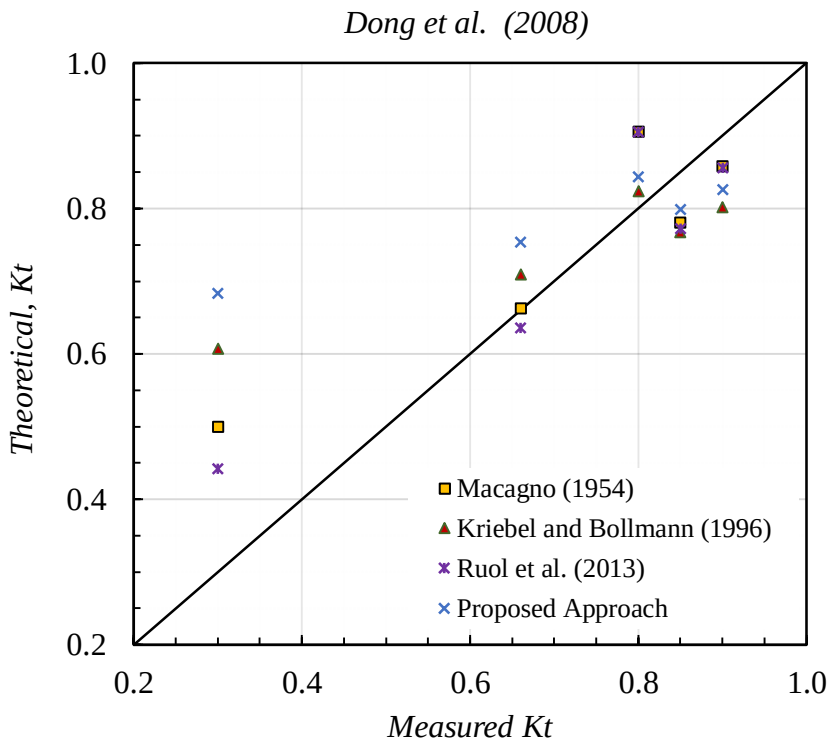
Dong et al. (2008)
1.0
0.8
0.6
0.4
0.2
Theoretical, Kt
0.2
0.4
0.6
0.8
1.0
Measured Kt
Macagno (1954)
Kriebel and Bollmann (1996)
Ruol et al. (2013)
Proposed Approach

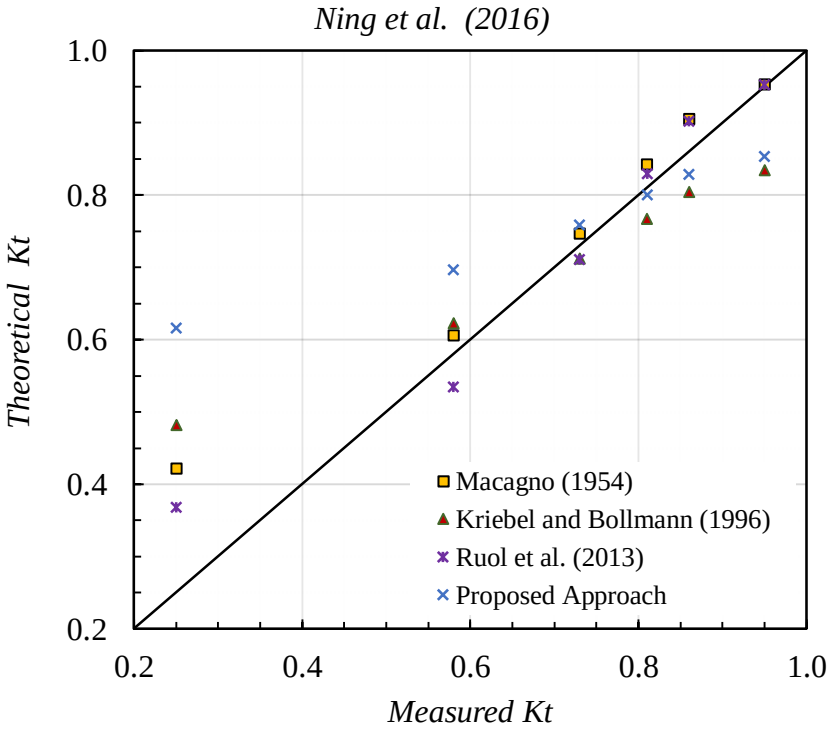
Ning et al. (2016)
1.0
0.8
0.6
0.4
0.2
Theoretical Kt
0.2
0.4
0.6
0.8
1.0
Measured Kt
Macagno (1954)
Kriebel and Bollmann (1996)
Ruol et al. (2013)
Proposed Approach

`

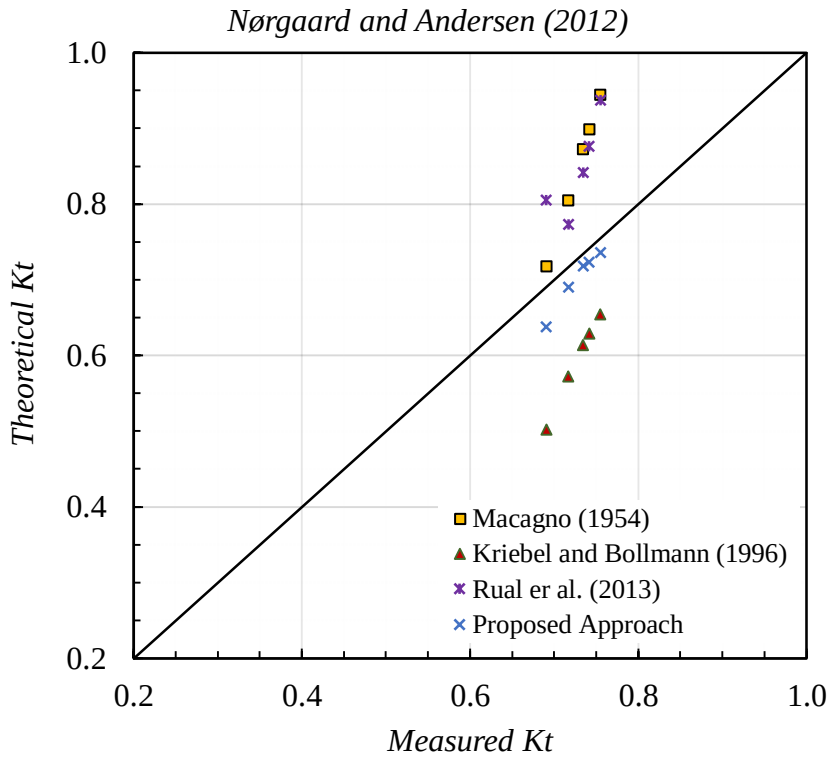

Figure 5.1: Measured versus calculated transmission coefficients for different applications using several theoretical models for Box-type FB.

In the case of the WD, for which field wave climate data were used, the proposed methodology depicted the best estimate compared to the other theoretical models. The average difference between the measured and calculated K_t was less than 4% using the proposed model, around 16% using the models developed by Macagno (1954) and Ruol et al. (2013), and 28% using Kriebel and Bollmann's (1996) model. The proposed model fits the WD experimental results better because the WD is completely heave-free, as it is moored by a single cable. The present approximation was developed under such assumptions; therefore, it gives better estimations with slack mooring systems, where the impact of heaving oscillation is not resisted by the mooring forces.

Figure 5.2 compares the measured and calculated transmission coefficients for the two experimental studies on π-shaped FBs (i.e., Koutandos et al., 2005 and Cox et al., 2007); and the four theoretical models including the model of current study. In the case

`

of Koutandos et al. (2005), it can be observed that the present model gives the closest expectations to measured K_t, especially under long wave conditions (i.e., B/L < 0.2); meanwhile, all the other theories produce overestimated values. In the case of the case of Cox et al. (2007), the present approach also gives the best K_t estimations and the lowest mean square error between the calculated and measured values which can be seen in Table 5.2.

Table 5.2**:** The mean square error between the measured and calculated transmission coefficient values for π-shaped floating structures.

Model	Koutandos et al. (2005)	Cox et al. (2007)
Macagno (1954)	0.074	0.032
Kriebel and Bollmann (1996)	0.031	0.038
Ruol et al. (2013)	0.071	0.035
Proposed Approach	0.014	0.006

A better correlation between the present theory and the experimental results can be seen in case of the study of Cox et al. (2007) since the FB was allowed to oscillate vertically with more freedom than in the case of Koutandos et al. (2005). This observation is similar to the situation of the box-type WEC WD in which the best agreement between the theoretical and the measured K_t was obtained.

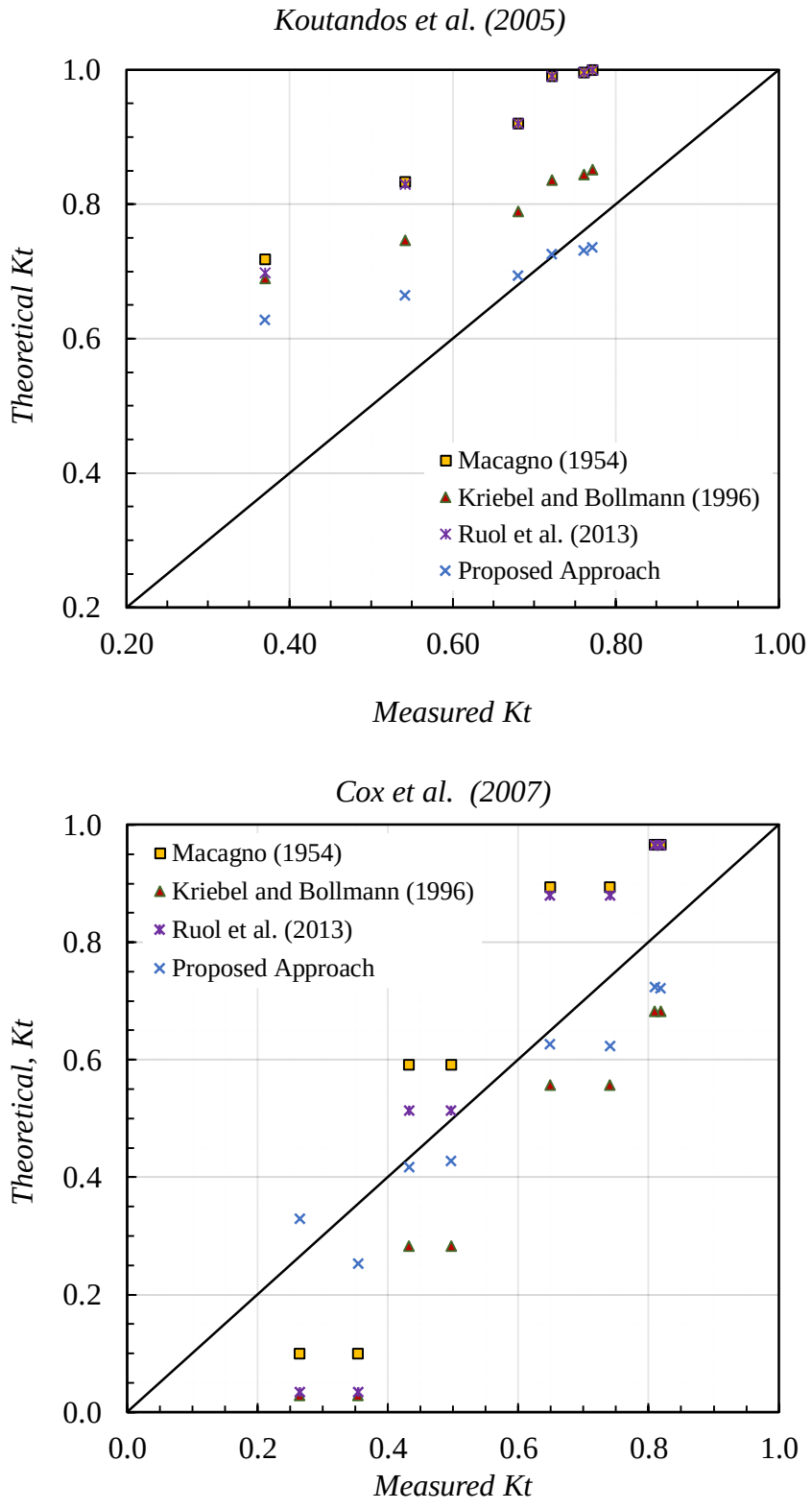

Figure 5.2: Measured versus calculated transmission coefficients for different applications using several theoretical models for π-shaped FB.

`

5.1.2 Effect of Draft and Water Depth

The floating structure, which is used as wave attenuator, can be extended downward to the seabed to block nearly all the incident wave power, but as it is basically floating, the draft depth is typically much smaller than the water depth. In the case of short period waves, the orbital velocity decreases rapidly as the water depth increases. Hence, a deeper draft may not change the transmitted wave power. In contrast, the orbital velocity of long-period waves expands toward the seabed. Therefore, a larger draft is required to block the incident wave power. However, this situation is problematic owing to large possible mooring forces (Hals, 1981; Oliver et al., 1994).

A deeper draft typically reflects more power and allows less energy to transfer to the lee side. The effect of relative draft on the transmission coefficient under constant wave climate and structure width has been determined using the proposed approach. The results show that as the draft increases (a higher value of *D/d*), the transmission coefficient decreases, indicating better blocking wave power transfer and successful additional attenuation of the transferred wave height (Figure 5.3).

`

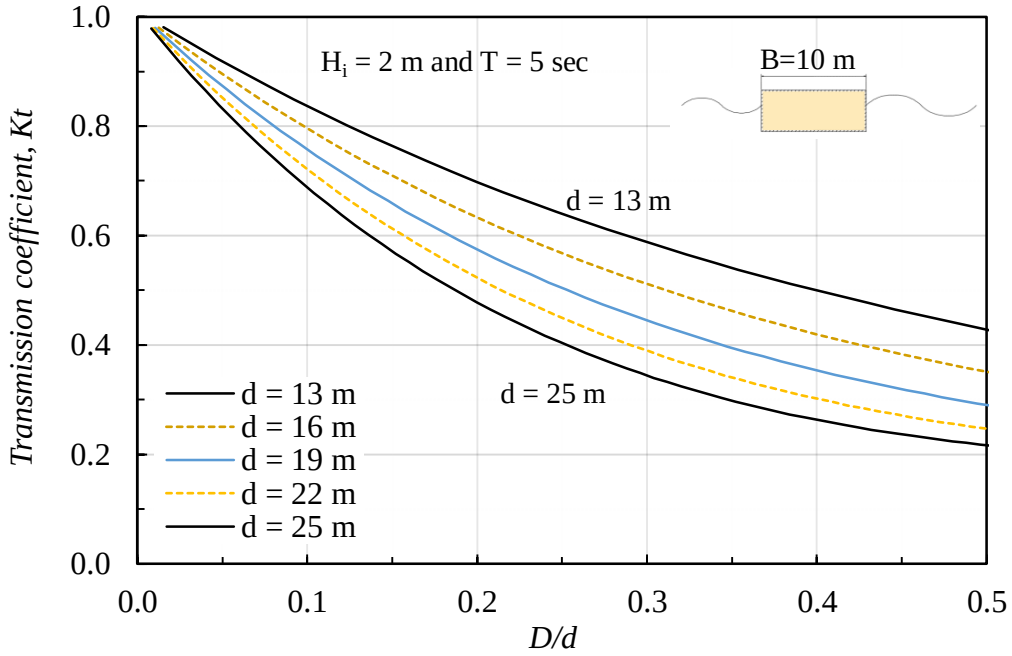

Figure 5.3: Effect of relative draft *D/d* on the transmission coefficient.

For a constant relative draft value (e.g., *D/d* = 0.2 in Figure. 5.3), another important finding is the reduction of the transmission coefficient with respect to the increasing sea depth. Thus, the floating structure's wave reduction performance is better in deep water because a deeper draft is required to keep *D/d* constant. As the orbital velocity (hence the wave power) is greater close to the sea surface, the deeper draft blocks more wave power from transferring to the lee side generating a lower transmission coefficient.

Practically, the selection of the right location for a floating structure that is utilized as a breakwater is controlled by the degree of protection required, the available budget for installation, and the available space. For a certain structure as the one shown in Figure. 5.3, the best option should be at *D/d* around 0.3 at water depth of 25 m since the transmission coefficient is not significantly decreases after this point and increasing the draft will increase the cost.

`

5.1.3 Effect of Incident Wave Height

In general, according to the definition of the transmission coefficient given in Eq. (3.1), as the incident wave hits the floating structure, the transmitted percentage of the kinetic part of the incident wave power and the induced pressure part of the incident wave power are constant. However, pursuant to the proposed methodology, the kinetic energy flux resulting from the oscillation of a heaving floating structure changes with the incident wave height. Figure 5.4, which is plotted based on the proposed model of this study, shows that, under the same wave period condition, as the incident wave height increases, the transmission coefficient of the floating structure also increases. This result is expected, as the H_i is a factor that affects the calculation of the K_t. The kinetic energy flux resulting from the heaving movement of the floating structure and its hydrodynamic mass is a function of H_i, and it increases with wave height, leading to additional power transmission. Therefore, better wave attenuation (a lower value of K_t) is achieved in case of non-fixed floating structures experiencing short wave heights. This finding distinguishes the present model of this study from previous theoretical approaches, which ignored the effect of the incident wave height.

`

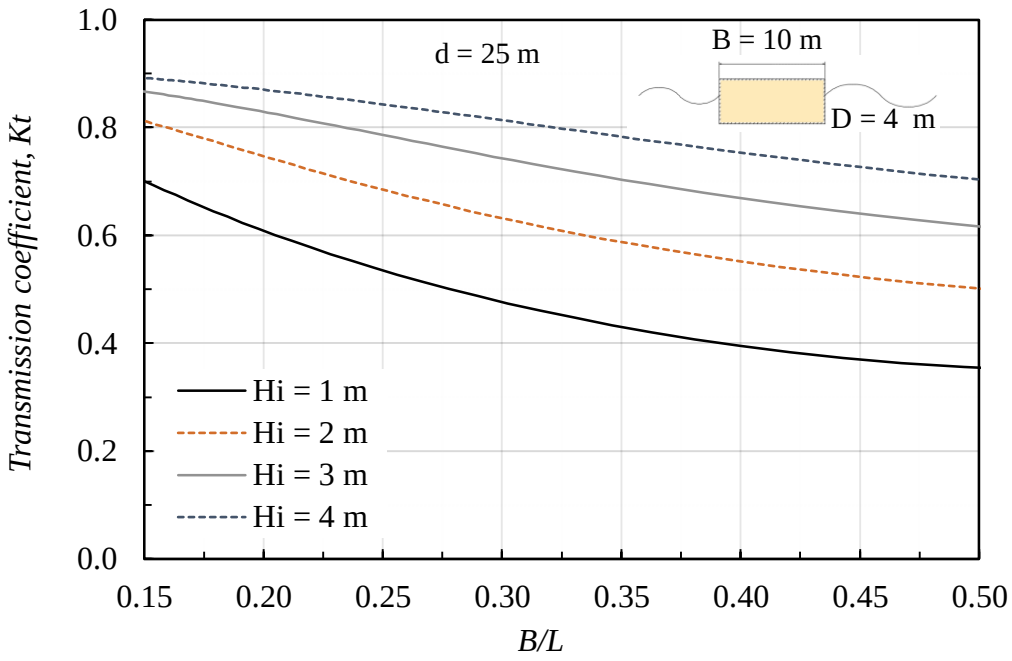

Figure 5.4: Effect of incident wave height H_i on the transmission coefficient.

5.2 Conclusions

An analytical approach was developed to evaluate the wave attenuation capability of two types of non-fixed floating structures namely box-type and π-shaped. The proposed model was based on linear wave and power transmission theories, and it considers the effect of the structure's heaving oscillation. Since the model was developed based on a 2D assumption, diffraction effects due to the finite length of the floating structure were not considered. However, in practice, floating structures are usually connected to each other, or at least arranged such that they can be considered as a single long body. The proposed approach was validated using laboratory-scale experimental data obtained from the literature (two studies on box-type FBs, two studies on box-type WECs and two studies on π-shaped FBs).

The results obtained using the proposed methodology of this research agreed with the small-scale results in the literature for waves with long periods and low steepness, in

`

accordance with linear wave theory. Some scatter is to be expected, because it is difficult to adequately consider the effect of mooring stiffness in a simple approach. Part of the scatter is also attributed to scale effects that are likely to influence the transmission behavior, especially for higher waves, ignoring overtopping. Therefore, this approach may be inaccurate when applied to waves higher than the freeboard of the floating structure.

The aim was to find answers to the research questions raised at the beginning of the study and this was achieved along the study. The summary of the answers is as below:

The methodology takes in consideration the transport of the wave kinetic energy. This energy transport is usually ignored when linear wave theory is used since the derivation of this theory is limited to a second-order approximation and the kinetic part of the wave power is of third order. Therefore, the magnitude of this part of wave power is negligible comparing to the part of the wave power due to the wave pressure. However, this research proposes to take the kinetic part into account because in the typical wave conditions, under which the FBs and WECs are commonly set up, the wave amplitudes are relatively large and the water is deep. In these conditions, the linear wave theory is still applicable and the wave kinetic energy transport fairly increases. The results of this study show that this part of the wave power affect the resultant transmission coefficient by increasing the total transmitted wave power when combined under the structure with the kinetic energy flux owing to the heaving oscillation of the floating structure.

The results show that the heave motion of the floating structure creates an additional kinetic energy due to the acceleration of the mass of the structure. In addition, the

`

added mass, which is the hydrodynamic mass attached to the floating structures and accelerates simultaneously with it, creates another additional kinetic energy. The transport of these parts of kinetic energy in the direction of the wave propagation increases the total transmitted wave power and thus the transmission coefficient of the floating structure.

Investigation on the effects of the floating structure draft and water depth indicated that at deeper drafts, the transmission coefficient of the floating structure decreases, and less power is transmitted to the lee side, thereby better reducing waves. In addition, for the same floating structure, wave attenuation achieved in deep water is better than that achieved in shallow water.

Most significantly, this approach can be distinguished from other theoretical approaches proposed previously by the fact that H_i influences the calculation of the K_t via changes in the kinetic energy flux resulting from the heaving motions of the floating structure.

5.3 Recommendations for Future Researches

The model of this study is developed to provide a simplified but more reliable technique to estimate the transmission coefficient for two specific types of floating structures (i.e., box and π-shaped). Future studies may test the model with other types of floating structures such as double pontoon, cylindrical, and etc. Further, the impact of the overtopping can be investigated since it was ignored in this study due to the insufficient information about the freeboard height in the experimental studies. Moreover, the impacts of some other factors such as bottom closeness, mooring stiffness, and

`

wave energy dissipation due to turbulence and friction can be investigated. These factors need to be investigated experimentally under different wave climates and structures' dimensions and for different types of floating structures, and then can be incorporated with the analytical model.

`

REFERENCES

Alamailes, A., and Türker, U. (2019). Using analytical approach to estimate wave transmission coefficient in floating structures. *J. Waterway Port Coastal Ocean Eng.*, 145(3), pp 04019010. DIO: 10.1061/(ASCE)WW.1943-5460.0000513

Beels, C. (2009). Optimization of the lay-out of a farm of wave energy converters in the North Sea: Analysis of wave power resources, wake effects, production and cost. Ph.D. thesis. Department of Civil Engineering, Ghent University.

Beels, C., Troch, P., De Visch, K., Kofoed, J. P., and De Backer, G. (2010). Application of the time-dependent mild-slope equations for the simulation of wake effects in the lee of a farm of wave dragon wave energy converters."*Renewable Energy,* 35(8), 1644–1661.

Bevilacqua, G., and Zanuttigh, B. (2011). Overtopping Wave Energy Converters: general aspects and stage of development. Universitia Di Bolonga, Italy, pp. 1-21.

Bouwmeester, E. C., and Van der Breggen, H. M. (1984). Floating breakwaters: Literature review. Delft University of Technology.

Burcharth, H.F., Zanuttigh, B., Andersen, T.L., Lara, J.L., Steendam, G.J., Ruol, P., Sergent, P., Ostrowski, R., Silva, R., Martinelli, L. and Nørgaard, J.Q.H., 2015. Innovative engineering solutions and best practices to mitigate coastal risk. In: Coast. *Risk Management in a Changing Climate*. Butterworth Heinemann, Boston, 55-170.

`

Carr, J. H. (1951). Mobile breakwaters. *Coastal Engineering Proceedings*, *1*(2), 25.

Cox, R., Coghlan, I., and Kerry, C. (2007). Floating breakwater performance in irregular waves with particular emphasis on wave transmission and reflection, energy dissipation, motions and restraining forces. In *Coastal Structures,* 351-362.

Dean, R. G., and Dalrymple, R. A. (1991). *Water wave mechanics for engineers and scientists* (Vol. 2). World Scientific Publishing Company, Singapore.

Diaconu, S., and Rusu, E. (2013). The environmental impact of a wave dragon array operating in the Black Sea. *Sci. World J.*, 498013.

Diamantoulaki, I., and Angelides, D. C. (2011). Modeling of cable-moored floating breakwaters connected with hinges. *Eng. Struct.*, 33(5), 1536–1552.

Dong, G., Zheng, Y., Li, Y., Teng, B., Guan, C., and Lin, D. (2008). Experiments on wave transmission coefficients of floating breakwaters. *Ocean Eng.*, 35(8), 931–938.

Goggins, J., and Finnegan, W. (2014). Shape optimisation of floating wave energy converters for a specified wave energy spectrum. *Renewable Energy*, 71, 208–220.

Hales, L. Z. (1981). Floating breakwaters: State-of-the-art literature review. *Technical Rep. TR81-1*. United States Army Corps of Engineers, Springfield, VA.

`

Holthuijsen, L. H. (2010). *Waves in oceanic and coastal waters.* Cambridge University Press, Cambridge, U.K.

Ji, C., Chen, X., Cui, J., Yuan, Z., and Incecik, A. (2015). "Experimental study of a new type of floating breakwater." *Ocean Eng.,* 105, 295–303.

Kramer, M. M., and Frigaard, P. B. (2002). Efficient wave energy amplification with wave reflectors. *Proc., 12th Int. Offshore and Polar Eng. Conf.,* Kitakyushu, Japan, 707–712.

Kriebel, D. L., and Bollmann, C. A. (1996). Wave transmission past vertical wave barriers. *Proc., 25th Int. Conf. on Coastal Eng. (ICCE),* ASCE, Reston, Va., 2470–2483.

Koutandos, E., Prinos, P., and Gironella, X. (2005). Floating breakwaters under regular and irregular wave forcing: Reflection and transmission characteristics. *J. Hydraulic Res.,* 43(2), 174–188.

Macagno, E. O. (1954). Houle dans un canal présentant un passage en charge. *La Houille Blanche,* 1(1), 10–37 (in French).

Martinelli, L., Ruol, P., and Zanuttigh, B. (2008). Wave basin experiments on floating breakwaters with different layouts. *Appl. Ocean Res.,* 30(3), 199–207.

McCartney, B. L. (1985). Floating breakwater design. *J. Waterway Port Coastal Ocean Eng.,* 111(2), 304–318.

`

Ning, D., Zhao, X., Göteman, M., and Kang, H. (2016). Hydrodynamic performance of a pile-restrained WEC-type floating breakwater: An experimental study. *Renewable Energy*, 95, 531–541.

Nørgaard, J. H., and Andersen, T. L. (2012). Investigation of wave transmission from a floating wave dragon wave energy converter. *22nd Int. Offshore and Polar Eng. Conf.*, International Society of Offshore and Polar Engineers.

Oliver, J., Aristaghes, P., Cederwall, K., Davidson, D., De Graaf, F., Thackery, M., and Torum, A. (1994). Floating breakwaters: A practical guide for design and construction. *PIANC Report, Working Group 13*, Permanent International Association of Navigation Congresses, Belgium.

Palha, A., Mendes, L., Fortes, C. J., Brito-Melo, A., and Sarmento, A. (2010). The impact of wave energy farms in the shoreline wave climate: Portuguese pilot zone case study using pelamis energy wave devices. *Renewable Energy, 35*(1), 62–77.

Parmeggiani, S., Kofoed, J., and Friis-Madsen, E. (2013). Experimental study related to the mooring design for the 1.5 MW Wave Dragon WEC demonstrator at Dan-WEC. *Energies*, *6*(4), 1863-1886.

Peña, E., Ferreras, J., and Sanchez-Tembleque, F. (2011). Experimental study on wave transmission coefficient, mooring lines and module connector forces with different designs of floating breakwaters. *Ocean Engineering*, *38*(10), 1150-1160.

`

Ruol, P., Martinelli, L., and Pezzutto, P. (2013). Formula to predict transmission for π-type floating breakwaters. *J. Waterway Port Coastal Ocean Eng.*, 10.1061/(ASCE)WW.1943-5460.0000153, 1–8.

Ruol, P., Zanuttigh, B., Martinelli, L., Kofoed, P., and Frigaard, P. (2011). Near-shore floating wave energy converters: Applications for coastal protection. *Coastal Eng. Proc.*, 1(32), 61.

Sorensen, R. M. (2005). *Basic coastal engineering.* Springer Science and Business Media, Berlin/Heidelberg, Germany.

Türker, U., and Kabdaslı, M. (2004). Average sediment dislocation analysis for barred profiles. *Ocean Eng.*, 31(14), 1741–1756.

Türker, U. (2014). Excess energy approach for wave energy dissipation at submerged structures. *Ocean Eng.*, 88, 194–203.

Ursell, F. (1947). The effect of a fixed vertical barrier on surface waves in deep water. *Math. Proc. Cambridge*, 43(3) 374–382.

Venugopal, V., and Smith, G. H. (2007). Wave climate investigation for an array of wave power devices. In *Proceedings of the 7th European wave and tidal energy conference, Porto, Portugal*, pp. 11-14.

Wiegel, R. L. (1960). Transmission of waves past a rigid vertical thin barrier. *J. Waterways Harbors Div.*, 86(1), 1–12.

`

Yamamoto, T., Nath, J. H., and Slotta, L. S. (1974). Wave forces on cylinders near plane boundary." *Journal of Waterways, Harbors and Coast Eng Div, 100* (10961 Proceeding).